

A unified test for regression discontinuity designs

Koki Fusejima*, Takuya Ishihara[†], and Masayuki Sawada[‡]

Abstract

Diagnostic tests for regression discontinuity design face a size-control problem. We document a massive over-rejection of the diagnostic restriction among empirical studies in the top five economics journals. At least one diagnostic test was rejected for 19 out of 59 studies, whereas less than 5% of the collected 787 tests rejected the null hypotheses. In other words, one-third of the studies rejected at least one of their diagnostic tests, whereas their underlying identifying restrictions appear plausible. Multiple testing causes this problem because the median number of tests per study was as high as 12. Therefore, we offer unified tests to overcome the size-control problem. Our procedure is based on the new joint asymptotic normality of local polynomial mean and density estimates. In simulation studies, our unified tests outperformed the Bonferroni correction. We implement the procedure as an R package `rdtest` with two empirical examples in its vignettes.

*Hitotsubashi Institute for Advanced Study, Hitotsubashi University; 2-1 Naka, Kunitachi, Tokyo 186-8601, Japan; k.fusejima@r.hit-u.ac.jp

[†]Graduate School of Economics and Management, Tohoku University; 27-1 Kawauchi, Aoba-ku, Sendai, Miyagi 980-8576, Japan; takuya.ishihara.b7@tohoku.ac.jp

[‡]Corresponding Author. Institute of Economic Research, Hitotsubashi University; 2-1 Naka, Kunitachi, Tokyo 186-8601, Japan; m-sawada@ier.hit-u.ac.jp

1 Introduction

Diagnostic tests are vital to regression discontinuity (RD) design. The typical procedure evaluates the testable restrictions which are expected to hold under a non-testable identifying restriction (Hahn, Todd, and der Klaauw, 2001). All such testable restrictions are expected to hold whenever identification holds. Hence, one must test the null hypothesis of *all restrictions hold* against the alternative hypothesis of *at least one restriction fails*.

However, these restrictions are often tested separately without appropriate size control. Throughout this study, we consider the *continuity-based* framework.¹ In this framework, most empirical studies test these restrictions as null hypotheses for the density test (McCrary, 2008) and the balance or placebo test (Lee, 2008). These tests are well-established separately but are rarely evaluated jointly. Hence, the multiple-testing problem plagues size control. Consequently, empirical studies may over-reject the underlying null hypothesis that all restrictions hold under identification.

In this study, we document the severe over-rejection of the diagnostic restriction in a meta-analysis of 59 empirical RD studies published recently in the top five economics journals.² We found that 19 out of 59 studies rejected at least one testable restriction, leading to the underlying restriction being questioned in 32% of the studies.

Nevertheless, each test appeared valid. Among 787 tests run separately, only 4.3% of the restrictions were rejected, and their p-values uniformly distributed over $[0, 1]$, suggesting that the test statistics are drawn from the null hypothesis that all testable restrictions hold. Hence, the underlying identification was plausible; nonetheless, we ended up with an incorrect conclusion for 19 studies rather than three.

We conclude that this over-rejection was caused by multiple testing problems. In 59 studies, the median number of tests was 12 per study. Furthermore, we found only five studies out of 59 reporting some type of joint testing. No study has reported a joint test that combines the density and balance or placebo tests because no test has been proposed to handle them jointly.

¹In Cattaneo, Idrobo, and Titiunik(2019; 2024), the *continuity-based* framework is a contrasting concept against the alternative *local randomization* framework for a finite sample analysis in which explicit randomization is considered within a small range as studied in Cattaneo, Frandsen, and Titiunik (2015); Cattaneo, Titiunik, and Vazquez-Bare (2016); Cattaneo, Titiunik, and Vazquez-Bare (2017).

²See Online Appendix B for the search criterion.

In this study, we propose a unified diagnostic test to resolve this over-rejection problem. This involves two major challenges. First, no tests consider the joint nature of the density and balance tests. Second, the test statistics are nonparametric estimates. Only one of the five studies considered the nonparametric nature of the test statistics. To address these two challenges, we derived the joint asymptotic normality of the nonparametric density estimation and nonparametric conditional mean estimation. We find that nonparametric density estimates and conditional mean estimates are asymptotically orthogonal. Based on this finding, we provide the first unified test with density and balance test statistics based on our new theoretical results from their nonparametric bias-corrected estimates.

Our unified test aggregates the vector of the density and balance test statistics; however, possible aggregation is not unique. An appropriate aggregation depends on the underlying alternative hypothesis. We considered two different aggregations: (1) a Wald (chi-squared) statistic of the sum of the squared statistics of the vector and (2) a Max test statistic of the maximum squared statistics of the vector. The two test statistics complement each other in detecting different types of alternative hypotheses.

The Wald statistic detects the alternative hypothesis that a large fraction of the original vector deviates from the null hypothesis. The Max statistic detects the alternative hypothesis that only a small fraction of the vector deviates from the null hypothesis. Nevertheless, the conventional Wald statistic did not attain the nominal size, possibly because of poor inverse estimation of the variance matrix. We bypass this problem by standardizing only the diagonal elements instead of multiplying the inverse of the variance matrix and propose it as the *standardized* Wald (hereafter, sWald) statistic.

In numerical simulations, the sWald and Max statistics exhibit appropriate size control properties for a moderate number of covariates when the sample size is as large as 1000. In particular, the sWald test is superior to other methods in size control performance for any number of covariates up to 25 in cases where even the Bonferroni correction may fail to achieve size control.³

We verified the superior power properties of the proposed methods. The Max test is superior to the Bonferroni correction in its power against the alternative hypothesis

³We conjecture that the reason for this failure is that Bonferroni correction with 25 covariates evaluates the thin tail of the nonparametric test statistic distribution, which could be imprecisely estimated.

that only one covariate sees a jump in the conditional mean. The sWald test is superior to the Bonferroni correction in its power against the alternative hypothesis that all covariates see jumps in their conditional means. In conclusion, we recommend the Max test if a user has a few particularly concerning covariates. Otherwise, we recommend the sWald test for better size control and power in other scenarios. ⁴

This study contributes to the literature on diagnostic procedures for RD design. ⁵ McCrary (2008) has developed the density test. Several theoretical studies have improved these procedures. ⁶ Otsu, Xu, and Matsushita (2013) have proposed an empirical likelihood-based density test, Cattaneo, Jansson, and Ma (2020) have considered a test based on a local polynomial estimation of the density function, and Bugni and Canay (2021) have proposed an approximate sign test for the density test. Nevertheless, none of these studies have considered the joint procedure for these tests. Diagnostic test practices follow a similar pattern: separate multiple testing of these diagnostic tests or some joint procedure without considering the nonparametric nature of the test statistics. In this study, we provide unified testing for the null hypothesis that all these diagnostic restrictions hold, suggesting that identification is plausible. We also provide a statistical software *rdtest*, which is an explicit wrapper of two standard packages, *rdrobust* (Calonico, Cattaneo, Farrell, and Titiunik, 2017) and *rddensity* (Cattaneo, Jansson, and Ma, 2018). Therefore, we provide an easy-to-implement unified diagnostic procedure for the widely used continuity-based framework.

⁴We also compare our methods with the resampling based method of Romano and Wolf (2005, 2016) using a *stata* package *rwolf2* (Clarke, 2021) in Online Appendix D. We note that the applicability of Romano and Wolf (2005) is not necessarily guaranteed for the RD context, and *rwolf2* can accept the balance tests only. Hence, our simulation comparisons with *rwolf2* are limited to the balance tests only. In the simulation, the Romano and Wolf correction exhibits a bimodal performance: it achieves a good power for the large effect sizes with high correlations, but the power is much lower than our methods when the effect sizes are small. Hence, we continue to support our methods for the purpose of detecting possibly small violations in diagnostic testings.

⁵See the latest textbooks Cattaneo et al.(2019; 2024) for an extensive survey of RD literature.

⁶Several theoretical studies also provide other forms of testing procedures in regression discontinuity designs. For example, Hsu and Shen (2019) and Hsu and Shen (2021) provide tests for the presence of treatment effect heterogeneity across covariate values and for monotonicity in the conditional treatment effects; Bertanha and Imbens (2020) provide tests for exogeneity and external validity in fuzzy designs.

Moreover, we contribute to the asymptotic theory of nonparametric estimates. We show the joint asymptotic normality of multiple local polynomial estimates for the conditional mean and density functions. Calonico, Cattaneo, and Titiunik (2014) show the asymptotic normality of a single local polynomial estimate for a conditional mean function at a boundary point after bias correction. Cattaneo et al. (2020) also show the asymptotic normality of a local polynomial estimate of a density function at a boundary point. We developed the joint normality results based on these results. The marginal bias and variance expressions are identical to those in Calonico et al. (2014) and Cattaneo et al. (2020), and we impose no restrictions on the choice of bandwidth apart from the original rate conditions. Consequently, we succeeded in accommodating the same mean squared error (MSE) optimal estimates for the balance and placebo tests (Calonico et al., 2014)⁷ and density tests (Cattaneo et al., 2020).

The remainder of the paper proceeds as follows. Section 2 demonstrates the multiple testing problem in the meta-analysis, and Section 3.1 explains the joint asymptotic normality of the nonparametric estimates. Subsequently, Section 3.2 presents our joint tests, Section 4 demonstrates the performance of our tests in the simulation, and Section 5 considers the two extensions for our procedure: equivalence testing which flips the null and alternative hypotheses, and pretesting analysis in view of Roth (2022). Finally, Section 6 concludes the article by recommending practices and proposing future research questions. In Online Appendix A, we provide all the formal results and the proofs.

2 Current practices of diagnostic tests

Most empirical studies diagnose their designs using two continuity restrictions: the density function of the running variable and the conditional mean functions of the pretreatment covariates. In this study, we focus on the two major practices that are routinely evaluated with well-established packages. There are other popular diagnoses such as the *placebo cutoff* analysis. See Cattaneo and Titiunik (2022, Section 4) and Cattaneo et al. (2019, Section 5) for further diagnostic concepts.

⁷Recently, another bandwidth selector of coverage error optimal bandwidths has been proposed by Calonico, Cattaneo, and Farrell (2020) along with theoretical background Calonico, Cattaneo, and Farrell (2022). In our numerical analyses and implementation, we used the default option for MSE optimal bandwidths.

The logic behind the diagnoses is that “the RD design offers an array of empirical methods that, under reasonable assumptions, can provide useful evidence about the plausibility of its assumptions.” (Cattaneo et al., 2019) In the continuity-based framework, identification holds when the conditional mean function of the potential outcome is continuous in the conditioning running variable at the cutoff. In other words, the units near the cutoff must be similar in the unobserved characteristics of the potential outcomes.

However, units often know the cutoff value and hence they may manipulate the running variable to be eligible for treatment. A typical idea to assess such manipulation is that “if units lack the ability to precisely manipulate the score value they receive, there should be no systematic differences between units with similar values of the score” (Cattaneo et al., 2019). This idea conveys a testable restriction that the observed characteristics must be balanced near the cutoff.

Similar idea is that “if units do not have the ability to precisely manipulate the value of the score that they receive, the number of treated observations just above the cutoff should be approximately similar to the number of control observations below it” (Cattaneo et al., 2019). This latter idea conveys another testable restriction that the observed density function of the running variable must be continuous at the cutoff. The former restriction is often conducted as the balance or placebo test, and the latter restriction is evaluated as the density test.

All those testable restrictions stem from the ideas that support identification. Hence, if we claim the plausibility of identification, all those diagnostic restrictions should hold, and none of them must be violated.⁸

In other words, we must test the null hypothesis that *all testable restrictions hold* against the alternative hypothesis that *at least one restriction fails* to diagnose the underlying designs. However, most studies have tested these restrictions separately as density tests (McCrary, 2008; Cattaneo et al., 2020, for example) and balance or placebo tests (Lee, 2008; Lee and Lemieux, 2010, for example). Running these tests separately would over-reject the underlying null hypothesis that all testable restrictions hold because of the multiple testing problem.

⁸Without additional restrictions, these restrictions have no direct connection with identification. For example, the density test is neither necessary nor sufficient for identification (McCrary, 2008). See Ishihara and Sawada (2023) for conditions under which the null hypothesis of the density test implies identification.

We quantified the size control problem by conducting a meta-analysis of RD studies published in the top five economics journals. Among 59 papers that satisfied our search criteria up to November 2021, we collected 787 reported test statistics.⁹ Our meta-analysis found two facts: (1) the reported test statistics appear to conform to the null hypothesis that all restrictions hold; (2) nonetheless, 32% (19) studies had at least one rejected test.

2.1 Fact 1: Test statistics are likely drawn from the null distributions

First, we document the reported test statistics likely to be drawn from null distributions. Table 1 presents the percentage of tests rejected from the reported ones. Among 787 tests reported in 59 studies, we found that less than 5% rejected null hypotheses. Figure 1 shows the quantile plot of the p-values. The quantile plot aligns with the 45-degree line, and the distribution is likely to be uniform over $[0, 1]$.¹⁰ Both lines of evidence support the null hypothesis that all restrictions hold and hence identification is plausible.

Table 1: Percentage of rejected tests

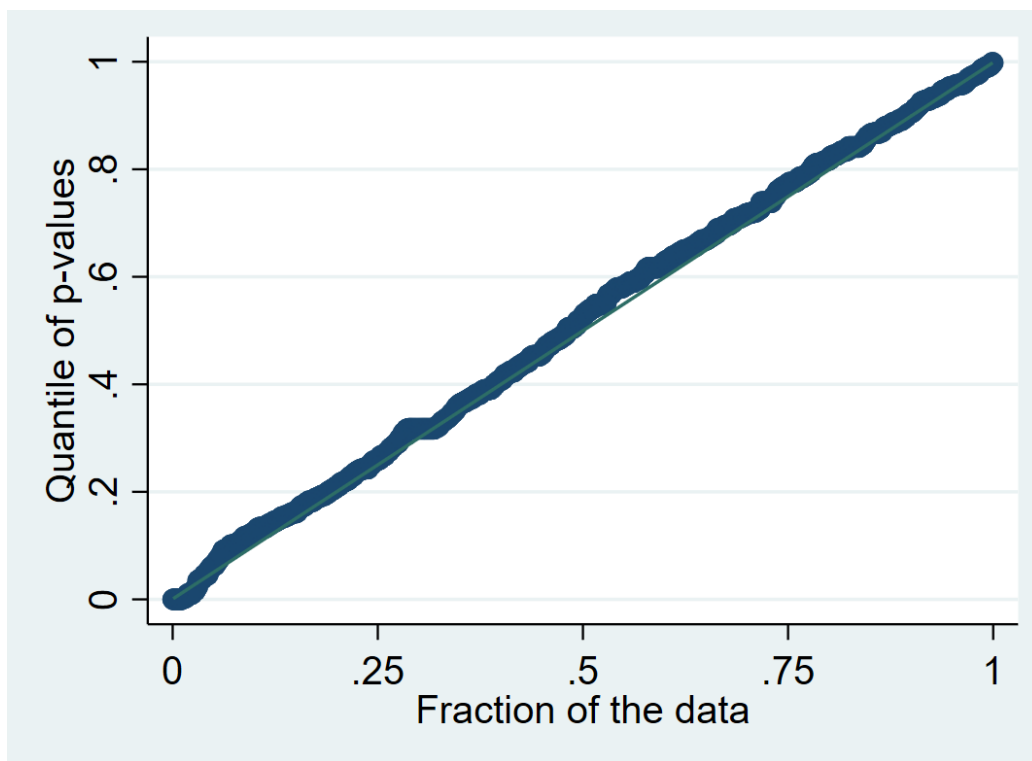
	Balance	Density	Total
Rejected	4.32%	4.35%	4.32%
Not	95.68%	95.65%	95.68%
Number of tests	764	23	787

Notes: Percentages of tests reported as *rejected* and *non-rejected* among 764 balance tests, 23 density tests, and 787 tests in total. See Online Appendix B for details.

⁹Many studies aim to demonstrate their robustness with different specifications of the same tests with different bandwidths, order of polynomials, or kernels. We screen the *main* specification for each test, and our reported results are the lower bounds of their over-rejections. See Online Appendix B for details.

¹⁰This is also true among the rejected studies. See Appendix Figure 7 for the histogram of p-values among the rejected studies.

Figure 1: Quantile plot of p-values of tests



Notes: The quantile plot of p-values that are reported or computed from t-statistics. Plot aligned with the solid 45 degree line implies similarity to the uniform distribution over $[0, 1]$.

2.2 Fact 2: The underlying null hypothesis is over-rejected because of multiple testing

From Fact 1, approximately three studies out of 59 should have shown any test rejection because the null hypotheses appear valid. However, Table 2 suggests that 32% of the studies (19 of 59) rejected at least one null hypothesis. Among 19 studies, 8 studies rejected more than once. As shown in Table 2 and Figure 2, many studies ran more than 10 diagnostic tests without appropriate size control.¹¹ Hence, we blame the multiple testing problem for over-rejecting the null hypothesis of *all restrictions*

¹¹Also, studies with many rejections tend to run excessively many tests. See Appendix Figure 8 for the scatter plot of the number of rejected tests and the number of tests.

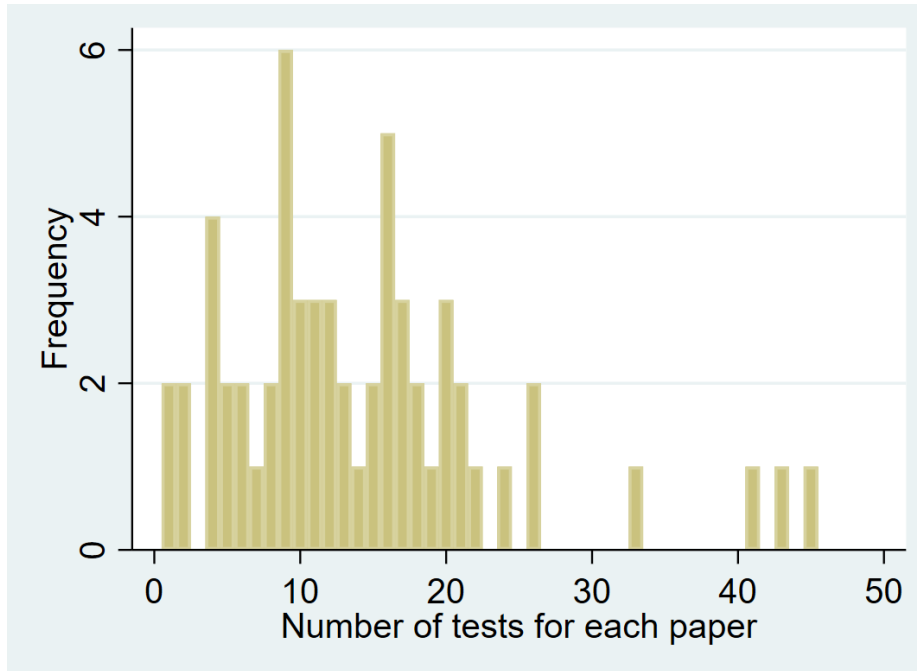
hold.

Table 2: Fraction of rejecting at least one hypothesis.

	mean	median	sd
Number of tests per study	14.20	12	9.59
Fraction rejecting at least one test	0.32	-	0.47
Number of rejected tests per study	0.69	0	1.52
Number of studies	59		

Notes: The table shows the mean, median, and standard deviation for the number of tests per study, the fraction of rejecting at least one test per study, and the number of rejected tests per study out of 59 studies.

Figure 2: Histogram of the number of tests



Notes: This figure is the histogram of the number of tests reported in each study.

2.3 How does empirical studies respond to their rejections

Upon rejection of their diagnostic tests, most studies defended their statistical significance in diagnostic tests by making some supporting arguments such as stating *economical* insignificance of their rejected test statistics. Those supporting arguments are indeed desirable. However, the majority of the studies did not address the root cause of their rejections, the multiple testing problem.

Notably, only five studies reported joint testing for balance tests. All but one study did not consider the nonparametric nature of the test statistics.¹² Furthermore, no studies have reported joint testing of the balance and density tests because no method is available for the joint test.

We emphasize that only a few studies made explicit argument that *testing many hypotheses* can result in their rejections of the diagnostic tests. Furthermore, their arguments were all informal without any multiple testing corrections. For example, Tyrefors Hinnerich and Pettersson-Lidbom (2014) stated that “Only one of the 44 estimates is significant at the 5 percent level. However, that is to be expected since, if 100 specifications are tested, it is likely that five will be statistically significant by chance” (page 981). With a unified diagnostic test, these studies could have formally concluded that their rejections were by chance in their data.

3 Unified test based on joint asymptotic normality

As shown in Section 2, the multiple-testing problem causes the over-rejection of the underlying restriction which suggests plausible identification. We introduce a notation to formally state the problem. Let $(Z_{1,i}, \dots, Z_{d,i}, X_i)'$, $i = 1, \dots, n$ denote the observed random sample, where X_i is the running variable with density $f(x)$ with respect to the Lebesgue measure and $Z_i = (Z_{1,i}, \dots, Z_{d,i})'$ denote the pre-treatment covariates. Given a known threshold \bar{x} , which we set to $\bar{x} = 0$ without loss of generality, let the running variable X_i determine whether unit i is assigned a treatment ($X_i \geq 0$) against ($X_i < 0$). In this notation, empirical applications frequently consider two different types of restrictions: the density function $f(x)$ is continuous at $x = 0$, and the conditional

¹²We confirm some sort of joint testing in the following five studies: Meyersson (2014); Abdulkadiroğlu, Angrist, and Pathak (2014); Johnson (2020); Fort, Ichino, and Zanella (2020); Jäger, Schoefer, and Heining (2021). Fort et al. (2020) use a nonparametric procedure by Canay and Kamat (2018).

mean functions of Z_k , $\mu_{Z_k}(x) = E[Z_{k,i}|X_i = x]$ for $k = 1, \dots, d$, are continuous at $x = 0$. Specifically, the following $d + 1$ restrictions must hold simultaneously

$$f_+ = f_-, \mu_{Z_1+} = \mu_{Z_1-}, \dots, \mu_{Z_d+} = \mu_{Z_d-}$$

where $f_+ = \lim_{x \rightarrow 0^+} f(x)$, $f_- = \lim_{x \rightarrow 0^-} f(x)$ and $\mu_{Z_k+} = \lim_{x \rightarrow 0^+} \mu_{Z_k}(x)$, $\mu_{Z_k-} = \lim_{x \rightarrow 0^-} \mu_{Z_k}(x)$. Hence, one must conduct the following test:

$$H_0 : (\tau_f, \tau_{Z_1}, \dots, \tau_{Z_d}) = 0 \quad \text{vs} \quad H_1 : (\tau_f, \tau_{Z_1}, \dots, \tau_{Z_d}) \neq 0,$$

to determine whether identification is plausible where $\tau_f = f_+ - f_-$ and $\tau_{Z_k} = \mu_{Z_k+} - \mu_{Z_k-}$. However, if one runs $d + 1$ tests separately:

$$\begin{aligned} H_{0f} : \tau_f = 0 & \quad \text{vs} \quad H_{1f} : \tau_f \neq 0, \\ H_{01} : \tau_{Z_1} = 0 & \quad \text{vs} \quad H_{11} : \tau_{Z_1} \neq 0, \\ & \quad \vdots \\ H_{0d} : \tau_{Z_d} = 0 & \quad \text{vs} \quad H_{1d} : \tau_{Z_d} \neq 0, \end{aligned}$$

the null hypothesis H_0 is over-rejected as documented in Section 2.

We resolved the size control problem by presenting a unified test in two steps. First, we present the theoretical basis for our unified test. Second, we propose two test statistics for the unified test against multiple testing.

3.1 New joint normality result

First, we derive the joint asymptotic normality of the nonparametric local polynomial estimators for f and $(\mu_{Z_1}, \dots, \mu_{Z_d})$ evaluated at the boundary of the support.

Following Calonico et al. (2014) and Cattaneo et al. (2020), we use local polynomial regressions to approximate the unknown functions $f(x)$ and $\mu_{Z_k}(x)$ for $k = 1, \dots, d$ flexibly near the cutoff $\bar{x} = 0$; see Fan and Gijbels (1996) for a review of local polynomial regressions. Based on the testing problem, we must obtain two distinct estimands for each function using the two subsamples $\{X_i : X_i \geq 0\}$ (approximation from the right) and $\{X_i : X_i < 0\}$ (approximation from the left) at a boundary point $x = 0$. These estimators are recommended owing to their excellent boundary properties.

Using a polynomial expansion, we construct smooth local one-sided approximations of the sample average of $Z_{k,i}$ and obtain the estimators $\hat{\mu}_{Z_k+,l}(h_{k,n})$ and $\hat{\mu}_{Z_k-,l}(h_{k,n})$ as intercepts in the local polynomial regression. Specifically, we estimate τ_{Z_k} using

the following l th-order local polynomial estimators: for some $l \geq 1$ and for each $k = 1, \dots, d$,

$$\hat{\tau}_{Z_k, l}(h_{k, n}) = \hat{\mu}_{Z_k+, l}(h_{k, n}) - \hat{\mu}_{Z_k-, l}(h_{k, n}),$$

$$\hat{\mu}_{Z_k+, l}(h_{k, n}) = e'_0 \hat{\beta}_{Z_k+, l}(h_{k, n}), \quad (3.1)$$

$$\hat{\mu}_{Z_k-, l}(h_{k, n}) = e'_0 \hat{\beta}_{Z_k-, l}(h_{k, n}), \quad (3.2)$$

where

$$\hat{\beta}_{Z_k+, l}(h_{k, n}) = \arg \min_{\beta \in \mathbb{R}^{l+1}} \sum_{i=1}^n 1\{X_i \geq 0\} (Z_{k, i} - r_l(X_i)' \beta)^2 K(X_i/h_{k, n})/h_{k, n}, \quad (3.3)$$

$$\hat{\beta}_{Z_k-, l}(h_{k, n}) = \arg \min_{\beta \in \mathbb{R}^{l+1}} \sum_{i=1}^n 1\{X_i < 0\} (Z_{k, i} - r_l(X_i)' \beta)^2 K(X_i/h_{k, n})/h_{k, n}, \quad (3.4)$$

$e_0 = (1, 0, \dots, 0)'$ is the first $(l+1)$ -dimensional unit vector, $r_l(x) = (1, x, \dots, x^l)'$ is a l th order polynomial expansion, $K(\cdot)$ is a kernel function, and $h_{k, n}$ is a positive-bandwidth sequence.

Similarly, using a polynomial expansion, we construct smooth local one-sided approximations of the empirical distribution of X_i and obtain the estimators $\hat{f}_{+, p}(h_{f, n})$ and $\hat{f}_{-, p}(h_{f, n})$ as the slope coefficients in the local polynomial regression. Specifically, we estimate τ_f using the following p th-order local polynomial estimator. For some $p \geq 2$,

$$\hat{\tau}_{f, p}(h_{f, n}) = \hat{f}_{+, p}(h_{f, n}) - \hat{f}_{-, p}(h_{f, n}),$$

$$\hat{f}_{+, p}(h_{f, n}) = e'_1 \hat{\beta}_{f+, p}(h_{f, n}), \quad (3.5)$$

$$\hat{f}_{-, p}(h_{f, n}) = e'_1 \hat{\beta}_{f-, p}(h_{f, n}), \quad (3.6)$$

where

$$\hat{\beta}_{f+, p}(h_{f, n}) = \arg \min_{\beta \in \mathbb{R}^{p+1}} \sum_{i=1}^n 1\{X_i \geq 0\} (\tilde{F}(X_i) - r_p(X_i)' \beta)^2 K(X_i/h_{f, n})/h_{f, n}, \quad (3.7)$$

$$\hat{\beta}_{f-, p}(h_{f, n}) = \arg \min_{\beta \in \mathbb{R}^{p+1}} \sum_{i=1}^n 1\{X_i < 0\} (\tilde{F}(X_i) - r_p(X_i)' \beta)^2 K(X_i/h_{f, n})/h_{f, n}, \quad (3.8)$$

$e_1 = (0, 1, 0, \dots, 0)'$ is the second $(p+1)$ -dimensional unit vector; $\tilde{F}(x) \equiv n^{-1} \sum_{i=1}^n 1\{X_i \leq x\}$ is the empirical distribution function of X_i , and $h_{f, n}$ is the positive-bandwidth sequence.

We derive the asymptotic distributions of the local polynomial estimators based

on the assumptions in Calonico et al. (2014) and Cattaneo et al. (2020), as follows.

Assumption 1. *For some $\kappa_0 > 0$, the following holds true for $(-\kappa_0, 0) \cup (0, \kappa_0)$ around the cutoff $\bar{x} = 0$.*

- (a) *$f(x)$ is R times continuously differentiable for some $R \geq 1$ and bounded away from zero.*
- (b) *For $k = 1, \dots, d$, $\mu_{Z_k}(x)$ is S times continuously differentiable for some $S \geq 1$, $\text{Var}(Z_{k,i}|X_i = x)$ is continuous and bounded away from zero, and $E[|Z_{k,i}|^4|X_i = x]$ is bounded.*

Assumption 1 is a set of basic regularity conditions for the data generation process. Assumption 1 (a) ensures that the density of the running variable is well defined and sufficiently smooth and that the observed values are arbitrarily close to the cutoff for large samples. Assumption 1 (b) ensures that the conditional expectations and variances of the pre-treatment covariates are well defined and have sufficient smoothness with the existence of the fourth moments.

Assumption 2. *For some $\kappa > 0$, the kernel function $K(\cdot) : \mathbb{R} \rightarrow \mathbb{R}$ is symmetric, bounded, and non-negative; it is zero outside the support, and positive and continuous on $(-\kappa, \kappa)$.*

Assumption 2 is a set of standard conditions for the kernel function and is satisfied for kernels such as triangular and uniform kernels, commonly used in empirical work. Our results can be extended to accommodate kernels with unbounded supports or asymmetric kernels with more complex notations.

We provide a joint asymptotic distribution for the local polynomial estimators. In the following, let $l, p \in \mathbb{N}$; $h_n = (h_{1,n}, \dots, h_{d,n})'$; $h_{max,n} = \max\{h_{1,n}, \dots, h_{d,n}\}$; $h_{min,n} = \min\{h_{1,n}, \dots, h_{d,n}\}$; we assume that all the limits are $n \rightarrow \infty$ (and $h_{k,n}, h_{f,n} \rightarrow 0$), unless stated otherwise. Whenever there was no confusion, we dropped the sample size n sub-index notation. For derivatives $\mu_{Z_k}^{(s)}(x)$ and $f^{(s)}(x)$, let $\mu_{Z_k+}^{(s)} = \lim_{x \rightarrow 0^+} \mu_{Z_k}^{(s)}(x)$, $\mu_{Z_k-}^{(s)} = \lim_{x \rightarrow 0^-} \mu_{Z_k}^{(s)}(x)$, $f_+^{(s)} = \lim_{x \rightarrow 0^+} f^{(s)}(x)$, and $f_-^{(s)} = \lim_{x \rightarrow 0^-} f^{(s)}(x)$.

Theorem 3.1. *Suppose that Assumptions 1 and 2 hold, with $R \geq p + 1$ and $S \geq l + 2$.*

If $nh_{\min} \rightarrow \infty$, $nh_f^2 \rightarrow \infty$, $n(h_{\max})^{2l+5} \rightarrow 0$ and $n(h_f)^{2p+3} \rightarrow 0$, then

$$\sqrt{n} \begin{bmatrix} \sqrt{h_1}(\hat{\tau}_{Z_1,l}(h_1) - \tau_{Z_1} - (h_1)^{1+l} B_{Z_1,l,l+1}(h_1)) \\ \vdots \\ \sqrt{h_d}(\hat{\tau}_{Z_d,l}(h_d) - \tau_{Z_d} - (h_d)^{1+l} B_{Z_d,l,l+1}(h_d)) \\ \sqrt{h_f}(\hat{\tau}_{f,p}(h_f) - \tau_f - h_f^p B_{f,p,p+1}(h_f)) \end{bmatrix} \xrightarrow{d} N_{d+1}(0, V_{l,p}),$$

where $N_{d+1}(\mu, \Sigma)$ denotes the multivariate normal distribution with $(d+1)$ -dimensional mean vector μ and $(d+1) \times (d+1)$ covariance matrix Σ ,

$$\begin{aligned} B_{Z^k,l,r}(h_k) &= B_{Z^{k+},l,r}(h_k) - B_{Z^{k-},l,r}(h_k) \\ &= \frac{\mu_{Z^{k+}}^{(r)}}{r!} \mathcal{B}_{+,0,l,r}(h_k) - \frac{\mu_{Z^{k-}}^{(r)}}{r!} \mathcal{B}_{-,0,l,r}(h_k), \end{aligned}$$

$$\begin{aligned} B_{f,p,q}(h_f) &= B_{f,+,p,q}(h_f) - B_{f,-,p,q}(h_f) \\ &= \frac{f_+^{(q-1)}}{(q-1)!} \mathcal{B}_{+,1,p,q}(h_f) - \frac{f_-^{(q-1)}}{(q-1)!} \mathcal{B}_{-,1,p,q}(h_f), \end{aligned}$$

and

$$V_{l,p} = \begin{pmatrix} V_{Z,l} & 0 \\ 0 & V_{f,p} \end{pmatrix}.$$

The exact forms of $\mathcal{B}_{+,s,l,r}(h)$ and $\mathcal{B}_{-,s,l,r}(h)$ are provided in Online Appendix A.2. The exact forms of $V_{Z,l}$ and $V_{f,p}$ are provided in Online Appendix A.4.

Theorem 3.1 shows that the joint asymptotic distribution of $\hat{\tau}_{f,p}(h_f)$ and $\hat{\tau}_{Z_k,l}(h_k)$ is a multivariate normal distribution under the same set of conditions as in Calonico et al. (2014) for $\hat{\tau}_{Z_k,l}(h_k)$ and Cattaneo et al. (2020) for $\hat{\tau}_{f,p}(h_f)$. Hence, the proposed joint distributional approximation is a natural generalization of the distributional approximation of each local polynomial estimator in these studies.

We emphasize that the covariance matrix of $(\hat{\tau}_{Z_1,l}(h_1), \dots, \hat{\tau}_{Z_d,l}(h_d))'$ and the variance of $\hat{\tau}_{f,p}(h_f)$ are asymptotically orthogonal. Orthogonality simplifies the estimation of the overall asymptotic covariance matrix because the asymptotic covariance of $\hat{\tau}_{f,p}(h_f)$ and $\hat{\tau}_{Z_k,l}(h_k)$ is known to be zero. We derive this orthogonality from the well-known fact that $\text{Cov}(Z_{k,i} - \mu_{Z_k}(X_i), g(X_i)) = 0$ for any function g .

Orthogonality affects the nature of the multiple testing problem in various ways. When the test statistics are independent, the multiple testing problem is likely worse. Hence, the size control problem in the naive test procedure becomes worse. In turn, a typical multiple test correction such as Bonferroni correction may become less

conservative. For our procedure, we have one less parameter to estimate, and the orthogonality may help stabilizing our procedure.

Remark 1 (Increasing the polynomial order for bias correction). We use bias-corrected estimators for the following analyses. In general, bias correction is critical in empirical contexts (Hyytinen, Meriläinen, Saarimaa, Toivanen, and Tukiainen, 2018). As highlighted in Calonico et al. (2014) and Cattaneo et al. (2020), bias correction is important for inference. As provided in Online Appendix A.2, $\mathcal{B}_{+,s,l,r}(h)$ and $\mathcal{B}_{-,s,l,r}(h)$ are the observed quantities, and the bias-corrected estimators are constructed by replacing $\mu_{Z_{k+}}^{(r)}$, $\mu_{Z_{k-}}^{(r)}$, $f_+^{(q-1)}$, and $f_-^{(q-1)}$ with their local polynomial estimators. Nevertheless, as shown in Calonico et al. (2014), if the same bandwidth and kernel function are used for estimating $\mu_{Z_{k+}}^{(r)}$ and $\mu_{Z_{k-}}^{(r)}$, the bias-corrected estimator is numerically equivalent to $\hat{\tau}_{Z_k,l+1}(h_k)$ (with no bias-correction). A bias correction based on similar results has been adopted by Cattaneo et al. (2020) for their local polynomial density estimators. This same bandwidth choice is shown to be optimal for the uniform kernel (Calonico et al., 2022). Following their approach, we implement bias correction by increasing the order of the local polynomial estimators.¹³

Remark 2 (Bandwidth selection). We allow the bandwidths to differ for each estimator as long as the conditions stated in Theorem 3.1 are satisfied and the marginal bias and variance expressions are identical to those in Calonico et al. (2014) and Cattaneo et al. (2020). Hence, we may apply the original data-driven bandwidth selection provided in Calonico et al. (2014) for h_1, \dots, h_d and Cattaneo et al. (2020) for h_f to our joint distributional approximation. As described above, we used bias-corrected local polynomial estimators. Specifically, h_k is the MSE-optimal bandwidth for $\hat{\tau}_{Z_k,l}(h_k)$, and h_f is the MSE-optimal bandwidth for $\hat{\tau}_{f,p}(h_f)$. We construct the test statistics based on $\hat{\tau}_{Z_k,l+1}(h_k)$ and $\hat{\tau}_{f,p+1}(h_f)$. The latter implementation via $\hat{\tau}_{f,p+1}(h_f)$ is the default for *rddensity*, based on Cattaneo et al. (2020).

Remark 3 (Asymptotic covariance matrix). We estimate the asymptotic covariance matrix as follows.

$$\hat{V}_{l,p}(h) = \begin{pmatrix} \hat{V}_{Z,l}(h) & 0 \\ 0 & \hat{V}_{f,p}(h_f) \end{pmatrix},$$

where

$$\hat{V}_{Z,l}(h) \xrightarrow{P} V_{Z,l}, \quad \hat{V}_{f,p}(h_f) \xrightarrow{P} V_{f,p}.$$

¹³See Online Appendix A.3 for details.

We employed the estimators proposed by Calonico et al. (2014) and Cattaneo et al. (2020) for the asymptotic variances of $\hat{\tau}_{Z_k,l}(h_k)$ and $\hat{\tau}_{f,p}(h_f)$ for each diagonal element of the asymptotic covariance matrix $\hat{V}_{Z,l}(h)$ and $\hat{V}_{f,p}(h_f)$. For the covariance estimators of $\hat{\tau}_{Z_j,l}(h_j)$ and $\hat{\tau}_{Z_k,l}(h_k)$, we follow Calonico et al. (2014). Specifically, we propose to estimate the elements of $\hat{V}_{Z,l}(h)$ based on the nearest-neighbor estimation, which may be more robust than plugging in the corresponding residuals of nonparametric regressions in finite samples. We provide the exact forms of $\hat{V}_{Z,l}(h)$ and $\hat{V}_{f,p}(h_f)$ in Online Appendix A.4.

3.2 Proposed unified tests

Given the joint asymptotic normality result, we introduce a unified test for the plausibility of identification. We constructed the test statistics based on the bias-corrected local polynomial estimators $\hat{\tau}_{Z_k,l+1}(h_k)$ and $\hat{\tau}_{f,p+1}(h_f)$, where the bandwidth was chosen as MSE-optimal for $\hat{\tau}_{Z_k,l}(h_k)$ and $\hat{\tau}_{f,p}(h_f)$. Our unified test has two forms: one aggregates the vector of the density and balance test statistics with the L^2 -norm, and the other aggregates them via the L^∞ -norm.

The Wald (chi-squared) test statistic with the L^2 -norm has the following form.

$$\hat{\chi}_{l+1,p+1}^2(h) = \|(\hat{V}_{l+1,p+1}(h))^{-1/2}\hat{T}_{l+1,p+1}(h)\|_2^2,$$

where

$$\hat{T}_{l,p}(h) = \sqrt{n}[\sqrt{h_1}\hat{\tau}_{Z_1,l}(h_1), \dots, \sqrt{h_d}\hat{\tau}_{Z_d,l}(h_d), \sqrt{h_f}\hat{\tau}_{f,p}(h_f)]'.$$

This conventional test statistic suffers from severe size distortions in finite samples. In particular, the inverse of the asymptotic covariance matrix estimator becomes unstable for a sufficiently large dimension d .

Instead, we propose a *sWald* test statistic that modifies the Wald test statistic. Specifically, we standardize only the diagonal elements instead of multiplying the entire matrix by the inverse of the asymptotic covariance matrix. The sWald test statistic has the following form:

$$\tilde{\chi}_{l+1,p+1}^2(h) = \|\tilde{T}_{l+1,p+1}(h)\|_2^2,$$

where

$$\tilde{T}_{l,p}(h) = \text{diag}\{(\hat{V}_{Z_1,l}(h_1))^{-1/2}, \dots, (\hat{V}_{Z_d,l}(h_d))^{-1/2}, (\hat{V}_{f,p}(h_f))^{-1/2}\}\hat{T}_{l,p}(h),$$

and $\text{diag}(a_1, \dots, a_n)$ is the $(n \times n)$ diagonal matrix with diagonal elements a_1, \dots, a_n .

We obtain the asymptotic distribution of $\tilde{\chi}_{l+1,p+1}^2(h)$ from the joint asymptotic distribution for the local polynomial estimators, with their diagonal elements standardized by their standard errors $(\hat{V}_{f,p+1}(h_f))^{1/2}$ and $(\hat{V}_{Z_k,l+1}(h_k))^{1/2}$. We construct the standard errors of τ_{Z_k} as $\hat{V}_{Z_k,l+1}(h_k) \xrightarrow{P} V_{Z_k,l+1}$, where $V_{Z_k,l+1}$ is the asymptotic variance of $\sqrt{nh_k}(\hat{\tau}_{Z_k,l+1}(h_k) - \tau_{Z_k})$. The asymptotic covariance matrix of the standardized local polynomial estimators is the asymptotic correlation matrix of the local polynomial estimators for τ_f and τ_{Z_k} . The correlation matrix $V_{l+1,p+1}^*$ is

$$V_{l+1,p+1}^* = \begin{pmatrix} V_{Z,l+1}^* & 0 \\ 0 & 1 \end{pmatrix},$$

where $V_{Z,l}^* = \text{diag}(V_{Z_1,l}^{-1/2}, \dots, V_{Z_d,l}^{-1/2})V_{Z,l}\text{diag}(V_{Z_1,l}^{-1/2}, \dots, V_{Z_d,l}^{-1/2})$; our estimator of $V_{l+1,p+1}^*$ is

$$\hat{V}_{l+1,p+1}^*(h) = \begin{pmatrix} \hat{V}_{Z,l+1}^*(h) & 0 \\ 0 & 1 \end{pmatrix},$$

where

$$\hat{V}_{Z,l}^*(h) = D_{\hat{V}}(h)\hat{V}_{Z,l}(h)D_{\hat{V}}(h) \text{ with } D_{\hat{V}}(h) = \text{diag}\{(\hat{V}_{Z_1,l}(h_1))^{-1/2}, \dots, (\hat{V}_{Z_d,l}(h_d))^{-1/2}\}.$$

In the following proposition, we show that the finite-sample distribution of $\tilde{\chi}_{l+1,p+1}^2(h)$ is approximated by the distribution of the sum of the squares of the $(d+1)$ -dimensional multivariate normal random vector.

Proposition 3.1. *Suppose Assumptions 1 and 2 hold with $R \geq p+2$ and $S \geq l+3$, and the asymptotic covariance matrix $V_{l+1,p+1}$ is nonsingular. If $nh_{\min} \rightarrow \infty$, $nh_f^2 \rightarrow \infty$, $n(h_{\max})^{2l+5} \rightarrow 0$, and $n(h_f)^{2p+3} \rightarrow 0$, then*

$$\begin{aligned} \text{Under } H_0 : \lim_{n \rightarrow \infty} P(\tilde{\chi}_{l+1,p+1}^2(h) \geq \hat{c}_{l+1,p+1}(\alpha)) &= \alpha, \\ \text{Under } H_1 : \lim_{n \rightarrow \infty} P(\tilde{\chi}_{l+1,p+1}^2(h) \geq \hat{c}_{l+1,p+1}(\alpha)) &= 1, \end{aligned}$$

where $\hat{c}_{l+1,p+1}(\alpha)$ is the $(1-\alpha)$ -quantile of the distribution of $\|N_{d+1}(0, \hat{V}_{l+1,p+1}^*(h))\|_2^2$.

Proposition 3.1 establishes the asymptotic validity and consistency of the α -level testing procedure, which rejects H_0 if $\hat{c}_{l+1,p+1}(\alpha)$ exceeds $\tilde{\chi}_{l+1,p+1}^2(h)$. The critical value $\hat{c}_{l+1,p+1}(\alpha)$ is obtained numerically by generating $(d+1)$ -dimensional standard normal random vectors using Monte Carlo simulation.

The *Max* test statistic with L^∞ norm takes the following form.

$$\hat{M}_{l+1,p+1}(h) = \|\tilde{T}_{l+1,p+1}(h)\|_\infty^2.$$

Similar to the sWald statistic, the Max statistic is constructed by standardizing diagonal elements. The following statement shows that the finite sample distribution of $\hat{M}_{l+1,p+1}(h)$ is approximated by the distribution of the maximum value of the $(d+1)$ -dimensional multivariate normal random vector.¹⁴

Proposition 3.2. *Suppose Assumptions 1 and 2 hold with $R \geq p+2$ and $S \geq l+3$, and the asymptotic covariance matrix $V_{l+1,p+1}$ is nonsingular. If $nh_{\min} \rightarrow \infty$, $nh_f^2 \rightarrow \infty$, $n(h_{\max})^{2l+5} \rightarrow 0$ and $n(h_f)^{2p+3} \rightarrow 0$,*

$$\text{Under } H_0 : \lim_{n \rightarrow \infty} P(\hat{M}_{l+1,p+1}(h) \geq \hat{m}_{l+1,p+1}(\alpha)) = \alpha,$$

$$\text{Under } H_1 : \lim_{n \rightarrow \infty} P(\hat{M}_{l+1,p+1}(h) \geq \hat{m}_{l+1,p+1}(\alpha)) = 1,$$

where $\hat{m}_{l+1,p+1}(\alpha)$ is the $(1-\alpha)$ -quantile of the distribution $\|N_{d+1}(0, \hat{V}_{l+1,p+1}^*(h))\|_\infty^2$.

Proposition 3.2 establishes the asymptotic validity and consistency of the α -level testing procedure, which rejects H_0 if $\hat{M}_{l+1,p+1}(h)$ exceeds $\hat{m}_{l+1,p+1}(\alpha)$. The critical value $\hat{m}_{l+1,p+1}(\alpha)$ is obtained numerically by generating $(d+1)$ -dimensional standard normal random vectors using Monte Carlo simulation.

Remark 4 (Max test against Bonferroni correction). The Max test is more powerful than the Bonferroni correction. The Bonferroni correction conducts asymptotic t tests separately with an altered size of $\alpha/(d+1)$. The Bonferroni correction rejects H_0 if

$$\hat{M}_{l+1,p+1}(h) \geq z^2(\alpha/2(d+1)),$$

where $z(\alpha/2(d+1))$ is the $\left(1 - \frac{\alpha}{2(d+1)}\right)$ -quantile of $N(0,1)$, suggesting that the same $\hat{M}_{l+1,p+1}(h)$ is used for the Bonferroni correction and Max test. For any correlation matrix V , we obtain

$$P(\|N_{d+1}(0, V)\|_\infty^2 \geq z^2(\alpha/2(d+1))) \leq \alpha.$$

Furthermore, $z^2(\alpha/2(d+1))$ must be greater than $\hat{m}_{l+1,p+1}(\alpha)$ because $\hat{m}_{l+1,p+1}(\alpha)$ is the $(1-\alpha)$ -quantile of distribution $\|N_{d+1}(0, \hat{V}_{l+1,p+1}^*(h))\|_\infty^2$. Therefore, the rejection probability of the Max test is always higher than that of the Bonferroni correction.

¹⁴This construction via simulation is similar to the plug-in sup-t implementation in Montiel Olea and Plagborg-Møller (2019).

Remark 5. In general, neither Max test nor sWald test might not dominate the other in their power properties. On the one hand, the sWald (and Wald) test has the rejection region which is more sensitive to multiple small jumps than that of the Max test. On the other hand, the rejection region of the Max test is more sensitive to a single large jump than that of the sWald test. Since both cases are sensible in assessing the plausibility of the RD design, it may be difficult to conclude which tests are superior. In the simulation in Section 4, we confirmed this feature in the power analysis.

Remark 6. Multiple testing problem for multiple outcomes is also a serious concern. Our *rdtest* package handles a special case of the test for the balance tests only, and the proposed tests are readily applicable to a joint testing for multiple outcomes.

4 Simulation evidences for the unified tests

Given the established theoretical properties of the proposed tests, their performance was evaluated using the Monte Carlo experiment. We conducted 3000 replications to generate a random sample $\{(X_i, Z_{1,i}, \dots, Z_{d,i})' : i = 1, \dots, n\}$ with size $n = \{500, 1000\}$ for each of them.¹⁵

We specify the distribution of running variable X_i as the weighted average of two truncated normal distributions, where $\bar{p} \geq 0.5$ determines the weights. The density of X_i is shown in Figure 3. The density $f(x)$ is continuous at $x = 0$ if and only if $\bar{p} = 0.5$ but jumps at $x = 0$ when $\bar{p} > 0.5$.

¹⁵The detailed simulation data generating process is in Online Appendix C.

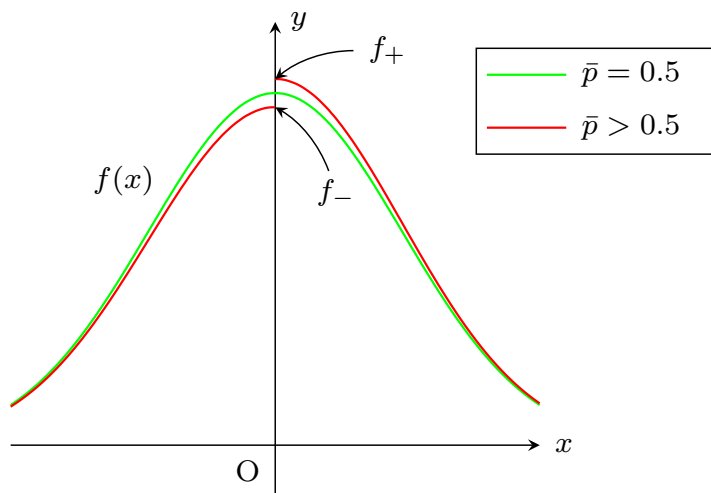


Figure 3: Graph of $f(x)$

For covariates Z_i , we consider two specifications: first, one of the d covariates sees a jump; second, all d covariates see a jump, with each jump size divided by d . For the first specification, we have $\mu_{Z_k}(x) = E[Z_{k,i}|X_i = x], k = 1 \dots, d$ as follows.

$$\mu_{Z_k}(x) = \lambda(x) \text{ for } k = 1, \dots, d-1 \quad \text{and} \quad \mu_{Z_d}(x) = \begin{cases} \lambda(x) & \text{if } x < 0 \\ \lambda(x) + a & \text{if } x \geq 0, \end{cases}$$

where only the d th covariate sees a jump, and the functional form of $\lambda(x)$ is obtained from the simulated data close to the data in Lee (2008) following Calonico et al. (2014), where $a \geq 0$ is the level of discontinuity of $\mu_{Z_d}(x)$ at $x = 0$. For the second specification, we have $\mu_{Z_k}(x) = E[Z_{k,i}|X_i = x], k = 1, \dots, d$ as follows.

$$\mu_{Z_k}(x) = \begin{cases} \lambda(x) & \text{if } x < 0 \\ \lambda(x) + a/d & \text{if } x \geq 0, \end{cases}$$

where a/d denotes the discontinuity level for each $\mu_{Z_k}(x)$ at $x = 0$, For both cases, let $1 > \rho \geq 0$ denote the conditional correlation between $Z_{j,i}$ and $Z_{k,i}$, given $X_i = x$. In this data-generating process, the null hypothesis for the joint manipulation test, $H_0 : (\tau_f, \tau_{Z_1}, \dots, \tau_{Z_d}) = 0$ is true if and only if $\bar{p} = 0.5$ and $a = 0$; $\tau_f > 0$ when $\bar{p} > 0.5$; $\tau_{Z_d} = a > 0$ when $a > 0$.

We conducted the tests with size $\alpha = 0.05$, employing local polynomial estimators $(\hat{\tau}_{Z_1,2}(h_1), \dots, \hat{\tau}_{Z_d,2}(h_d), \hat{\tau}_{f,3}(h_f))$ described in Section 3.1 with $K(u) = (1 - |u|) \vee 0$, where the bandwidths are chosen to be MSE-optimal for $\hat{\tau}_{Z_k,1}(h_k)$ and $\hat{\tau}_{f,2}(h_f)$. The

selection of the kernel function and polynomial order follows Calonico et al. (2014) and Cattaneo et al. (2020).¹⁶ Below, we report the empirical sizes and powers of the conventional and proposed testing methods.

We compared five testing methods: (i) naive testing; (ii) Bonferroni correction of naive testing; (iii) Wald (chi-square) test; (iv) Max test proposed in Section 3.2; (v) sWald test proposed in Section 3.2. Naive testing separately conducts $d + 1$ asymptotic t tests, as described in Calonico et al. (2014) and Cattaneo et al. (2020) with a size α for each of the $d + 1$ restrictions of the null hypothesis, $\tau_f = 0, \tau_{Z_1} = 0, \dots, \tau_{Z_d} = 0$. Naive testing rejects the null hypothesis if at least one test rejects it. The Bonferroni correction conducts asymptotic t tests separately, but the size is changed to $\alpha/(d + 1)$ to restrict type 1 error of the null hypothesis that all $d + 1$ restrictions hold.¹⁷

In Tables 3–5, we compare the empirical size of each test under the null hypothesis (where $\bar{p} = 0.5$ and $a = 0$) with different correlation coefficients $\rho = 0, 0.5, 0.9$. Notably, naive testing suffers from size distortion, and over-rejection worsens when d is large. Similarly, the Wald test without correction suffers from size distortion as d increases. As discussed in Section 3.2, the effective sample size may be too small compared to a large d . When d is large, the covariance matrix increases, and inverse matrix estimation becomes unstable when the effective sample size is limited.

¹⁶As mentioned in the previous sections, the polynomial orders are chosen so that the estimates are bias-corrected for their valid inference. This choice of polynomial order is the default for *rddensity* and available as $\rho = 1$ option for *rdrobust*.

¹⁷We do not benefit from rejecting more than one test for evaluating the underlying identifying restriction. Thus, Holm correction for Bonferroni test does not improve the following results because the probability of rejecting at least one null hypothesis remains the same in two corrections.

Table 3: Empirical size of tests (i)–(v) ($\rho = 0$)

dim	n: 500					n: 1000				
	naive	bonfe	Wald	Max	sWald	naive	bonfe	Wald	Max	sWald
1	0.095	0.050	0.047	0.060	0.051	0.081	0.035	0.039	0.048	0.046
3	0.185	0.056	0.068	0.064	0.049	0.173	0.049	0.054	0.054	0.043
5	0.289	0.070	0.112	0.077	0.055	0.271	0.052	0.073	0.057	0.044
10	0.464	0.086	0.271	0.088	0.055	0.425	0.059	0.132	0.060	0.041
25	0.787	0.114	0.896	0.116	0.034	0.748	0.074	0.517	0.071	0.032

Table 4: Empirical size of tests (i)–(v) ($\rho = 0.5$)

dim	n: 500					n: 1000				
	naive	bonfe	Wald	Max	sWald	naive	bonfe	Wald	Max	sWald
3	0.177	0.053	0.072	0.061	0.060	0.167	0.045	0.054	0.051	0.050
5	0.252	0.058	0.107	0.071	0.060	0.234	0.051	0.072	0.060	0.055
10	0.362	0.076	0.248	0.092	0.068	0.327	0.051	0.119	0.062	0.054
25	0.545	0.076	0.862	0.097	0.060	0.500	0.058	0.468	0.073	0.051

Table 5: Empirical size of tests (i)–(v) ($\rho = 0.9$)

dim	n: 500					n: 1000				
	naive	bonfe	Wald	Max	sWald	naive	bonfe	Wald	Max	sWald
3	0.132	0.042	0.066	0.055	0.060	0.124	0.033	0.051	0.049	0.053
5	0.150	0.036	0.090	0.059	0.048	0.149	0.035	0.068	0.054	0.050
10	0.186	0.037	0.216	0.072	0.070	0.169	0.023	0.104	0.050	0.050
25	0.226	0.024	0.820	0.060	0.056	0.204	0.018	0.406	0.047	0.047

Notes: (i) “naive”: empirical size of naive testing; (ii) “bonfe”: empirical size of Bonferroni correction; (iii) “Max”: empirical size of the Max test; (iv) “Wald”: empirical size of the Wald (chi-square) test; (v) “sWald”: standardized Wald (chi-square) test; “dim”: dimension of the pre-treatment covariates $Z_i = (Z_{1,i}, \dots, Z_{d,i})'$; Columns under “n: 500” and “n: 1000” report the results obtained with size $n = 500$ and $n = 1000$, respectively.

The performances of the other methods vary according to sample size, dimension of covariates, and correlation coefficients. For the relatively small sample size of $n = 500$, the superiority of these methods is ambiguous. For a relatively small number of covariates $dim \in \{1, 3, 5\}$, the sWald test controls for size by 6%, whereas the Max

test and Bonferroni correction control for size by approximately 7%. For a larger number of covariates, the Bonferroni correction and Max test may fail to control size by 10%, whereas the sWald test controls size by 7% throughout. For a larger sample size of $n = 1000$, the sWald test dominates the Bonferroni correction for size control. The sWald test controls size by 5.5% for any correlation and number of covariates up to 25.¹⁸ For a moderate number of covariates up to $dim = 5$ or 10, the Max test can control the size by 6% and is not substantially worse than the Bonferroni correction. Therefore, when the sample size is not small, the sWald test can control the size for any dimension up to $dim = 25$; the Max test and Bonferroni correction can control the size up to $dim = 5$ or 10.

Given the results of size control, we evaluate their empirical power properties. We compare the empirical power of the (ii) Bonferroni correction, (iv) Max test, and (v) sWald test under $\bar{p} = 0.575$ and $\tau_{Z_a}(= a) = 0, 0.5, 1, 1.5, 2$ for different dimensions $d = 1, 3, 5$. Figure 4 presents the results for the scalar covariate. Figures 5, and 6 present the results when one of the d covariates sees a jump. Further, Figures 7 and 8 show the results when all d covariates see a jump. However, each jump size is divided by d for $d = 3, 5$. In Figures 5–8, each figure presents the results for different correlations $\rho = 0.5, 0.9$.¹⁹

In all cases, the Max test exhibits higher power than the Bonferroni correction. When one of the covariates jumps (Figures 5 and 6), the Max test outperforms the Bonferroni correction and sWald test, and the gap among the three methods expands as the correlation and dimension increase. While the sWald test has relatively less power to detect small jumps in the covariate, the power of the sWald test catches up quickly as the jump size increases.

When all covariates have seen jumps (see Figure 7 and 8), the sWald test outperforms the Max test and Bonferroni correction in most cases. When the correlation is weak, the sWald test is substantially superior to the other two methods; however, the Max test approaches the sWald test as the correlation and dimensions increase. In Online Appendix D, we report qualitatively similar simulation results for other specifications, including lower or negative correlation coefficients.

¹⁸We consider that the failure in the Bonferroni correction comes from challenges in evaluating the tail of the nonparametric test statistics.

¹⁹In Online Appendix D, we present the results for weaker correlations and results containing negative correlations.

To summarize, we recommend the Max test when one suspects that a few covariates exhibit jumps but not the others among a moderate number of covariates. We recommend the sWald test for other cases because it has superior size control and power properties for detecting jumps among many covariates.

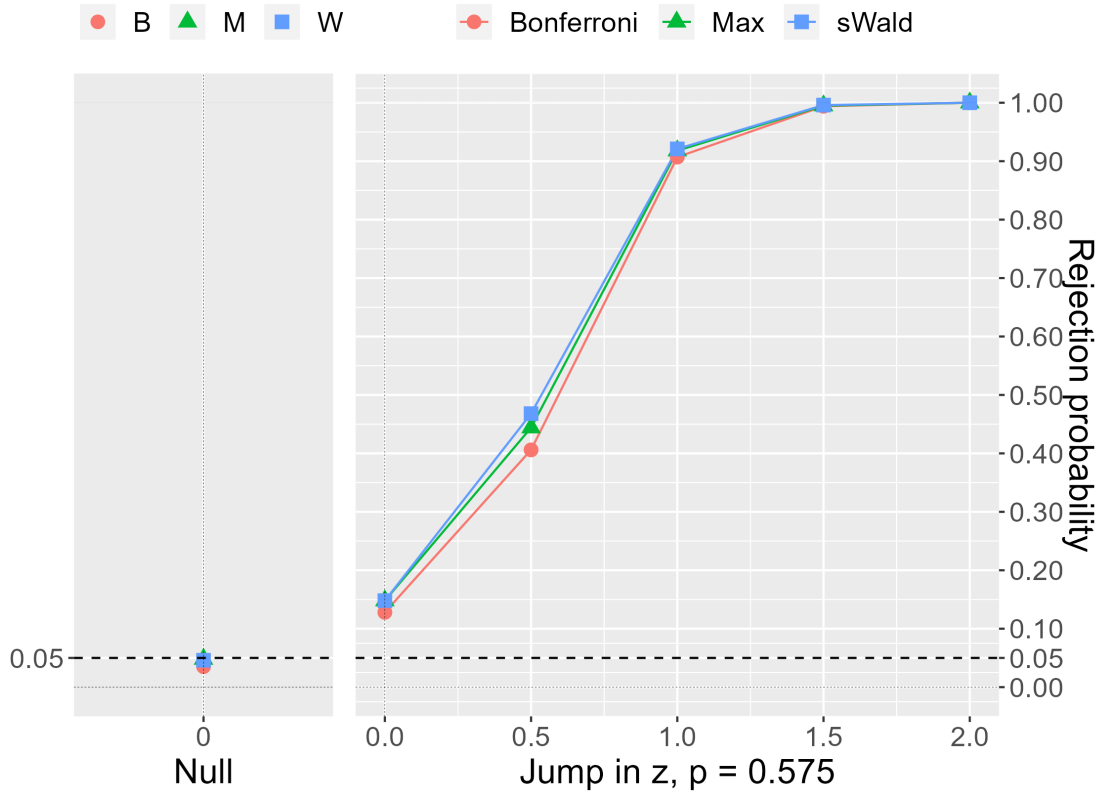
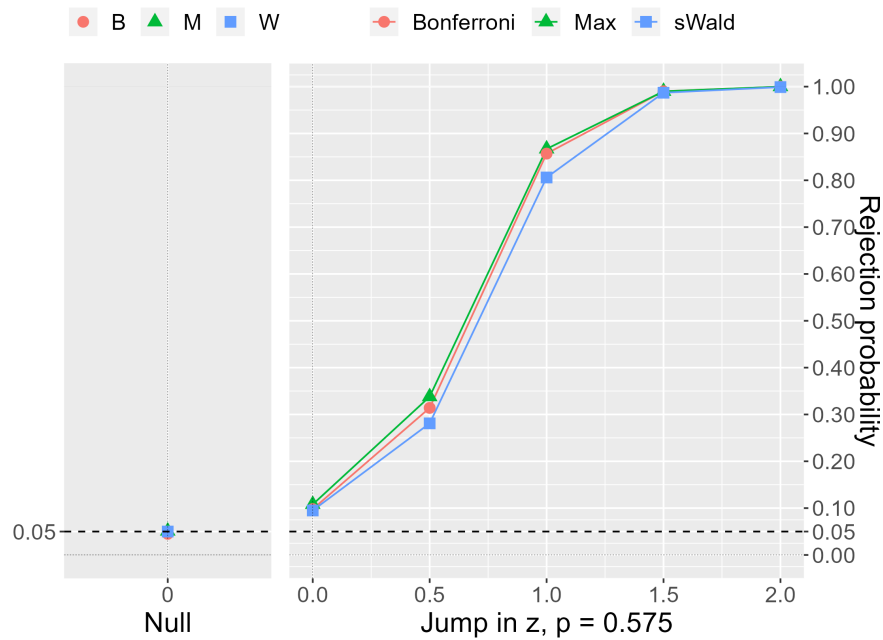
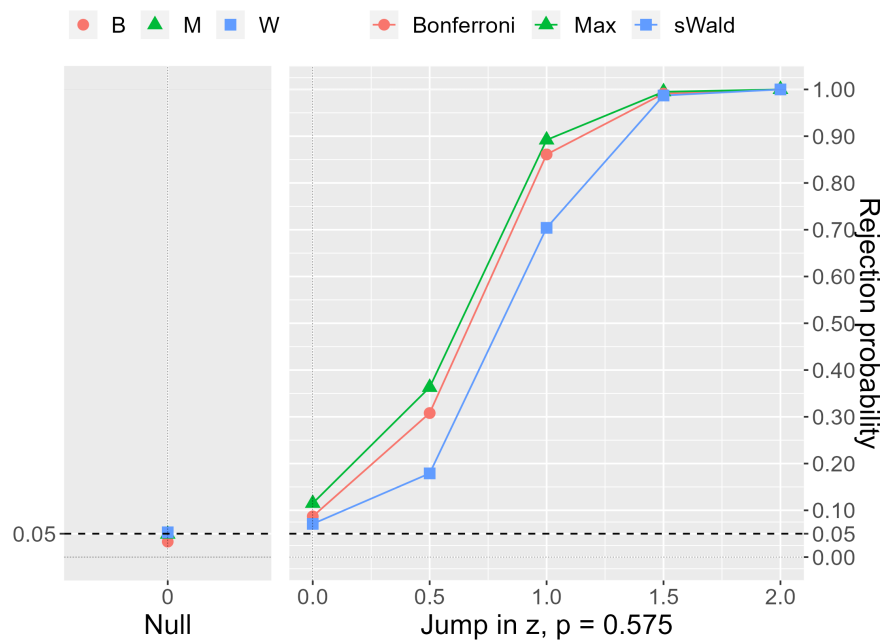


Figure 4: A jump in a scalar Z and a density test, $n = 1000$

Notes: Jump in z is relative to its standard deviation of the error term. The density has the discontinuity with the density ratio of $0.575/0.425 = 1.353$.

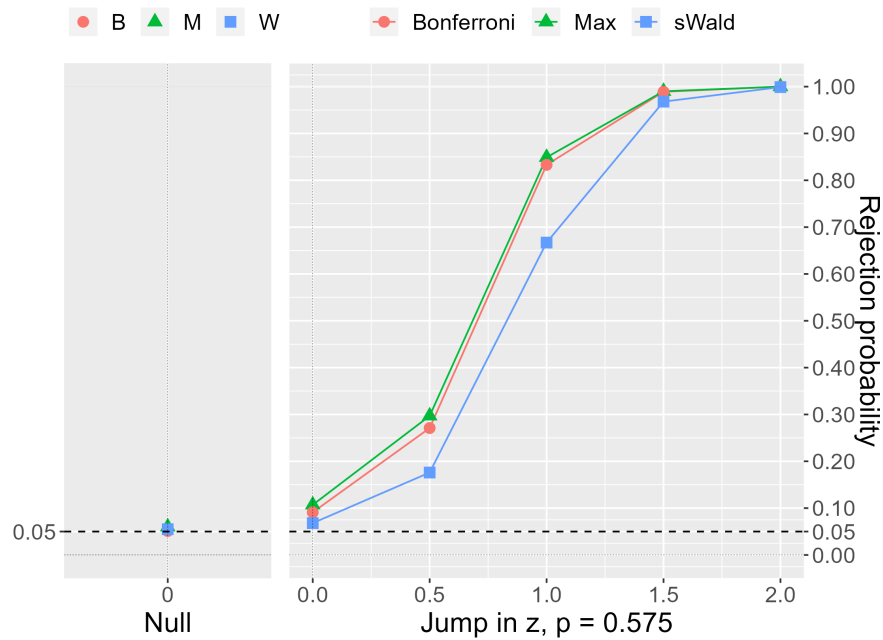


(a) Covariates have the same pairwise correlation coefficient of 0.5

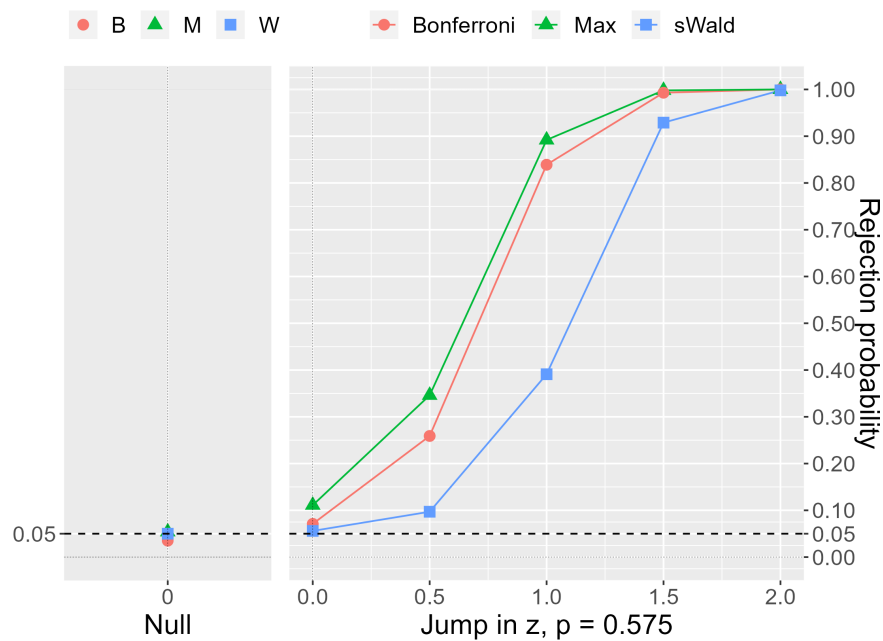


(b) Covariates have the same pairwise correlation coefficient of 0.9

Figure 5: A jump in the three covariates with a density, $n = 1000$
Notes: Jump in z is relative to its standard deviation of the error term. The density has the discontinuity with the density ratio of $0.575/0.425 = 1.353$.



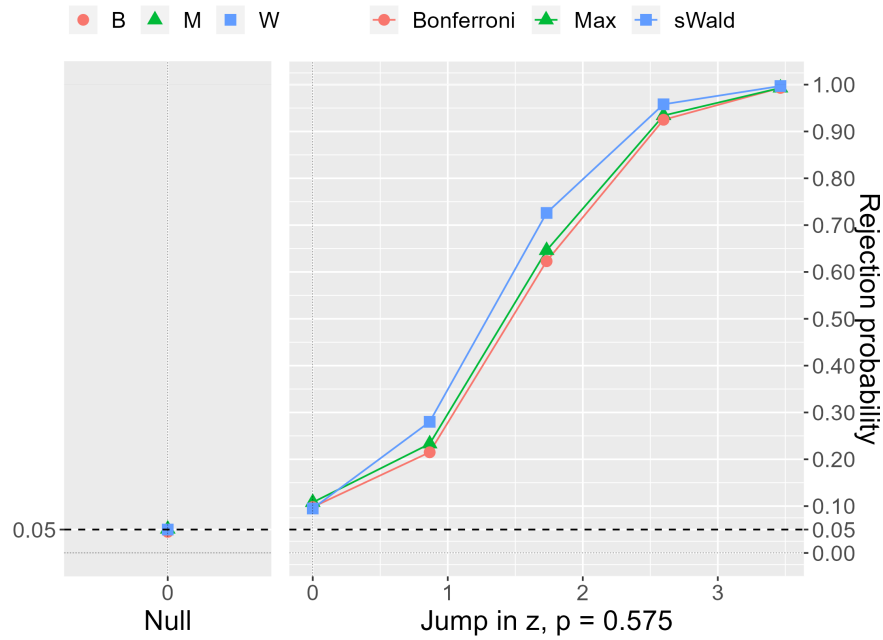
(a) Covariates have the same pairwise correlation coefficient of 0.5



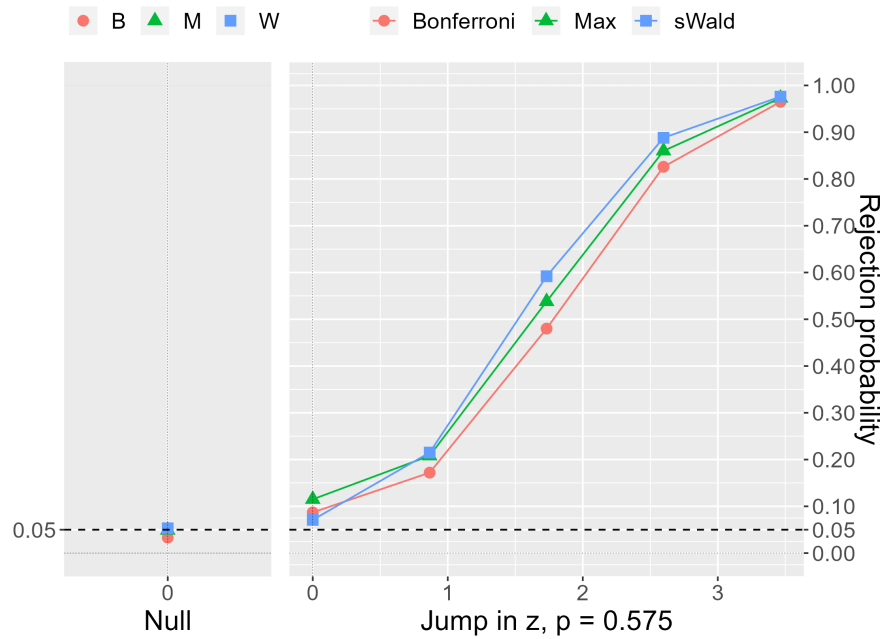
(b) Covariates have the same pairwise correlation coefficient of 0.9

Figure 6: A jump in the five covariates with a density, $n = 1000$

Notes: Jump in z is relative to its standard deviation of the error term. The density has the discontinuity with the density ratio of $0.575/0.425 = 1.353$.

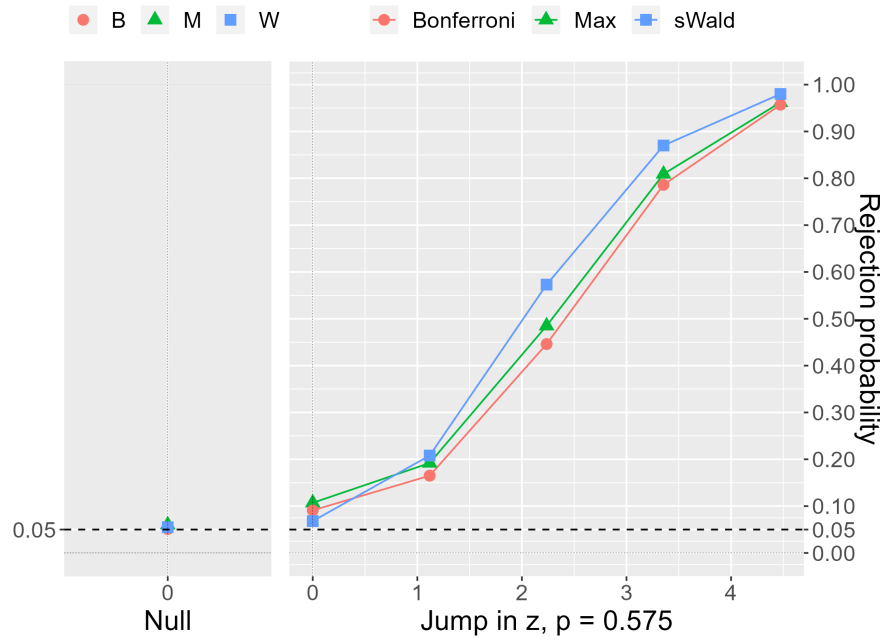


(a) Covariates have the same pairwise correlation coefficient of 0.5

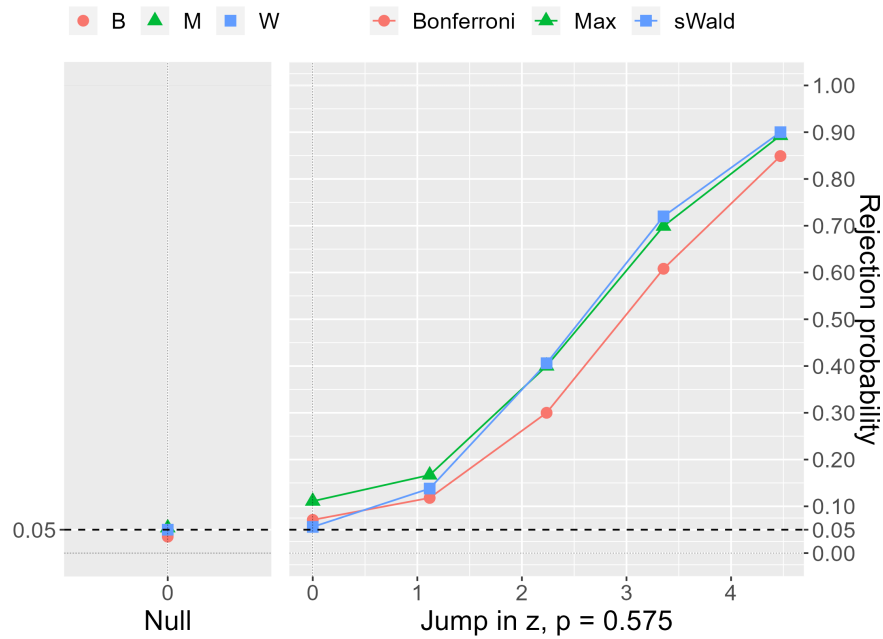


(b) Covariates have the same pairwise correlation coefficient of 0.9

Figure 7: 1/3 of jumps in all the three covariates with density, $n = 1000$
Notes: Jump in z divided by the number of covariates is relative to its standard deviation of the error term. The density has the discontinuity with the density ratio of $0.575/0.425 = 1.353$.



(a) Covariates have the same pairwise correlation coefficient of 0.5



(b) Covariates have the same pairwise correlation coefficient of 0.9

Figure 8: 1/5 of jumps in all the five covariates with density, $n = 1000$
Notes: Jump in z divided by the number of covariates is relative to its standard deviation of the error term. The density has the discontinuity with the density ratio of $0.575/0.425 = 1.353$.

5 Extension

Our unified test solves the over-rejection problem prevalent in empirical studies. Below, we consider two extensions of our analysis to supplement our unified test.

5.1 Equivalence Testing

The diagnostic test evaluates the null hypothesis that suggests the plausibility of the underlying identification. Hence, the diagnostic procedure tests whether the *desired* null hypothesis can be rejected, and we control the probability of falsely rejecting the *desired* null hypothesis of no imbalance or discontinuity. In other words, the roles of type I and type II errors are flipped.

Several studies propose *equivalence* or *non-inferiority* testing as alternatives to flipped testing for the desirable null hypothesis. See, for example, Wellek (2010) and Hartman and Hidalgo (2018) for further details. In RD designs, Hartman (2021) propose equivalence tests for diagnostic testing of each covariate and density. As before, the existing equivalence tests are uni-variate, and a unified alternative is necessary. Hence, we developed a unified equivalent test for multivariate balance tests and a density test in terms of the max test based on Wellek (2010) with a rectangular equivalence domain.

Recall that we want to verify whether the following $d + 1$ restrictions hold simultaneously

$$f_+ = f_-, \quad \mu_{Z_1+} = \mu_{Z_1-}, \quad \dots, \quad \mu_{Z_d+} = \mu_{Z_d-}.$$

An appropriate set of hypotheses for the equivalence test is as follows:

$$\begin{aligned} H_0 : \min\{\tau_f, \tau_{Z_1}, \dots, \tau_{Z_d}\} \leq -\varepsilon \quad \text{or} \quad \max\{\tau_f, \tau_{Z_1}, \dots, \tau_{Z_d}\} \geq \varepsilon \\ \text{vs } H_1 : -\varepsilon < \tau_f < \varepsilon \quad \text{and} \quad -\varepsilon < \tau_{Z_k} < \varepsilon \quad \text{for all } k = 1, \dots, d, \end{aligned} \quad (5.1)$$

where $\varepsilon > 0$ determines the range within which the imbalance or discontinuity is sufficiently small.

To conduct an equivalence test, the researcher must select an appropriate equivalence range $(-\varepsilon, \varepsilon)$. We follow Hartman and Hidalgo (2018) and Hartman (2021) to focus on the equivalence confidence interval, which is the shortest equivalence range $(-\varepsilon, \varepsilon)$ such that the alternative hypothesis with the equivalence range would not be detected at the prespecified level α for the observed data. Hence, we achieve an equivalence confidence interval without manually selecting ε .

Denote

$$\begin{aligned} & \hat{\psi}_{1,l,p}(h) \\ &= \max \left\{ \frac{\sqrt{n}\sqrt{h_f}(\hat{\tau}_{f,p}(h_f) - \varepsilon)}{\hat{V}_{f,p}(h_f)}, \frac{\sqrt{n}\sqrt{h_1}(\hat{\tau}_{Z_1,l}(h_1) - \varepsilon)}{\hat{V}_{Z_1,l}(h_1)}, \dots, \frac{\sqrt{n}\sqrt{h_d}(\hat{\tau}_{Z_d,l}(h_d) - \varepsilon)}{\hat{V}_{Z_d,l}(h_d)} \right\} \end{aligned}$$

and

$$\begin{aligned} & \hat{\psi}_{2,l,p}(h) \\ &= \min \left\{ \frac{\sqrt{n}\sqrt{h_f}(\hat{\tau}_{f,p}(h_f) + \varepsilon)}{\hat{V}_{f,p}(h_f)}, \frac{\sqrt{n}\sqrt{h_1}(\hat{\tau}_{Z_1,l}(h_1) + \varepsilon)}{\hat{V}_{Z_1,l}(h_1)}, \dots, \frac{\sqrt{n}\sqrt{h_d}(\hat{\tau}_{Z_d,l}(h_d) + \varepsilon)}{\hat{V}_{Z_d,l}(h_d)} \right\}. \end{aligned}$$

The following proposition demonstrates the asymptotic validity of the proposed equivalence test for a prespecified level α .

Proposition 5.1. *Suppose Assumptions 1 and 2 hold with $R \geq p + 2$ and $S \geq l + 3$, and the asymptotic covariance matrix $V_{l+1,p+1}$ is nonsingular. If $nh_{\min} \rightarrow \infty$, $nh_f^2 \rightarrow \infty$, $n(h_{\max})^{2l+5} \rightarrow 0$ and $n(h_f)^{2p+3} \rightarrow 0$,*

$$\text{Under } H_0 : \limsup_{n \rightarrow \infty} P \left(\hat{\psi}_{1,l+1,p+1}(h) \leq z_{\alpha/2} \text{ or } \hat{\psi}_{2,l+1,p+1}(h) \geq z_{1-\alpha/2} \right) \leq \alpha,$$

$$\text{Under } H_1 : \lim_{n \rightarrow \infty} P \left(\hat{\psi}_{1,l+1,p+1}(h) \leq z_{\alpha/2} \text{ or } \hat{\psi}_{2,l+1,p+1}(h) \geq z_{1-\alpha/2} \right) = 1,$$

where $z_{\alpha/2}$ and $z_{1-\alpha/2}$ are the $\alpha/2$ and $(1 - \alpha/2)$ quantiles of $N(0, 1)$, respectively.

5.2 Pretesting Analysis

Following Roth (2022), we analyze the bias of the treatment effect estimator induced by conducting a pretest. Let $\hat{\tau}_Y, \hat{\tau}_Z, \hat{\tau}_f$ be the local polynomial estimators of $\lim_{x \rightarrow 0^+} E[Y_i | X_i = x] - \lim_{x \rightarrow 0^-} E[Y_i | X_i = x]$, $(\mu_{Z_1+} - \mu_{Z_1-}, \dots, \mu_{Z_d+} - \mu_{Z_d-})'$, $f_+ - f_-$, respectively.²⁰ For simplicity, suppose that $d = 1$ and $(\hat{\tau}_Y, \hat{\tau}_Z, \hat{\tau}_f)'$ is multivariate normally distributed; that is,

$$\begin{pmatrix} \hat{\tau}_Y \\ \hat{\tau}_Z \\ \hat{\tau}_f \end{pmatrix} \sim N \left(\begin{pmatrix} \tau_Y \\ 0 \\ 0 \end{pmatrix} + \begin{pmatrix} \delta_Y \\ \delta_Z \\ \delta_f \end{pmatrix}, \begin{pmatrix} \sigma_{YY} & \sigma_{YZ} & 0 \\ \sigma_{YZ} & \sigma_{ZZ} & 0 \\ 0 & 0 & \sigma_{ff} \end{pmatrix} \right),$$

where τ_f is the treatment effect and $\delta = (\delta_Y, \delta_Z, \delta_f)'$ is the unconditional bias from the imbalance at the cutoff. Because Theorem 3.1 implies that the asymptotic covariance

²⁰To apply Theorem 3.1, we use the bias-corrected estimators as $\hat{\tau}_Y, \hat{\tau}_Z, \hat{\tau}_f$.

between $(\hat{\tau}_Y, \hat{\tau}_Z)'$ and $\hat{\tau}_f$ is zero, we assume that $\hat{\tau}_f$ is independent of $\hat{\tau}_Y$ and $\hat{\tau}_Z$.

Let $\mathcal{T}(\Sigma) \subset \mathbb{R}^2$ be the acceptance region, which potentially depends on the covariance matrix $\Sigma = (\sigma_{ZZ}, \sigma_{ff})$. From Proposition 1 in Roth (2022), the expectation of $\hat{\tau}_Y$ conditional on passing the pretest can be written as

$$E[\hat{\tau}_Y | (\hat{\tau}_Z, \hat{\tau}_f)' \in \mathcal{T}(\Sigma)] = \tau_Y + \delta_Y + \frac{\sigma_{YZ}}{\sigma_{ZZ}} \{E[\hat{\tau}_Z | (\hat{\tau}_Z, \hat{\tau}_f)' \in \mathcal{T}(\Sigma)] - \delta_Z\}. \quad (5.2)$$

Equation (5.2) implies that the expectation of $\hat{\tau}_Y$ conditional on passing the pretest is the sum of the treatment effect τ_Y , the unconditional bias δ_Y , and the pretest bias $\frac{\sigma_{YZ}}{\sigma_{ZZ}} \{E[\hat{\tau}_Z | (\hat{\tau}_Z, \hat{\tau}_f)' \in \mathcal{T}(\Sigma)] - \delta_Z\}$. When considering the max test, the acceptance region can be written as

$$\mathcal{T}(\Sigma) = \{(t_Z, t_f)' \in \mathbb{R}^2 : |t_Z| \leq c_Z \text{ and } |t_f| \leq c_f\},$$

where c_Z and c_f are positive constants that depend on Σ . Because $\hat{\tau}_f$ is independent of $\hat{\tau}_Z$, (5.2) becomes

$$E[\hat{\tau}_Y | (\hat{\tau}_Z, \hat{\tau}_f)' \in \mathcal{T}(\Sigma)] = \tau_Y + \delta_Y + \frac{\sigma_{YZ}}{\sigma_{ZZ}} \{E[\hat{\tau}_Z - c_Z \leq \hat{\tau}_Z \leq c_Z] - \delta_Z\}. \quad (5.3)$$

Hence, when we use the Max test as the pretest, the density test statistic $\hat{\tau}_f$ does not affect the pretest bias, which disappears if $\delta_Z = 0$.

To discuss the sign of the pretest bias, we consider the following model:

$$Y_i = \tau_Y 1\{X_i \geq 0\} + \mu_Y(X_i) + \beta Z_i + \epsilon_i,$$

where μ_Y is a continuous function, and ϵ_i is an error term satisfying $E[\epsilon_i | X_i, Z_i] = 0$. Then, we have

$$\lim_{x \rightarrow 0^+} E[Y_i | X_i = x] - \lim_{x \rightarrow 0^-} E[Y_i | X_i = x] = \tau_Y + \beta \delta_Z,$$

where we use $\lim_{x \rightarrow 0^+} E[Z_i | X_i = x] - \lim_{x \rightarrow 0^-} E[Z_i | X_i = x] = \delta_Z$. This implies that the unconditional bias becomes $\delta_Y = \beta \delta_Z$. Hence, if $\beta > 0$ and $\sigma_{YZ} > 0$, then the sign of the pretest bias is opposite to that of the unconditional bias δ_Y . Therefore, in this case, the pretest can reduce bias. In Online Appendix E, we conduct a numerical analysis using simulated and calibrated datasets. The numerical results also support our theoretical analysis that pretesting may reduce bias.

An analogous analysis for the variance implies that the variance of the treatment effect estimate is likely to be smaller after pretesting. Similar to Proposition 3 of Roth

(2022), we obtain

$$V[\hat{\tau}_Y | (\hat{\tau}_Z, \hat{\tau}_f)' \in \mathcal{T}(\Sigma)] = \sigma_{YY} + \left(\frac{\sigma_{YZ}}{\sigma_{ZZ}}\right)^2 \{V[\hat{\tau}_Z | (\hat{\tau}_Z, \hat{\tau}_f)' \in \mathcal{T}(\Sigma)] - \sigma_{ZZ}\}. \quad (5.4)$$

If the max test is conducted, the acceptance region is convex. Hence, Proposition 4 in Roth (2022) implies that

$$V[\hat{\tau}_Z | (\hat{\tau}_Z, \hat{\tau}_f)' \in \mathcal{T}(\Sigma)] - \sigma_{ZZ} \leq 0.$$

Hence, the variance is likely to be smaller after pretesting.²¹

6 Conclusion

Diagnostic tests are vital for applied studies of RD designs; however, their inappropriate use frustrates their purpose. The diagnostic procedure for RD design aims to test the underlying null hypothesis that all pre-determined covariates balance and the density function is continuous. Current practices test these restrictions separately without appropriate size control—they over-reject the null hypothesis that the identifying restriction for the RD design is plausible.

We demonstrate an extraordinary over-rejection of the null hypothesis, where each testable restriction is valid. Among the 59 studies published in the top five economics journals, 32% (19 studies) rejected at least one testable restriction. Nevertheless, less than 5% of the 787 tests were rejected. Hence, we conclude that the plausibility of identification is highly over-rejected where the underlying null hypotheses appear to hold. We blame the multiple testing problem for the over-rejection because most studies run more than 10 covariates balance tests separately.

We provide a solution to this over-rejection problem. We demonstrate the joint asymptotic normality of RD design estimators and provide alternative unified testing procedures. We show two different unified tests: the standardized Wald (sWald) test and the Max test. In the numerical simulations, the sWald and Max statistics achieved appropriate size-control properties for a moderate number of covariates when

²¹The above analysis indicates that pretesting can reduce the bias and variance of the treatment effect estimates. Its implication for the power of the test for the treatment effect is indefinite. For example, pretesting reduces the variance of estimator when the bias is zero $\delta_Y = \delta_Z = 0$. The smaller variance may increase the power when τ_Y is away from 0 and decrease the power when τ_Y is close to 0.

the sample size was 1000. The sWald test is particularly superior to other methods in size control, as it can control for any dimension of covariates up to 25 where the Bonferroni correction may fail to control the size. The power properties vary according to the underlying alternative hypotheses. The Max test is superior to the Bonferroni correction when only one covariate exhibits a jump in the conditional mean. The sWald test is superior to the Bonferroni correction when all the covariates jump in their conditional means.

In conclusion, we recommend the Max test for a design with a moderate number of covariates when only a few covariates which critically matter for the plausibility of identification such as placebo outcomes. We recommend the sWald test for other designs. This test is appropriate for most practical designs where there is no ex-ante concern regarding covariate and testing many covariate balancing is the norm.

Our unified test provides a formal judgment for whether the rejected diagnostic tests were spurious and by luck or not. In RD designs, rejections in the diagnostic tests can be genuine signals for their designs being implausible while they may be spurious. Hence, our procedure offers a transparent decision rule that is essential to the users if the diagnostic tests are part of the assessment in RD designs.

Furthermore, our procedure is complementary with the other current practices. For example, practitioners often conduct an additional inspection for a covariate with an apparent graphical evidence for a jump. We continue to recommend graphical analyses and those careful inspections because such procedure is complementary with our unified tests. With our unified test, practitioners may have stronger argument for a plausible design in the following combination of arguments: our unified test suggests that the rejections were spurious; furthermore, other anecdotes conclude that the spurious rejections were immaterial to the plausibility of the design. Hence, our procedure shall be an essential support for effectively justifying designs with a few rejected diagnostic tests when the underlying design is genuinely valid.

Based on our findings, we consider several topics for future research. First, finding another use for testable restrictions may be preferable. To validate the plausibility of identification, we must focus on the underlying null hypothesis rather than detecting which restrictions fail. Nevertheless, if we detect a particular subgroup of covariates that threatens the plausibility of identification, such a finding may provide valuable information. Diagnostic procedures using such information may improve design validation. Second, although we focused on the statistical inference of testable

restrictions, a graphical analysis of testable restrictions is also important. Recent studies, such as Calonico, Cattaneo, and Titiunik (2015), have considered the optimal procedure for visualization, and Korting, Lieberman, Matsudaira, Pei, and Shen (2023) have demonstrated that tuning parameters in visualization is critical. We recommend our unified testing along with graphical analysis, with multiple testing problems in graphical analyses as a future research topic. Finally, evaluating the joint distribution of testing statistics that are nonparametric estimates is challenging. We will consider these issues as future research questions.

Acknowledgements

The study was supported by JSPS KAKENHI Grant Numbers JP20J20046, JP23K18799 (Fusejima), JP22K13373 (Ishihara), and JP21K13269 (Sawada). This study is derived from a chapter of Koki Fusejima’s dissertation. We thank Eiji Kurozumi, Yukitoshi Matsushita, Katsumi Shimotsu, and Kohei Yata, the anonymous referees and associate editor as well as seminar participants at Hitotsubashi University, The University of Tokyo, Kansai Keiryō Keizaigaku Kenkyukai, Japanese Joint Statistical Meeting, International Conference on Econometrics and Statistics, and the Asian Meeting of the Econometric Society in East and South-East Asia. Moreover, we thank Masaki Oguni and Yuri Sugiyama for their excellent research assistance.

A Formal results

Appendix A provides formal theoretical results and proofs.

A.1 Setup and Notation

Let $|\cdot|$ denote the Euclidean matrix norm, that is, $|A|^2 = \text{trace}(A'A) = \sum_{j=1}^n \sum_{i=1}^m a_{ij}^2$ for $(m \times n)$ matrix $A = \{a_{ij}\}_{i=1, \dots, m}^{j=1, \dots, n}$, and $|a|^4 = |aa'|^2 = \sum_{j=1}^n \sum_{i=1}^n a_i^2 a_j^2$ for $(n \times 1)$ vector $a = (a_1, \dots, a_n)'$. Let $a_n \lesssim b_n$ denote $a_n \leq Cb_n$ for a positive constant C , which is independent of n .

The estimands of the local polynomial estimators are

$$\beta_{Z_k+,l} = \left[\mu_{Z_k+}, \frac{\mu_{Z_k+}^{(1)}}{1!}, \dots, \frac{\mu_{Z_k+}^{(l)}}{l!} \right]', \quad \beta_{Z_k-,l} = \left[\mu_{Z_k-}, \frac{\mu_{Z_k-}^{(1)}}{1!}, \dots, \frac{\mu_{Z_k-}^{(l)}}{l!} \right]',$$

$$\beta_{f_{+,p}} = \left[F_+, \frac{f_+}{1!}, \frac{f_+^{(1)}}{2!}, \dots, \frac{f_+^{(p-1)}}{p!} \right]', \quad \beta_{f_{-,p}} = \left[F_-, \frac{f_-}{1!}, \frac{f_-^{(1)}}{2!}, \dots, \frac{f_-^{(p-1)}}{p!} \right]',$$

where $F(x) = E[1\{X \leq x\}]$, $F_+ = \lim_{x \rightarrow 0^+} F(x)$, $F_- = \lim_{x \rightarrow 0^-} F(x)$.

We set $Z_k = (Z_{k,1}, \dots, Z_{k,n})'$, $\tilde{F} = (\tilde{F}(X_1), \dots, \tilde{F}(X_n))'$, $K_h(u) = K(u/h)/h$, $H_p(h) = \text{diag}(1, h, \dots, h^p)$, $X_p(h) = [r_p(X_1/h), \dots, r_p(X_n/h)]'$,

$$W_+(h) = \text{diag}(1\{X_1 \geq 0\}K_h(X_1), \dots, 1\{X_n \geq 0\}K_h(X_n)),$$

$$W_-(h) = \text{diag}(1\{X_1 < 0\}K_h(X_1), \dots, 1\{X_n < 0\}K_h(X_n)),$$

$$\Gamma_{+,p}(h) = \frac{1}{n} X_p(h)' W_+(h) X_p(h), \quad \Gamma_{-,p}(h) = \frac{1}{n} X_p(h)' W_-(h) X_p(h),$$

The local polynomial estimators are as follows.

$$\hat{\beta}_{Z_{k+,l}}(h_k) = \frac{1}{n} H_l^{-1}(h_k) \Gamma_{+,l}^{-1}(h_k) X_l(h_k)' W_+(h_k) Z_k,$$

$$\hat{\beta}_{Z_{k-,l}}(h_k) = \frac{1}{n} H_l^{-1}(h_k) \Gamma_{-,l}^{-1}(h_k) X_l(h_k)' W_-(h_k) Z_k,$$

and

$$\hat{\beta}_{f_{+,p}}(h_f) = \frac{1}{n} H_p^{-1}(h_f) \Gamma_{+,p}^{-1}(h_f) X_p(h_f)' W_+(h_f) \tilde{F},$$

$$\hat{\beta}_{f_{-,p}}(h_f) = \frac{1}{n} H_p^{-1}(h_f) \Gamma_{-,p}^{-1}(h_f) X_p(h_f)' W_-(h_f) \tilde{F}.$$

Let

$$\Delta \hat{\mu}_{Z_{k+,l}}(h_k) \equiv \sqrt{nh_k} [\hat{\mu}_{Z_{k+,l}}(h_k) - \mu_{Z_{k+}}], \quad \Delta \hat{\mu}_{Z_{k-,l}}(h_k) \equiv \sqrt{nh_k} [\hat{\mu}_{Z_{k-,l}}(h_k) - \mu_{Z_{k-}}],$$

$$\Delta \hat{f}_{+,p}(h_f) \equiv \sqrt{nh_f} [\hat{f}_{+,p}(h_f) - f_+], \quad \Delta \hat{f}_{-,p}(h_f) \equiv \sqrt{nh_f} [\hat{f}_{-,p}(h_f) - f_-].$$

Letting $\mathcal{X}_n = (X_1, \dots, X_n)'$, we decompose $\Delta \hat{\mu}_{Z_{k+,l}}(h_k)$ and $\Delta \hat{\mu}_{Z_{k-,l}}(h_k)$ as

$$\Delta \hat{\mu}_{Z_{k+,l}}(h_k) = \Delta^M \hat{\mu}_{Z_{k+,l}}(h_k) + \Delta^B \hat{\mu}_{Z_{k+,l}}(h_k),$$

$$\Delta \hat{\mu}_{Z_{k-,l}}(h_k) = \Delta^M \hat{\mu}_{Z_{k-,l}}(h_k) + \Delta^B \hat{\mu}_{Z_{k-,l}}(h_k),$$

where

$$\Delta^M \hat{\mu}_{Z_{k+,l}}(h_k) \equiv \sqrt{nh_k} \{ \hat{\mu}_{Z_{k+,l}}(h_k) - E[\hat{\mu}_{Z_{k+,l}}(h_k) | \mathcal{X}_n] \},$$

$$\Delta^M \hat{\mu}_{Z_{k-,l}}(h_k) \equiv \sqrt{nh_k} \{ \hat{\mu}_{Z_{k-,l}}(h_k) - E[\hat{\mu}_{Z_{k-,l}}(h_k) | \mathcal{X}_n] \}$$

and

$$\Delta^B \hat{\mu}_{Z_{k+,l}}(h_k) \equiv \sqrt{nh_k} \{ E[\hat{\mu}_{Z_{k+,l}}(h_k) | \mathcal{X}_n] - \mu_{Z_{k+}} \},$$

$$\Delta^B \hat{\mu}_{Z_{k-,l}}(h_k) \equiv \sqrt{nh_k} \{ E[\hat{\mu}_{Z_{k-,l}}(h_k) | \mathcal{X}_n] - \mu_{Z_{k-}} \}.$$

$\Delta^B \hat{\mu}_{Z_k+,l}(h_k)$ and $\Delta^B \hat{\mu}_{Z_k-,l}(h_k)$ represent the smoothing bias. We consider the distributional approximations of $\Delta^M \hat{\mu}_{Z_k+,l}(h_k)$ and $\Delta^M \hat{\mu}_{Z_k-,l}(h_k)$.

We define $\tilde{f}_{+,p}(h_f)$ and $\tilde{f}_{-,p}(h_f)$ as slope coefficients in the following local polynomial regressions.

$$\tilde{f}_{+,p}(h_f) = e'_1 \tilde{\beta}_{f+,p}(h_f), \quad \tilde{f}_{-,p}(h_f) = e'_1 \tilde{\beta}_{f-,p}(h_f),$$

where

$$\begin{aligned} \tilde{\beta}_{f+,p}(h_f) &= \arg \min_{\beta \in \mathbb{R}^{p+1}} \sum_{i=1}^n 1\{X_i \geq 0\} (F(X_i) - r_p(X_i)' \beta)^2 K_{h_f}(X_i), \\ \tilde{\beta}_{f-,p}(h_f) &= \arg \min_{\beta \in \mathbb{R}^{p+1}} \sum_{i=1}^n 1\{X_i < 0\} (F(X_i) - r_p(X_i)' \beta)^2 K_{h_f}(X_i). \end{aligned}$$

$\tilde{f}_{+,p}(h_f)$ and $\tilde{f}_{-,p}(h_f)$ are obtained from p th-order local polynomial one-sided approximations of the true distribution of X_i . We decompose $\Delta \hat{f}_{+,p}(h_f)$ and $\Delta \hat{f}_{-,p}(h_f)$ as

$$\Delta \hat{f}_{+,p}(h_f) = \Delta^{M_0} \hat{f}_{+,p}(h_f) + \Delta^{B_0} \hat{f}_{+,p}(h_f), \quad \Delta \hat{f}_{-,p}(h_f) = \Delta^{M_0} \hat{f}_{-,p}(h_f) + \Delta^{B_0} \hat{f}_{-,p}(h_f),$$

where

$$\begin{aligned} \Delta^{M_0} \hat{f}_{+,p}(h_f) &\equiv \sqrt{nh_f} \{ \hat{f}_{+,p}(h_f) - \tilde{f}_{+,p}(h_f) \}, \\ \Delta^{M_0} \hat{f}_{-,p}(h_f) &\equiv \sqrt{nh_f} \{ \hat{f}_{-,p}(h_f) - \tilde{f}_{-,p}(h_f) \} \end{aligned}$$

and

$$\Delta^{B_0} \hat{f}_{+,p}(h_f) \equiv \sqrt{nh_f} \{ \tilde{f}_{+,p}(h_f) - f_+ \}, \quad \Delta^{B_0} \hat{f}_{-,p}(h_f) \equiv \sqrt{nh_f} \{ \tilde{f}_{-,p}(h_f) - f_- \}.$$

$\Delta^{B_0} \hat{f}_{+,p}(h_f)$ and $\Delta^{B_0} \hat{f}_{-,p}(h_f)$ represent smoothing bias. We set

$F = (F(X_1), \dots, F(X_n))'$, $\iota = (1, \dots, 1)'$, which are n -dimensional.

$$U_{+,p}(h_f) \equiv \frac{1}{n(n-1)} \sum_{i,j:i \neq j}^n \psi_{+,p,h_f}(X_i, X_j),$$

$$U_{-,p}(h_f) \equiv \frac{1}{n(n-1)} \sum_{i,j:i \neq j}^n \psi_{-,p,h_f}(X_i, X_j),$$

where

$$\psi_{+,p,h_f}(X_i, X_j) \equiv 1\{X_i \geq 0\} r_p(X_i/h_f) (1\{X_j \leq X_i\} - F(X_i)) K_{h_f}(X_i),$$

$$\psi_{-,p,h_f}(X_i, X_j) \equiv 1\{X_i < 0\} r_p(X_i/h_f) (1\{X_j \leq X_i\} - F(X_i)) K_{h_f}(X_i).$$

We further decompose $\Delta^{M_0} \hat{f}_{+,p}(h_f)$ and $\Delta^{M_0} \hat{f}_{-,p}(h_f)$ as follows.

$$\begin{aligned}\Delta^{M_0} \hat{f}_{+,p}(h_f) &= \Delta^{M_1} \hat{f}_{+,p}(h_f) + \Delta^{B_1} \hat{f}_{+,p}(h_f), \\ \Delta^{M_0} \hat{f}_{-,p}(h_f) &= \Delta^{M_1} \hat{f}_{-,p}(h_f) + \Delta^{B_1} \hat{f}_{-,p}(h_f),\end{aligned}$$

where

$$\begin{aligned}\Delta^{M_1} \hat{f}_{+,p}(h_f) &\equiv \left(1 - \frac{1}{n}\right) \sqrt{\frac{n}{h_f}} e_1' \Gamma_{+,p}^{-1}(h_f) U_{+,p}(h_f), \\ \Delta^{M_1} \hat{f}_{-,p}(h_f) &\equiv \left(1 - \frac{1}{n}\right) \sqrt{\frac{n}{h_f}} e_1' \Gamma_{-,p}^{-1}(h_f) U_{-,p}(h_f),\end{aligned}$$

and

$$\begin{aligned}\Delta^{B_1} \hat{f}_{+,p}(h_f) &\equiv \frac{1}{\sqrt{nh_f}} \frac{1}{n} e_1' \Gamma_{+,p}^{-1}(h_f) X_p(h_f)' W_+(h_f) (\iota - F), \\ \Delta^{B_1} \hat{f}_{-,p}(h_f) &\equiv \frac{1}{\sqrt{nh_f}} \frac{1}{n} e_1' \Gamma_{-,p}^{-1}(h_f) X_p(h_f)' W_-(h_f) (\iota - F).\end{aligned}$$

$U_{+,p}(h_f)$ and $U_{-,p}(h_f)$ are considered second-order U-statistics (where the kernels $\psi_{+,p,h_f}(X_i, X_j)$ and $\psi_{-,p,h_f}(X_i, X_j)$ are $(p+1)$ -dimensional and depend on the bandwidth h_f), and $\Delta^{B_1} \hat{f}_{+,p}(h_f)$ and $\Delta^{B_1} \hat{f}_{-,p}(h_f)$ represent the leave-in bias. These terms arise because the empirical distribution function $\tilde{F}(X_i)$ is approximated, which leads to double summation. Note that $E[\psi_{+,p,h_f}(X_i, X_j)] = 0$ and $E[\psi_{-,p,h_f}(X_i, X_j)] = 0$. U-statistics can be decomposed as

$$U_{+,p}(h_f) = U_{1,+,p}(h_f) + U_{2,+,p}(h_f), \quad U_{-,p}(h_f) = U_{1,-,p}(h_f) + U_{2,-,p}(h_f)$$

with

$$U_{1,+,p}(h_f) \equiv \frac{1}{n} \sum_{i=1}^n E[\psi_{+,p,h_f}(X_j, X_i) | X_i], \quad U_{1,-,p}(h_f) \equiv \frac{1}{n} \sum_{i=1}^n E[\psi_{-,p,h_f}(X_j, X_i) | X_i]$$

for $j \neq i$ and

$$\begin{aligned}U_{2,+,p}(h_f) &\equiv \frac{1}{n(n-1)} \sum_{i,j:i \neq j}^n \varphi_{+,p,h_f}(X_i, X_j), \\ U_{2,-,p}(h_f) &\equiv \frac{1}{n(n-1)} \sum_{i,j:i \neq j}^n \varphi_{-,p,h_f}(X_i, X_j),\end{aligned}$$

where

$$\begin{aligned}\varphi_{+,p,h_f}(X_i, X_j) &\equiv \psi_{+,p,h_f}(X_i, X_j) + \psi_{+,p,h_f}(X_j, X_i) \\ &\quad - E[\psi_{+,p,h_f}(X_i, X_j) | X_j] - E[\psi_{+,p,h_f}(X_j, X_i) | X_i],\end{aligned}$$

$$\begin{aligned}\varphi_{-,p,h_f}(X_i, X_j) &\equiv \psi_{-,p,h_f}(X_i, X_j) + \psi_{-,p,h_f}(X_j, X_i) \\ &\quad - E[\psi_{-,p,h_f}(X_i, X_j)|X_j] - E[\psi_{-,p,h_f}(X_j, X_i)|X_i].\end{aligned}$$

This decomposition is often referred to as the Hoeffding decomposition (see, e.g., Serfling (1980)). $U_{2,+p}(h_f)$ and $U_{2,-p}(h_f)$ are degenerate U-statistics that are later shown to be asymptotically negligible under our assumptions. Let

$$\begin{aligned}\Delta^{B_2} \hat{f}_{+,p}(h_f) &\equiv \sqrt{\frac{n}{h_f}} e'_1 \Gamma_{+,p}^{-1}(h_f) U_{2,+p}(h_f), \\ \Delta^{B_2} \hat{f}_{-,p}(h_f) &\equiv \sqrt{\frac{n}{h_f}} e'_1 \Gamma_{-,p}^{-1}(h_f) U_{2,-p}(h_f), \\ \Delta^{B_3} \hat{f}_{+,p}(h_f) &\equiv -\frac{1}{\sqrt{nh_f}} e'_1 \Gamma_{+,p}^{-1}(h_f) U_{+,p}(h_f), \\ \Delta^{B_3} \hat{f}_{-,p}(h_f) &\equiv -\frac{1}{\sqrt{nh_f}} e'_1 \Gamma_{-,p}^{-1}(h_f) U_{-,p}(h_f).\end{aligned}$$

We can decompose $\Delta \hat{f}_{+,p}(h_f)$ and $\Delta \hat{f}_{-,p}(h_f)$ into

$$\Delta \hat{f}_{+,p}(h_f) = \Delta^M \hat{f}_{+,p}(h_f) + \Delta^B \hat{f}_{+,p}(h_f), \quad \Delta \hat{f}_{-,p}(h_f) = \Delta^M \hat{f}_{-,p}(h_f) + \Delta^B \hat{f}_{-,p}(h_f),$$

where

$$\Delta^M \hat{f}_{+,p}(h_f) \equiv \sqrt{\frac{n}{h_f}} e'_1 \Gamma_{+,p}^{-1}(h_f) U_{1,+p}(h_f), \quad \Delta^M \hat{f}_{-,p}(h_f) \equiv \sqrt{\frac{n}{h_f}} e'_1 \Gamma_{-,p}^{-1}(h_f) U_{1,-p}(h_f)$$

and

$$\Delta^B \hat{f}_{+,p}(h_f) \equiv \sum_{j=0}^3 \Delta^{B_j} \hat{f}_{+,p}(h_f), \quad \Delta^B \hat{f}_{-,p}(h_f) \equiv \sum_{j=0}^3 \Delta^{B_j} \hat{f}_{-,p}(h_f).$$

We consider distributional approximations of $\Delta^M \hat{f}_{+,p}(h_f)$ and $\Delta^M \hat{f}_{-,p}(h_f)$.

To characterize the bias and variance of the local polynomial estimators, we employ the following notation.

$$\begin{aligned}\sigma_{Z_k+}^2 &= \lim_{x \rightarrow 0^+} \sigma_{Z_k}^2(x), \quad \sigma_{Z_k-}^2 = \lim_{x \rightarrow 0^-} \sigma_{Z_k}^2(x), \quad \sigma_{Z_k}^2(x) = \text{Var}(Z_k | X = x), \\ \sigma_{Z_j Z_k+} &= \lim_{x \rightarrow 0^+} \sigma_{Z_j Z_k}(x), \quad \sigma_{Z_j Z_k-} = \lim_{x \rightarrow 0^-} \sigma_{Z_j Z_k}(x), \quad \sigma_{Z_j Z_k}(x) = \text{Cov}(Z_j, Z_k | X = x), \\ \varepsilon_{Z_k} &= (\varepsilon_{Z_k,1}, \dots, \varepsilon_{Z_k,n})' \text{ with } \varepsilon_{Z_k,i} = Z_{k,i} - \mu_{Z_k}(X_i), \\ \Sigma_{Z_k} &= E[\varepsilon_{Z_k} \varepsilon'_{Z_k} | \mathcal{X}_n] = \text{diag}(\sigma_{Z_k}^2(X_1), \dots, \sigma_{Z_k}^2(X_n)), \\ \Sigma_{Z_j Z_k} &= E[\varepsilon_{Z_j} \varepsilon'_{Z_k} | \mathcal{X}_n] = \text{diag}(\sigma_{Z_j Z_k}(X_1), \dots, \sigma_{Z_j Z_k}(X_n)),\end{aligned}$$

$$\begin{aligned}
S_p(h) &= [(X_1/h)^p, \dots, (X_n/h)^p]', \\
\vartheta_{+,p,q}(h) &= X_p(h)'W_+(h)S_q(h)/n, \quad \vartheta_{-,p,q}(h) = X_p(h)'W_-(h)S_q(h)/n, \\
\Psi_{Z_j Z_{k+},p,q}(h_j, h_k) &= X_p(h_j)'W_+(h_j)\Sigma_{Z_j Z_k} W_+(h_k)X_q(h_k)/n, \\
\Psi_{Z_j Z_{k-},p,q}(h_j, h_k) &= X_p(h_j)'W_-(h_j)\Sigma_{Z_j Z_k} W_-(h_k)X_q(h_k)/n, \\
\Psi_{Z_{k+},p}(h) &= \Psi_{Z_k Z_{k+},p,p}(h, h) = X_p(h)'W_+(h)\Sigma_{Z_k} W_+(h)X_p(h)/n, \\
\Psi_{Z_{k-},p}(h) &= \Psi_{Z_k Z_{k-},p,p}(h, h) = X_p(h)'W_-(h)\Sigma_{Z_k} W_-(h)X_p(h)/n, \\
\tilde{\Psi}_{Z_j Z_{k+},p,q}(h_j, h_k) &= \int_0^\infty K\left(\frac{h_{jk}u}{h_j}\right) K\left(\frac{h_{jk}u}{h_k}\right) r_p\left(\frac{h_{jk}u}{h_j}\right) r_q\left(\frac{h_{jk}u}{h_k}\right)' \sigma_{Z_j Z_k}^2(uh_{jk})f(uh_{jk})du, \\
\tilde{\Psi}_{Z_j Z_{k-},p,q}(h_j, h_k) &= \int_0^\infty K\left(\frac{h_{jk}u}{h_j}\right) K\left(\frac{h_{jk}u}{h_k}\right) r_p\left(\frac{h_{jk}u}{h_j}\right) r_q\left(\frac{h_{jk}u}{h_k}\right)' \sigma_{Z_j Z_k}^2(-uh_{jk})f(-uh_{jk})du, \\
\tilde{\Psi}_{Z_{k+},p}(h) &= \tilde{\Psi}_{Z_k Z_{k+},p,p}(h, h) = \int_0^\infty K(u)^2 r_p(u) r_p(u)' \sigma_{Z_k}^2(uh) f(uh) du, \\
\tilde{\Psi}_{Z_{k-},p}(h) &= \tilde{\Psi}_{Z_k Z_{k-},p,p}(h, h) = \int_0^\infty K(u)^2 r_p(u) r_p(u)' \sigma_{Z_k}^2(-uh) f(-uh) du, \\
\Gamma_p &= \int_0^\infty K(u) r_p(u) r_p(u)' du, \quad \vartheta_{p,q} = \int_0^\infty K(u) u^q r_p(u) du,
\end{aligned}$$

where $h_{jk} = (h_j h_k)^{1/2}$,

$$\begin{aligned}
&\Psi_{jk,p,q} \\
&= \begin{cases} \int_0^\infty K((c_{jk})^{1/2}u) K((c_{jk})^{-1/2}u) r_p((c_{jk})^{1/2}u) r_q((c_{jk})^{-1/2}u)' du & \text{if } \rho_{jk} \rightarrow c_{jk} \\ 0 & \text{otherwise} \end{cases} \\
&= \begin{cases} (c_{jk})^{1/2} \int_0^\infty K(c_{jk}u) K(u) r_p(c_{jk}u) r_q(u)' du & \text{if } \rho_{jk} \rightarrow c_{jk} \\ 0 & \text{otherwise,} \end{cases}
\end{aligned}$$

for $c_{jk} \in (0, \infty)$,

$$\begin{aligned}
\Psi_{p,q} &= \Psi_{kk,p,q} = \int_0^\infty K(u)^2 r_p(u) r_q(u)' du, \\
\Psi_{f,p} &= \int_0^\infty \int_0^\infty (u \wedge v) r_p(u) r_p(v)' K(u) K(v) dudv.
\end{aligned}$$

A.2 Preliminary lemmas

First, we present the asymptotic bias, variance, and distribution of the local polynomial estimators. We provide the proofs of the lemmas in Appendix A.5.

The following lemma describes the asymptotic behavior of the bias terms for the local polynomial estimators.

Lemma A.1. *Suppose Assumptions 1-2 hold with $S \geq l + 2$ and $R \geq p + 1$.*

(a) *If $nh_{\min} \rightarrow \infty$ and $h_{\max} \rightarrow 0$, then*

$$\begin{aligned} & \Delta^B \hat{\mu}_{Z_k+,l}(h_k) \\ &= \sqrt{n}(h_k)^{3/2+l} B_{Z_k+,l,l+1}(h_k) + \sqrt{n}(h_k)^{5/2+l} B_{Z_k+,l,l+2}(h_k)[1 + o_p(1)], \end{aligned} \quad (\text{A.1})$$

$$\begin{aligned} & \Delta^B \hat{\mu}_{Z_k-,l}(h_k) \\ &= \sqrt{n}(h_k)^{3/2+l} B_{Z_k-,l,l+1}(h_k) + \sqrt{n}(h_k)^{5/2+l} B_{Z_k-,l,l+2}(h_k)[1 + o_p(1)], \end{aligned} \quad (\text{A.2})$$

where

$$B_{Z_k+,l,r}(h_k) = \frac{\mu_{Z_k+}^{(r)}}{r!} \mathcal{B}_{+,0,l,r}(h_k), \quad B_{Z_k-,l,r}(h_k) = \frac{\mu_{Z_k-}^{(r)}}{r!} \mathcal{B}_{-,0,l,r}(h_k), \quad (\text{A.3})$$

$$\mathcal{B}_{+,s,l,r}(h_k) = s! e'_s \Gamma_{+,l}^{-1}(h_k) \vartheta_{+,l,r}(h_k) = s! e'_s \Gamma_l^{-1} \vartheta_{l,r} + o_p(1), \quad (\text{A.4})$$

$$\mathcal{B}_{-,s,l,r}(h_k) = s! e'_s \Gamma_{-,l}^{-1}(h_k) \vartheta_{-,l,r}(h_k) = (-1)^{s+r} s! e'_s \Gamma_l^{-1} \vartheta_{l,r} + o_p(1). \quad (\text{A.5})$$

(b) *If $nh_f \rightarrow \infty$ and $h_f \rightarrow 0$, then*

$$\begin{aligned} & \Delta^{B_0} \hat{f}_{+,p}(h_f) \\ &= \sqrt{n} h_f^{p+1/2} B_{f,+,p,p+1}(h_f) + \sqrt{n} h_f^{p+3/2} B_{f,+,p,p+2}(h_f)[1 + o_p(1)], \end{aligned} \quad (\text{A.6})$$

$$\Delta^{B_1} \hat{f}_{+,p}(h_f) = O_p((nh_f)^{-1/2}) = o_p(1),$$

$$\begin{aligned} & \Delta^{B_0} \hat{f}_{-,p}(h_f) \\ &= \sqrt{n} h_f^{p+1/2} B_{f,-,p,p+1}(h_f) + \sqrt{n} h_f^{p+3/2} B_{f,-,p,p+2}(h_f)[1 + o_p(1)], \end{aligned} \quad (\text{A.7})$$

$$\Delta^{B_1} \hat{f}_{-,p}(h_f) = o_p(1),$$

where

$$B_{f,+,p,q}(h_f) = \frac{f_+^{(q-1)}}{(q-1)!} \mathcal{B}_{+,1,p,q}(h_f), \quad B_{f,-,p,q}(h_f) = \frac{f_-^{(q-1)}}{(q-1)!} \mathcal{B}_{-,1,p,q}(h_f). \quad (\text{A.8})$$

(c) *If $nh_f^2 \rightarrow \infty$ and $h_f \rightarrow 0$, then*

$$\Delta^{B_2} \hat{f}_{+,p}(h_f) = O_p((nh_f^2)^{-1/2}) = o_p(1), \quad \Delta^{B_2} \hat{f}_{-,p}(h_f) = o_p(1). \quad (\text{A.9})$$

Observe that

$$\Delta^M \hat{\mu}_{Z_k+,l}(h_k) = \sqrt{\frac{h_k}{n}} e_0' \Gamma_{+,l}^{-1}(h_k) X_l(h_k)' W_+(h_k) \varepsilon_{Z_k},$$

$$\Delta^M \hat{\mu}_{Z_k-,l}(h_k) = \sqrt{\frac{h_k}{n}} e_0' \Gamma_{-,l}^{-1}(h_k) X_l(h_k)' W_-(h_k) \varepsilon_{Z_k}.$$

The following lemma is used to derive the asymptotic variance of the local polynomial estimators.

Lemma A.2. *Suppose Assumptions 1-2 hold with $S \geq l+2$ and $R \geq p+1$.*

(a) *If $nh_{\min} \rightarrow \infty$ and $h_{\max} \rightarrow 0$, then*

$$\begin{aligned} & \text{Cov} \left(\sqrt{\frac{h_j}{n}} X_l(h_j)' W_+(h_j) \varepsilon_{Z_j}, \sqrt{\frac{h_k}{n}} X_l(h_k)' W_+(h_k) \varepsilon_{Z_k} \right) \\ &= f_+ \sigma_{Z_j Z_k+} \Psi_{jk,l,l} + o(1) \end{aligned}$$

and

$$\begin{aligned} & \text{Cov} \left(\sqrt{\frac{h_j}{n}} X_l(h_j)' W_-(h_j) \varepsilon_{Z_j}, \sqrt{\frac{h_k}{n}} X_l(h_k)' W_-(h_k) \varepsilon_{Z_k} \right) \\ &= f_- \sigma_{Z_j Z_k-} H_l(-1) \Psi_{jk,l,l} H_l(-1) + o(1). \end{aligned}$$

(b) *If $nh_f^2 \rightarrow \infty$ and $h_f \rightarrow 0$, then*

$$\begin{aligned} & \text{Var} \left(\sqrt{\frac{n}{h_f}} U_{1,+p}(h_f) \right) \\ &= \frac{1}{h_f} f_+^2 (F_+ - F_+^2) \Gamma_p e_0 e_0' \Gamma_p + f_+^3 \Psi_{f,p} \\ & \quad + \{ -f_+^3 F_+ + f_+ f_+' (F_+ - F_+^2) \} \Gamma_p (e_1 e_0' + e_0 e_1') \Gamma_p + o(1) \end{aligned}$$

and

$$\begin{aligned} & \text{Var} \left(\sqrt{\frac{n}{h_f}} U_{1,-p}(h_f) \right) \\ &= \frac{1}{h_f} f_-^2 (F_- - F_-^2) H_p(-1) \Gamma_p e_0 e_0' \Gamma_p H_p(-1) + f_-^3 H_p(-1) \Psi_{f,p} H_p(-1) \\ & \quad - \{ -f_-^3 (F_- - 1) + f_- f_-' (F_- - F_-^2) \} H_p(-1) \Gamma_p (e_1 e_0' + e_0 e_1') \Gamma_p H_p(-1) \\ & \quad + o(1). \end{aligned}$$

(c)

$$\text{Cov} (X_l(h_k)' W_+(h_k) \varepsilon_{Z_k}, U_{1,+p}(h_f)) = 0$$

and

$$\text{Cov}(X_l(h_k)'W_-(h_k)\varepsilon_{Z_k}, U_{1,-,p}(h_f)) = 0.$$

We set

$$\begin{aligned} C_{Z_j Z_{k+},l} &= \frac{\sigma_{Z_j Z_{k+}}^2}{f_+} e_0' \Gamma_l^{-1} \Psi_{jk,l,l} \Gamma_l^{-1} e_0, & C_{Z_j Z_{k-},l} &= \frac{\sigma_{Z_j Z_{k-}}^2}{f_-} e_0' \Gamma_l^{-1} \Psi_{jk,l,l} \Gamma_l^{-1} e_0, \\ V_{Z_{k+},l} = C_{Z_k Z_{k+},l} &= \frac{\sigma_{Z_k^+}^2}{f_+} e_0' \Gamma_l^{-1} \Psi_l \Gamma_l^{-1} e_0, & V_{Z_{k-},l} = C_{Z_k Z_{k-},l} &= \frac{\sigma_{Z_k^-}^2}{f_-} e_0' \Gamma_l^{-1} \Psi_l \Gamma_l^{-1} e_0, \\ V_{f,+,p} &= f_+ e_1' \Gamma_p^{-1} \Psi_{f,p} \Gamma_p^{-1} e_1, & V_{f,-,p} &= f_- e_1' \Gamma_p^{-1} \Psi_{f,p} \Gamma_p^{-1} e_1. \end{aligned}$$

We further set

$$\begin{aligned} \tilde{\Delta} \hat{\mu}_{Z_{k+},l}(h_k) &\equiv \Delta \hat{\mu}_{Z_{k+},l}(h_k) - \sqrt{n}(h_k)^{3/2+l} B_{Z_{k+},l,l+1}(h_k), \\ \tilde{\Delta} \hat{\mu}_{Z_{k-},l}(h_k) &\equiv \Delta \hat{\mu}_{Z_{k-},l}(h_k) - \sqrt{n}(h_k)^{3/2+l} B_{Z_{k-},l,l+1}(h_k), \\ \tilde{\Delta} \hat{f}_{+,p}(h_f) &\equiv \Delta \hat{f}_{+,p}(h_f) - \sqrt{n} h_f^{p+1/2} B_{f,+,p,p+1}(h_f), \\ \tilde{\Delta} \hat{f}_{-,p}(h_f) &\equiv \Delta \hat{f}_{-,p}(h_f) - \sqrt{n} h_f^{p+1/2} B_{f,-,p,p+1}(h_f), \end{aligned}$$

Using Lemmas A.1 and A.2, the following provides an asymptotic distribution for the local polynomial estimators.

Lemma A.3. *Suppose Assumptions 1–2 hold with $S \geq l+2$ and $R \geq p+1$. If $nh_{\min} \rightarrow \infty$, $nh_f^2 \rightarrow \infty$, $n(h_{\max})^{2l+5} \rightarrow 0$, and $n(h_f)^{2p+3} \rightarrow 0$, then*

$$[\tilde{\Delta} \hat{\mu}_{Z_{1+},l}(h_1), \dots, \tilde{\Delta} \hat{\mu}_{Z_{d+},l}(h_d), \tilde{\Delta} \hat{f}_{+,p}(h_f)]' \xrightarrow{d} N_{d+1}(0, V_{+,l,p}), \quad (\text{A.10})$$

$$[\tilde{\Delta} \hat{\mu}_{Z_{1-},l}(h_1), \dots, \tilde{\Delta} \hat{\mu}_{Z_{d-},l}(h_d), \tilde{\Delta} \hat{f}_{-,p}(h_f)]' \xrightarrow{d} N_{d+1}(0, V_{-,l,p}), \quad (\text{A.11})$$

where

$$\begin{aligned} V_{+,l,p} &= \begin{pmatrix} V_{Z_{+,l}} & 0 \\ 0 & V_{f,+,p} \end{pmatrix}, & V_{Z_{+,l}} &= \{C_{Z_j Z_{k+},l}\}_{j,k=1,\dots,d}, \\ V_{-,l,p} &= \begin{pmatrix} V_{Z_{-,l}} & 0 \\ 0 & V_{f,-,p} \end{pmatrix}, & V_{Z_{-,l}} &= \{C_{Z_j Z_{k-},l}\}_{j,k=1,\dots,d}. \end{aligned}$$

Remark 7. In Lemma A.2 (b), the results for the estimators on the left and right sides are not analogous. The term

$$\{-f_+^3 F_+ + f_+ f_+'(F_+ - F_+^2)\} \Gamma_p (e_1 e_0' + e_0 e_1') \Gamma_p$$

for the right-hand-side estimator changes to

$$-\{ -f_-^3(F_- - 1) + f_- f_-'(F_- - F_-^2) \} H_p(-1) \Gamma_p(e_1 e_0' + e_0 e_1') \Gamma_p H_p(-1)$$

for the left-hand-side estimator. Nevertheless, we observe the following.

$$e_1' \Gamma_p^{-1} \Gamma_p (e_1 e_0' + e_0 e_1') \Gamma_p \Gamma_p^{-1} e_1 = e_1' (e_1 e_0' + e_0 e_1') e_1 = 0,$$

and the difference has no effect on the asymptotic variances $V_{f,+p}$ and $V_{f,-p}$. We outline the proof of Lemma A.2 (b) for the left-side estimator in Remark 8.

A.3 Result for implementation

As mentioned in the main text, we implemented bias correction by increasing the order of the local polynomial estimators constructed from the following (not bias-corrected) distributional approximation.

Theorem A.1. *Suppose that Assumptions 1 and 2 hold, with $R \geq p + 2$ and $S \geq l + 3$. If $nh_{\min} \rightarrow \infty$, $nh_f^2 \rightarrow \infty$, $n(h_{\max})^{2l+5} \rightarrow 0$, and $n(h_f)^{2p+3} \rightarrow 0$, then:*

$$\begin{aligned} & \sqrt{n} [\sqrt{h_1} (\hat{\tau}_{Z_1, l+1}(h_1) - \tau_{Z_1}), \dots, \sqrt{h_d} (\hat{\tau}_{Z_d, l+1}(h_d) - \tau_{Z_d}), \sqrt{h_f} (\hat{\tau}_{f, p+1}(h_f) - \tau_f)]' \\ & \xrightarrow{d} N_{d+1}(0, V_{l+1, p+1}). \end{aligned}$$

A.4 Asymptotic covariance matrix and standard error estimation

Using the asymptotic covariance matrices of $(\hat{\mu}_{Z_1, l}(h_1), \dots, \hat{\mu}_{Z_d, l}(h_d), \hat{f}_{+, p}(h_f))'$ and $(\hat{\mu}_{Z_1, -l}(h_1), \dots, \hat{\mu}_{Z_d, -l}(h_d), \hat{f}_{-, p}(h_f))'$, the asymptotic covariance matrix of $(\hat{\tau}_{Z_1, l}(h_1), \dots, \hat{\tau}_{Z_d, l}(h_d), \hat{\tau}_{f, p}(h_f))'$ is

$$V_{l, p} = V_{+, l, p} + V_{-, l, p} = \begin{pmatrix} V_{Z, l} & 0 \\ 0 & V_{f, p} \end{pmatrix},$$

where $V_{Z, l} = V_{Z_+, l} + V_{Z_-, l} = \{C_{Z_j Z_k +, l} + C_{Z_j Z_k -, l}\}_{j, k=1, \dots, d}$ and $V_{f, p} = V_{f, +, p} + V_{f, -, p}$. We propose the following estimator for the asymptotic covariance matrix:

$$\hat{V}_{l, p}(h) = \hat{V}_{+, l, p}(h) + \hat{V}_{-, l, p}(h) = \begin{pmatrix} \hat{V}_{Z, l}(h) & 0 \\ 0 & \hat{V}_{f, p}(h_f) \end{pmatrix},$$

where $\hat{V}_{Z,l}(h) = \hat{V}_{Z_+,l}(h) + \hat{V}_{Z_-,l}(h) = \{\hat{C}_{Z_j Z_{k+},l}(h_j, h_k) + \hat{C}_{Z_j Z_{k-},l}(h_j, h_k)\}_{j,k=1,\dots,d}$ and $\hat{V}_{f,p}(h_f) = \hat{V}_{f,+,p}(h_f) + \hat{V}_{f,-,p}(h_f)$. The diagonal elements of $\hat{V}_{Z,l}(h)$ are $\hat{V}_{Z_k,l}(h_k) = \hat{V}_{Z_{k+},l}(h_k) + \hat{V}_{Z_{k-},l}(h_k)$ for $k = 1, \dots, d$.

For $\hat{C}_{Z_j Z_{k+},l}(h_j, h_k)$, $\hat{C}_{Z_j Z_{k-},l}(h_j, h_k)$, $\hat{V}_{Z_{k+},l}(h)$, and $\hat{V}_{Z_{k-},l}(h)$, we follow an approach similar to the standard error estimators of Calonico et al. (2014) based on nearest-neighbor estimation. We define

$$\begin{aligned}\hat{C}_{Z_j Z_{k+},l}(h_j, h_k) &= h_{jk} e_0' \Gamma_{+,l}^{-1}(h_j) \hat{\Psi}_{Z_j Z_{k+},l}(h_j, h_k) \Gamma_{+,l}^{-1}(h_k) e_0, \\ \hat{C}_{Z_j Z_{k-},l}(h_j, h_k) &= h_{jk} e_0' \Gamma_{-,l}^{-1}(h_j) \hat{\Psi}_{Z_j Z_{k-},l}(h_j, h_k) \Gamma_{-,l}^{-1}(h_k) e_0, \\ \hat{V}_{Z_{k+},l}(h) &= \hat{C}_{Z_k Z_{k+},l}(h, h) = h e_0' \Gamma_{+,l}^{-1}(h) \hat{\Psi}_{Z_{k+},l}(h) \Gamma_{+,l}^{-1}(h) e_0, \\ \hat{V}_{Z_{k-},l}(h) &= \hat{C}_{Z_k Z_{k-},l}(h, h) = h e_0' \Gamma_{-,l}^{-1}(h) \hat{\Psi}_{Z_{k-},l}(h) \Gamma_{-,l}^{-1}(h) e_0\end{aligned}$$

with

$$\begin{aligned}\hat{\Psi}_{Z_j Z_{k+},l}(h_j, h_k) &= X_l(h_j)' W_+(h_j) \hat{\Sigma}_{Z_j Z_{k+}} W_+(h_k) X_l(h_k) / n, \\ \hat{\Psi}_{Z_j Z_{k-},l}(h_j, h_k) &= X_l(h_j)' W_-(h_j) \hat{\Sigma}_{Z_j Z_{k-}} W_-(h_k) X_l(h_k) / n, \\ \hat{\Psi}_{Z_{k+},l}(h) &= \hat{\Psi}_{Z_k Z_{k+},l}(h, h) = X_l(h)' W_+(h) \hat{\Sigma}_{Z_{k+}} W_+(h) X_l(h) / n, \\ \hat{\Psi}_{Z_{k-},l}(h) &= \hat{\Psi}_{Z_k Z_{k-},l}(h, h) = X_l(h)' W_-(h) \hat{\Sigma}_{Z_{k-}} W_-(h) X_l(h) / n, \\ \hat{\Sigma}_{Z_j Z_{k+}} &= \text{diag}(\hat{\sigma}_{Z_j Z_{k+}}^2(X_1), \dots, \hat{\sigma}_{Z_j Z_{k+}}^2(X_n)), \\ \hat{\Sigma}_{Z_j Z_{k-}} &= \text{diag}(\hat{\sigma}_{Z_j Z_{k-}}^2(X_1), \dots, \hat{\sigma}_{Z_j Z_{k-}}^2(X_n)), \\ \hat{\Sigma}_{Z_{k+}} &= \text{diag}(\hat{\sigma}_{Z_{k+}}^2(X_1), \dots, \hat{\sigma}_{Z_{k+}}^2(X_n)), \\ \hat{\Sigma}_{Z_{k-}} &= \text{diag}(\hat{\sigma}_{Z_{k-}}^2(X_1), \dots, \hat{\sigma}_{Z_{k-}}^2(X_n)), \\ \hat{\sigma}_{Z_j Z_{k+}}^2(X_i) &= 1\{X_i \geq 0\} \frac{M}{M+1} \left(Z_{j,i} - \sum_{m=1}^M \frac{Z_{j,l_m^+(i)}}{M} \right) \left(Z_{k,i} - \sum_{m=1}^M \frac{Z_{k,l_m^+(i)}}{M} \right), \\ \hat{\sigma}_{Z_j Z_{k-}}^2(X_i) &= 1\{X_i < 0\} \frac{M}{M+1} \left(Z_{j,i} - \sum_{m=1}^M \frac{Z_{j,l_m^-(i)}}{M} \right) \left(Z_{k,i} - \sum_{m=1}^M \frac{Z_{k,l_m^-(i)}}{M} \right), \\ \hat{\sigma}_{Z_{k+}}^2(X_i) &= 1\{X_i \geq 0\} \frac{M}{M+1} \left(Z_{k,i} - \sum_{m=1}^M \frac{Z_{k,l_m^+(i)}}{M} \right)^2, \\ \hat{\sigma}_{Z_{k-}}^2(X_i) &= 1\{X_i < 0\} \frac{M}{M+1} \left(Z_{k,i} - \sum_{m=1}^M \frac{Z_{k,l_m^-(i)}}{M} \right)^2,\end{aligned}$$

where $l_m^+(i)$ and $l_m^-(i)$ are the m th closest units to unit i among $\{X_i : X_i \geq 0\}$ and $\{X_i : X_i < 0\}$ respectively, and M denotes the number of neighbors. Calonico et al.

(2014) shows that, if $\sigma_{Z_j Z_k}^2(x)$ is Lipschitz continuous on $(-\kappa_0, \kappa_0)$, then, for any choice of $M \in \mathbb{N}_+$,

$$\hat{\Psi}_{Z_j Z_{k+}, l, l}(h_j, h_k) = \Psi_{Z_j Z_{k+}, l, l}(h_j, h_k) + o_p(\min\{h_j^{-1}, h_k^{-1}\}),$$

$$\hat{\Psi}_{Z_j Z_{k-}, l, l}(h_j, h_k) = \Psi_{Z_j Z_{k-}, l, l}(h_j, h_k) + o_p(\min\{h_j^{-1}, h_k^{-1}\})$$

hold, which leads to $\hat{V}_{Z, l}(h) \xrightarrow{P} V_{Z, l}$ combined with Lemma A.2.

For $\hat{V}_{f, p}(h_f)$, we employ the jackknife-based standard error estimator from Cattaneo et al. (2020), which may be more robust than plug-in estimations in finite samples. We define

$$\hat{V}_{f+, p}(h_f) = h_f^{-1} e_1' \Gamma_{+, p}^{-1}(h_f) \hat{\Psi}_{f+, p}(h_f) \Gamma_{+, p}^{-1}(h_f) e_1,$$

$$\hat{V}_{f-, p}(h_f) = h_f^{-1} e_1' \Gamma_{-, p}^{-1}(h_f) \hat{\Psi}_{f-, p}(h_f) \Gamma_{-, p}^{-1}(h_f) e_1,$$

with

$$\begin{aligned} \hat{\Psi}_{f+, p}(h_f) &= \frac{1}{n} \sum_{i=1}^n \left(\frac{1}{n-1} \sum_{j:j \neq i} \hat{\phi}_{+, p, h_f}^*(X_i, X_j) \right) \left(\frac{1}{n-1} \sum_{j:j \neq i} \hat{\phi}_{+, p, h_f}^*(X_i, X_j) \right)' \\ &\quad - \left(\frac{1}{n(n-1)} \sum_{i, j: i < j} \hat{\phi}_{+, p, h_f}^*(X_i, X_j) \right) \left(\frac{1}{n(n-1)} \sum_{i, j: i < j} \hat{\phi}_{+, p, h_f}^*(X_i, X_j) \right)', \end{aligned}$$

$$\begin{aligned} \hat{\Psi}_{f-, p}(h_f) &= \frac{1}{n} \sum_{i=1}^n \left(\frac{1}{n-1} \sum_{j:j \neq i} \hat{\phi}_{-, p, h_f}^*(X_i, X_j) \right) \left(\frac{1}{n-1} \sum_{j:j \neq i} \hat{\phi}_{-, p, h_f}^*(X_i, X_j) \right)' \\ &\quad - \left(\frac{1}{n(n-1)} \sum_{i, j: i < j} \hat{\phi}_{-, p, h_f}^*(X_i, X_j) \right) \left(\frac{1}{n(n-1)} \sum_{i, j: i < j} \hat{\phi}_{-, p, h_f}^*(X_i, X_j) \right)', \end{aligned}$$

$$\hat{\phi}_{+, p, h_f}^*(X_i, X_j) = \hat{\psi}_{+, p, h_f}^*(X_i, X_j) + \hat{\psi}_{+, p, h_f}^*(X_j, X_i),$$

$$\hat{\phi}_{-, p, h_f}^*(X_i, X_j) = \hat{\psi}_{-, p, h_f}^*(X_i, X_j) + \hat{\psi}_{-, p, h_f}^*(X_j, X_i),$$

$$\hat{\psi}_{+, p, h_f}^*(X_i, X_j) = 1\{X_i \geq 0\} r_p(X_i/h_f) (1\{X_j \leq X_i\} - r_p(X_i)' \hat{\beta}_{f+, p}(h_f)) K_{h_f}(X_i),$$

$$\hat{\psi}_{-, p, h_f}^*(X_i, X_j) = 1\{X_i < 0\} r_p(X_i/h_f) (1\{X_j \leq X_i\} - r_p(X_i)' \hat{\beta}_{f-, p}(h_f)) K_{h_f}(X_i).$$

These estimators can be motivated from another representations of $\Delta \hat{f}_{+, p}(h_f)$ and $\Delta \hat{f}_{-, p}(h_f)$. For $\Delta \hat{f}_{+, p}(h_f)$, one can show that

$$\Delta \hat{f}_{+, p}(h_f) = \sqrt{\frac{n}{h_f}} e_1' \Gamma_{+, p}^{-1}(h_f) U_{+, p}^*(h_f) + O_p\left(\frac{1}{\sqrt{nh_f}}\right),$$

where

$$U_{+,p}^*(h_f) = \frac{1}{n(n-1)} \sum_{i,j:i \neq j}^n \psi_{+,p,h_f}^*(X_i, X_j),$$

$$\psi_{+,p,h_f}^*(X_i, X_j) = 1\{X_i \geq 0\} r_p(X_i/h_f) (1\{X_j \leq X_i\} - r_p(X_i)' \beta_{f+,p}) K_{h_f}(X_i),$$

and $\hat{\Psi}_{f+,p}(h_f)$ is constructed to approximate the asymptotic variance of the second-order U-statistic $U_{+,p}^*(h_f)$.

A.5 Proof of the results

The proofs in this section use several auxiliary results (Lemma A.4) collected in Appendix A.6. For Lemmas A.1-A.3, we only provide proofs for the right-hand-side estimators ($\hat{\mu}_{Z_k+,l}(h_k)$, $\hat{f}_{+,p}(h_f)$), and the proofs of the left-hand-side estimators ($\hat{\mu}_{Z_k-,l}(h_k)$ and $\hat{f}_{-,p}(h_f)$) are analogous. Without loss of generality, we assume that $\kappa h_j < \kappa_0$ for $j = 1, \dots, d, f$ to bound the densities and error variances evaluated at uh_f where $u \in (-\kappa, \kappa)$.

Proof of Lemma A.1. For part (a), applying Lemma S.A.3 (B) of Calonico et al. (2014) to $E[\hat{\mu}_{Z_k+,l}(h_k)|\mathcal{X}_n]$ for $k = 1, \dots, d$ yields:

$$\begin{aligned} & \frac{1}{\sqrt{n}} \Delta^B \hat{\mu}_{Z_k+,l}(h_k) \\ &= (h_k)^{3/2+l} \frac{\mu_{Z_k+}^{(l+1)}}{(l+1)!} \mathcal{B}_{+,0,l,l+1}(h_k) + (h_k)^{5/2+l} \frac{\mu_{Z_k+}^{(l+2)}}{(l+2)!} \mathcal{B}_{+,0,l,l+2}(h_k) + o_p((h_k)^{5/2+l}). \end{aligned} \tag{A.12}$$

For $\Delta^{B_0} \hat{f}_{+,p}(h_f)$ in part (b), a derivation analogous to the proof of Lemma 2 in Cattaneo et al. (2020) gives

$$\begin{aligned} & \frac{1}{\sqrt{n}} \Delta^{B_0} \hat{f}_{+,p}(h_f) \\ &= h_f^{p+1/2} \frac{f_+^{(p)}}{(p+1)!} \mathcal{B}_{+,1,p,p+1}(h_f) + h_f^{p+3/2} \frac{f_+^{(p+1)}}{(p+2)!} \mathcal{B}_{+,1,p,p+2}(h_f) + o_p((h_f)^{p+3/2}). \end{aligned} \tag{A.13}$$

For $\Delta^{B_1} \hat{f}_{+,p}(h_f)$ in part (b), we observe that

$$\begin{aligned} & E \left[\frac{1}{n} |X_p(h_f)' W_+(h_f)(\iota - F)| \right] \\ & \leq \frac{1}{n} \sum_{i=1}^n E \left[|r_p(X_i/h_f)' 1\{X_i \geq 0\} K_{h_f}(X_i)(1 - F(X_i))| \right] \\ & \lesssim \int_0^\infty |r_p(u)| K(u) f(h_f u) = O(1), \end{aligned}$$

and using the Markov's inequality,

$$\frac{1}{n} X_p(h_f)' W_+(h_f)(\iota - F) = O_p(1).$$

Thus, we obtain $\Delta^{B_1} \hat{f}_{+,p}(h_f) = O_p(\frac{1}{\sqrt{nh_f}})$.

For part (c), we observe the following.

$$\begin{aligned} E[|U_{2+,p}(h_f)|^2] & \lesssim \frac{1}{n(n-1)} E[|\varphi_{+,p,h_f}(X_i, X_j)|^2] \\ & \lesssim \frac{1}{n(n-1)} E[|\psi_{+,p,h_f}(X_i, X_j) - E[\psi_{+,p,h_f}(X_i, X_j)|X_j]|^2] \\ & \quad + \frac{1}{n(n-1)} E[|\psi_{+,p,h_f}(X_j, X_i) - E[\psi_{+,p,h_f}(X_j, X_i)|X_i]|^2] \\ & \lesssim \frac{1}{n(n-1)} E[|\psi_{+,p,h_f}(X_i, X_j)|^2]. \end{aligned} \tag{A.14}$$

A derivation analogous to the proof of Lemma 4 in Cattaneo et al. (2020) provides

$$\begin{aligned} & \frac{1}{n(n-1)} E[|\psi_{+,p,h_f}(X_i, X_j)|^2] \\ & \lesssim \frac{1}{n(n-1)h_f} f_+(F_+ - F_+^2) \int_0^\infty K(u)^2 r_p(u)' r_p(u) du + O\left(\frac{1}{n^2}\right) = O_p\left(\frac{1}{n^2 h_f}\right), \end{aligned} \tag{A.15}$$

which implies that $U_{2+,p}(h_f) = O_p(\frac{1}{n\sqrt{h_f}})$ from Chebyshev's inequality. Hence part (c) follows from $\sqrt{\frac{n}{h_f}} U_{2+,p}(h_f) = O_p(\frac{1}{\sqrt{nh_f^2}})$. \square

Proof of Lemma A.2. Observe that

$$\begin{aligned} & \text{Cov} \left(\sqrt{\frac{h_j}{n}} X_l(h_j)' W_+(h_j) \varepsilon_{Z_j}, \sqrt{\frac{h_k}{n}} X_l(h_k)' W_+(h_k) \varepsilon_{Z_k} | \mathcal{X}_n \right) \\ & = \frac{h_{jk}}{n} X_l(h_j)' W_+(h_j) \Sigma_{Z_j Z_k} W_+(h_k) X_l(h_k) = h_{jk} \Psi_{Z_j Z_k +, l}(h_j, h_k) \end{aligned}$$

and part (a) follows from Lemma A.4 (a).

Note that

$$\begin{aligned} & E[\psi_{+,p,h_f}(X_j, X_i)|X_i] \\ &= \int_0^\infty r_p(u)(1(X_i \leq h_f u) - F(h_f u))K(u)f(h_f u)du, \end{aligned}$$

A derivation analogous to the proof of Lemma 3 in Cattaneo et al. (2020) provides

$$\begin{aligned} & \text{Var} \left(\int_0^\infty r_p(u)(1(X_i \leq h_f u) - F(h_f u))K(u)f(h_f u)du \right) \\ &= \int_0^\infty \int_0^\infty r_p(u)r_p(v)'K(u)K(v)f(h_f u)f(h_f v)\{F(h_f(u \wedge v)) - F(h_f u)F(h_f v)\}dudv \\ &= f_+^2(F_+ - F_+^2) \int_0^\infty \int_0^\infty r_p(u)r_p(v)'K(u)K(v)dudv + h_f f_+^3 \Psi_{f,p} \\ & \quad + h_f \{-f_+^3 F_+ + f_+ f_+'(F_+ - F_+^2)\} \int_0^\infty \int_0^\infty (u+v)r_p(u)r_p(v)'K(u)K(v)dudv + o(1), \end{aligned}$$

Hence, part (b) follows from

$$\int_0^\infty r_p(u)K(u)du = \Gamma_p e_0 \quad \text{and} \quad \int_0^\infty ur_p(u)K(u)du = \Gamma_p e_1.$$

Observe that

$$X_l(h_k)'W_+(h_k)\varepsilon_{Z_k} = \sum_{i=1}^n 1\{X_i \geq 0\}K_{h_k}(X_i)r_l(X_i/h_k)\varepsilon_{Z_k,i}$$

and part (c) follows from

$$\begin{aligned} & \text{Cov} \left(\sum_{i=1}^n 1\{X_i \geq 0\}K_{h_k}(X_i)r_l(X_i/h_k)\varepsilon_{Z_k,i}, \sum_{i=1}^n E[\psi_{+,p,h_f}(X_j, X_i)|X_i] \right) \\ &= \sum_{i=1}^n E[1\{X_i \geq 0\}K_{h_k}(X_i)r_l(X_i/h_k)\varepsilon_{Z_k,i}E[\psi_{+,p,h_f}(X_j, X_i)|X_i]] = 0 \end{aligned}$$

because $E[\varepsilon_{Z_k,i}|\mathcal{X}_n] = 0$. □

Remark 8. We now outline the proof of Lemma A.2 (b) for the left-hand-side

estimator. A derivation analogous to the proof for the right-side estimator yields

$$\begin{aligned}
& \text{Var} \left(E[\psi_{-,p,h_f}(X_j, X_i) | X_i] \right) \\
&= f_-^2 (F_- - F_-^2) H_p(-1) \int_0^\infty \int_0^\infty r_p(u) r_p(v)' K(u) K(v) dudv H_p(-1) \\
&+ h_f f_-^3 H_p(-1) \int_0^\infty \int_0^\infty \{(-u) \wedge (-v)\} r_p(u) r_p(v)' K(u) K(v) dudv H_p(-1) \\
&+ h_f \{-f_-^3 F_- + f_- f'_-(F_- - F_-^2)\} \\
&\times H_p(-1) \int_0^\infty \int_0^\infty -(u+v) r_p(u) r_p(v)' K(u) K(v) dudv H_p(-1) + o(1),
\end{aligned}$$

and the stated result follows from

$$(-u) \wedge (-v) = \frac{1}{2}(-u - v - |u - v|) = u \wedge v - (u + v).$$

Proof of Lemma A.3. We show that

$$\sum_{k=1}^d t_k \tilde{\Delta} \hat{\mu}_{Z_{k+1},l}(h_k) + t_f \tilde{\Delta} \hat{f}_{+,p} \xrightarrow{d} N(0, \tilde{t}' V_{+,l,p} \tilde{t}), \quad (\text{A.16})$$

The stated result follows from the Cramér-Wold theorem.

We set

$$\xi_{1,n} = \sum_{k=1}^d t_k \Delta^M \hat{\mu}_{Z_{k+1},l}(h_k) + t_f \Delta^M \hat{f}_{+,p}(h_f) \quad (\text{A.17})$$

and

$$\xi_{2,n} = \sum_{k=1}^d t_k \tilde{\Delta}^B \hat{\mu}_{Z_{k+1},l}(h_k) + t_f \tilde{\Delta}^B \hat{f}_{+,p}(h_f), \quad (\text{A.18})$$

where

$$\tilde{\Delta}^B \hat{\mu}_{Z_{k+1},l}(h_k) \equiv \Delta^B \hat{\mu}_{Z_{k+1},l}(h_k) - \sqrt{n}(h_k)^{3/2+l} B_{Z_{k+1},l,l+1}(h_k)$$

and

$$\tilde{\Delta}^B \hat{f}_{+,p}(h_f) \equiv \Delta^B \hat{f}_{+,p}(h_f) - \sqrt{n} h_f^{p+1/2} B_{f,+,p,p+1}(h_f).$$

To demonstrate (A.16), we decompose the left-hand-side as follows.

$$\sum_{k=1}^d t_k \tilde{\Delta} \hat{\mu}_{Z_{k+1},l}(h_k) + t_f \tilde{\Delta} \hat{f}_{+,p}(h_f) = \xi_{1,n} + \xi_{2,n}.$$

We show that $\xi_{1,n} \xrightarrow{d} N(0, \tilde{t}' V_{+,l,p} \tilde{t})$ and $\xi_{2,n} = o_p(1)$.

First, we demonstrate that $\xi_{2,n} = o_p(1)$. If $h_{max} \rightarrow 0$, then from Lemma A.1 (a),

$$\sum_{k=1}^d t_k \tilde{\Delta}^B \hat{\mu}_{Z_k+,l}(h_k) = O_p \left(\sqrt{n} \sum_{k=1}^d (h_k)^{5/2+l} \right) = O_p \left(\sqrt{n} (h_{max})^{5/2+l} \right). \quad (\text{A.19})$$

From Lemma A.2 (b), $E[|\sqrt{\frac{n}{h_f}} U_{1,+p}(h_f)|^2] = O(\frac{1}{h_f})$, implying

$\sqrt{\frac{n}{h_f}} U_{1,+p}(h_f) = O_p(\frac{1}{\sqrt{h_f}})$ from Chebyshev's inequality. Hence, we have $\Delta^{B_3} \hat{f}_{+,p}(h_f) = O_p(\frac{1}{n\sqrt{h_f}})$ and

$$\tilde{\Delta}^B \hat{f}_{+,p}(h_f) = O_p \left(\sqrt{n} h_f^{3/2+p} \right) + O_p \left(\frac{1}{\sqrt{n h_f^2}} \right).$$

Therefore, we have $\xi_{2,n} = o_p(1)$ for the bias.

Next, we demonstrate that $\xi_{1,n} \xrightarrow{d} N(0, 1)$. Let

$$\tilde{\Delta}^M \hat{\mu}_{Z_k+,l}(h_k) = \sqrt{\frac{h_k}{n}} f_+^{-1} e_0' \Gamma_l^{-1} X_l(h_k)' W_+(h_k) \varepsilon_{Z_k}$$

and

$$\tilde{\Delta}^M \hat{f}_{+,p}(h_f) = \sqrt{\frac{n}{h_f}} f_+^{-1} e_1' \Gamma_p^{-1} U_{1,+p}(h_f).$$

Subsequently, we have

$$\Delta^M \hat{\mu}_{Z_k+,l}(h_k) = \tilde{\Delta}^M \hat{\mu}_{Z_k+,l}(h_k) + o_p(1)$$

and

$$\Delta^M \hat{f}_{+,p}(h_f) = \tilde{\Delta}^M \hat{f}_{+,p}(h_f) + O_p \left(\sqrt{h_f} + \frac{1}{\sqrt{n h_f^2}} \right).$$

To demonstrate this, from Lemma S.A.1 in Calonico et al. (2014), we obtain

$$\Gamma_{+,p}(h_f) = f_+ \Gamma_p + O_p \left(h_f + \frac{1}{\sqrt{n h_f}} \right),$$

Hence, $|\Gamma_{+,p}(h_f) - f_+ \Gamma_p| < 1$ with a probability approaching one. Consequently, a well-known result for the matrix inverse yields

$$|\Gamma_{+,p}^{-1}(h_f) - f_+^{-1} \Gamma_p^{-1}| \leq \frac{|\Gamma_{+,p}(h_f) - f_+ \Gamma_p| |f_+^{-1} \Gamma_p^{-1}|^2}{1 - |\Gamma_{+,p}(h_f) - f_+ \Gamma_p| |f_+^{-1} \Gamma_p^{-1}|} = O_p \left(h_f + \frac{1}{\sqrt{n h_f}} \right)$$

with a probability approaching one. Hence, we obtain

$$\Gamma_{+,p}^{-1}(h_f) = f_+^{-1}\Gamma_p^{-1} + O_p\left(h_f + \frac{1}{\sqrt{nh_f}}\right),$$

and we have $\sqrt{\frac{h_k}{n}}X_l(h_k)'W_+(h_k)\varepsilon_{Z_k} = O_p(1)$ and $\sqrt{\frac{n}{h_f}}U_{1+,p}(h_f) = O_p\left(\frac{1}{\sqrt{h_f}}\right)$ from Lemma A.2 (a) and (b), respectively. Let

$$\tilde{\xi}_{1,n} = \sum_{k=1}^d t_k \tilde{\Delta}^M \hat{\mu}_{Z_k+,l}(h_k) + t_f \tilde{\Delta}^M \hat{f}_{+,p}(h_f).$$

Subsequently, from the previous definitions and derivations, $\xi_{1,n} = \tilde{\xi}_{1,n} + o_p(1)$.

Thus, it remains to show that $\tilde{\xi}_{1,n} \xrightarrow{d} N(0, \tilde{t}'V_{+,l,p}\tilde{t})$. Notably, $\tilde{\xi}_{1,n}$ can be represented as $\tilde{\xi}_{1,n} = \sum_{i=1}^n \hat{\omega}_i$ with

$$\hat{\omega}_i \equiv f_+^{-1} \left\{ e_0' \Gamma_l^{-1} \sum_{k=1}^d t_k \hat{\omega}_{k,i} \varepsilon_{Z_k,i} + t_f e_1' \Gamma_p^{-1} \hat{\omega}_{f,i} \right\},$$

where

$$\hat{\omega}_{k,i} \equiv \sqrt{\frac{h_k}{n}} \mathbf{1}\{X_i \geq 0\} K_{h_k}(X_i) r_l(X_i/h_k)$$

and

$$\hat{\omega}_{f,i} \equiv \frac{1}{\sqrt{nh_f}} E[\psi_{+,p,h_f}(X_j, X_i) | X_i].$$

$\{\hat{\omega}_i\} : 1 \leq i \leq n$ denotes a triangular array of independent random variables; We show that

$$E[\tilde{\xi}_{1,n}] = 0, \tag{A.20}$$

$$\text{Var}(\tilde{\xi}_{1,n}) = \tilde{t}'V_{+,l,p}\tilde{t} + o(1), \tag{A.21}$$

and

$$\sum_{i=1}^n E[|\hat{\omega}_i|^4] = o(1). \tag{A.22}$$

The Lyapunov Condition—a well-known sufficient condition for the Lindeberg condition—is satisfied by (A.22). Therefore, from (A.20), (A.21), and (A.22), applying the Lindeberg-Feller central limit theorem yields that $\tilde{\xi}_{1,n} \xrightarrow{d} N(0, \tilde{t}'V_{+,l,p}\tilde{t})$ (see, for example, Durrett (2019)).

First, from the definition, (A.20) follows from $E[\varepsilon_{Z_k,i} | \mathcal{X}_n] = 0$ and

$E[\psi_{+,p,h_f}(X_j, X_i)] = 0$. Next, from Lemmas A.2 (a) and (b), we have

$$\begin{aligned}\text{Var}(\tilde{\xi}_{1,n}) &= \text{Var}\left(\sum_{k=1}^d t_k \tilde{\Delta}^M \hat{\mu}_{Z_k+,l}(h_k)\right) + \text{Var}\left(t_f \tilde{\Delta}^M \hat{f}_{+,p}(h_f)\right) \\ &= t' V_{Z+,l} t + t_f^2 V_{f+,p} + o(1).\end{aligned}$$

Hence, we obtain (A.21). Finally, similar to the proof of Lemma S.A.3 (D) in Calonico et al. (2014), we obtain

$$\begin{aligned}\sum_{i=1}^n E[|\hat{\omega}_{k,i} \varepsilon_{Z_k,i}|^4] &\lesssim \sum_{i=1}^n E[|\hat{\omega}_{k,i}|^4] \\ &\lesssim \frac{1}{nh_k} \int_0^\infty K(u)^4 |r_p(u)|^4 f(h_k u) du = O\left(\frac{1}{nh_k}\right).\end{aligned}$$

The first inequality holds because, for two random variables W and Y , $E[|W + Y|^4 | X_i = x] \leq 8\{E[W^4 | X_i = x] + E[Y^4 | X_i = x]\}$ holds,

$$E[\varepsilon_{Z_k,i}^4 | X_i = x] \leq 8\{E[|Z_{k,i}|^4 | X_i = x] + \mu(x)^4\}. \quad (\text{A.23})$$

Hence, $E[\varepsilon_{Z_k,i}^4 | X_i = x]$ is bounded, based on Assumption 1. Similar to the proof of Lemma 3 in Cattaneo et al. (2020), we obtain

$$\begin{aligned}&\sum_{i=1}^n E[|\hat{\omega}_{f,i}|^4] \\ &\lesssim \int_0^\infty \int_0^\infty \int_0^\infty \int_0^\infty r_p(u_1) r_p(u_2)' r_p(u_3) r_p(u_4)' \prod_{j=1}^4 [K(u_j) f(h_f u_j)] du_1 du_2 du_3 du_4 \\ &= O\left(\frac{1}{nh_f^2}\right).\end{aligned}$$

Observe that

$$\begin{aligned}\sum_{i=1}^n E[|\hat{\omega}_{f,i}|^4] &\lesssim \sum_{i=1}^n \sum_{k=1}^d E[|t_k \hat{\omega}_{k,i} \varepsilon_{Z_k,i}|^4] + \sum_{i=1}^n E[|t_f \hat{\omega}_{f,i}|^4] \\ &\lesssim \sum_{k=1}^d \sum_{i=1}^n E[|\hat{\omega}_{k,i} \varepsilon_{Z_k,i}|^4] + \sum_{i=1}^n E[|\hat{\omega}_{f,i}|^4] \\ &\lesssim O\left(\frac{1}{nh_{\min}}\right) + O\left(\frac{1}{nh_f^2}\right).\end{aligned} \quad (\text{A.24})$$

The first inequality in (A.24) holds because, for two random variables W and Y ,

$E[|W + Y|^4] \leq 8\{E[W^4] + E[Y^4]\}$ holds iteratively. Therefore, (A.22) follows. \square

Proof of Theorem 3.1. The stated result follows from the same argument given in the proof of Lemma A.3 using the analogs of Lemmas A.1 and A.2, but is now applied to the estimator $(\hat{\tau}_{Z_1,l}(h_1), \dots, \hat{\tau}_{Z_d,l}(h_d), \hat{\tau}_{f,p}(h_f))'$. \square

Proof of Proposition 3.1. Let $c_{l,p}(\alpha)$ be the α -quantile of $\|N_{d+1}(0, V_{l,p}^*)\|_2^2$. Theorem 3.1 implies that $\tilde{\chi}_{l,p}^2(h) \xrightarrow{d} \|N_{d+1}(0, V_{l,p}^*)\|_2^2$ under H_0 . To prove Proposition 3.1 under H_0 , it suffices to show that $\hat{c}_{l,p}(\alpha) \xrightarrow{P} c_{l,p}(\alpha)$ because this implies that $\tilde{\chi}_{l,p}^2(h) - \hat{c}_{l,p}(\alpha) \xrightarrow{d} \|N_{d+1}(0, V_{l,p}^*)\|_2^2 - c_{l,p}(\alpha)$ under H_0 . Let $F(\cdot; V)$ be the distribution function of $\|N_{d+1}(0, V)\|_2^2$. Suppose that V_m and V are positive definite matrices for m and $V_m \rightarrow V$. Subsequently, for all $t \in \mathbb{R}$, it follows from the dominated convergence theorem that

$$\begin{aligned} F(t; V_m) &= \int \cdots \int 1\{u_1^2 + \cdots + u_{d+1}^2 \leq t\} \phi(u_1, \dots, u_{d+1}; V_m) du_1 \cdots du_{d+1} \\ &\rightarrow \int \cdots \int 1\{u_1^2 + \cdots + u_{d+1}^2 \leq t\} \phi(u_1, \dots, u_{d+1}; V) du_1 \cdots du_{d+1} = F(t; V), \end{aligned}$$

where $\phi(u_1, \dots, u_{d+1}; V)$ denotes the joint density function of $N_{d+1}(0, V)$. As $F(t; V)$ is continuous with respect to t , $F(\cdot; V_m)$ converges uniformly to $F(\cdot; V)$, according to Polya's theorem. As discussed in Section 3.9.4.2, in van der Vaart and Wellner (1996), the inverse map is continuous. Thus, $F^{-1}(\alpha; V_m) \rightarrow F^{-1}(\alpha; V)$ for any $\alpha \in (0, 1)$. Hence, $F^{-1}(t; V)$ is continuous with respect to V , and we obtain $\hat{c}_{l,p}(\alpha) \xrightarrow{P} c_{l,p}(\alpha)$ from the continuous-mapping theorem.

To prove Proposition 3.1 under H_1 , suppose that, without loss of generality, $\tau_{Z_k} \neq 0$. The proof for the case $\tau_f \neq 0$ follows from an analogous argument. Observe that

$$P\left(\frac{nh_k \hat{\tau}_{Z_k,l}^2(h_k)}{\hat{V}_{Z_k,l}(h_k)} \geq \hat{c}_{l,p}(\alpha)\right) \leq P(\tilde{\chi}_{l,p}^2(h) \geq \hat{c}_{l,p}(\alpha))$$

and

$$\begin{aligned} &P\left(\frac{nh_k \hat{\tau}_{Z_k,l}^2(h_k)}{\hat{V}_{Z_k,l}(h_k)} \geq \hat{c}_{l,p}(\alpha)\right) \\ &= P\left(\frac{nh_k (\hat{\tau}_{Z_k,l}(h_k) - \tau_{Z_k})^2}{\hat{V}_{Z_k,l}(h_k)} - \hat{c}_{l,p}(\alpha) \geq -\frac{nh_k (2\hat{\tau}_{Z_k,l}(h_k) - \tau_{Z_k})\tau_{Z_k}}{\hat{V}_{Z_k,l}(h_k)}\right). \end{aligned}$$

Because we have

$$\begin{aligned} \frac{nh_k(\hat{\tau}_{Z_k,l}(h_k) - \tau_{Z_k})^2}{\hat{V}_{Z_k,l}(h_k)} - \hat{c}_{l,p}(\alpha) &\xrightarrow{d} \|N(0,1)\|_2^2 - c_{l,p}(\alpha), \\ \frac{(2\hat{\tau}_{Z_k,l}(h_k) - \tau_{Z_k})\tau_{Z_k}}{\hat{V}_{Z_k,l}(h_k)} &\xrightarrow{P} \frac{2\tau_{Z_k}^2}{V_{Z_k,l}}, \end{aligned}$$

and $nh_k \rightarrow \infty$, we obtain

$$\lim_{n \rightarrow \infty} P \left(\frac{nh_k \hat{\tau}_{Z_k,l}^2(h_k)}{\hat{V}_{Z_k,l}(h_k)} \geq \hat{c}_{l,p}(\alpha) \right) = 1.$$

Hence, the stated result under H_1 follows. \square

Proof of Proposition 3.2. Let $m_{l,p}(\alpha)$ be the α -quantile of $\|N_{d+1}(0, V_{l,p}^*)\|_\infty^2$. Then, $\hat{m}_{l,p}(\alpha) \xrightarrow{P} m_{l,p}(\alpha)$ follows from the same argument as the proof of Proposition 3.1. Hence, the stated result under H_0 follows.

To prove Proposition 3.2 under H_1 , suppose that, without loss of generality, $\tau_{Z_k} \neq 0$. The proof for the case $\tau_f \neq 0$ follows from an analogous argument. Observe that

$$P \left(\frac{nh_k \hat{\tau}_{Z_k,l}^2(h_k)}{\hat{V}_{Z_k,l}(h_k)} \geq \hat{m}_{l,p}(\alpha) \right) \leq P(\hat{M}_{l,p}(h) \geq \hat{m}_{l,p}(\alpha)).$$

By an analogous argument as in the proof of Proposition 3.1, we obtain

$$\lim_{n \rightarrow \infty} P \left(\frac{nh_k \hat{\tau}_{Z_k,l}^2(h_k)}{\hat{V}_{Z_k,l}(h_k)} \geq \hat{m}_{l,p}(\alpha) \right) = 1.$$

Hence, the stated result under H_1 follows. \square

Proof of Proposition 5.1. We first prove the statement under H_0 . First, suppose that $\max\{\tau_f, \tau_{Z_1}, \dots, \tau_{Z_d}\} \geq \varepsilon$. Then, for the case of $\max\{\tau_f, \tau_{Z_1}, \dots, \tau_{Z_d}\} = \tau_{Z_k}$, observe that

$$\hat{\psi}_{1,l,p}(h) \geq \frac{\sqrt{n}\sqrt{h_k}(\hat{\tau}_{Z_k,l}(h_k) - \varepsilon)}{\hat{V}_{Z_k,l}(h_k)} \geq \frac{\sqrt{n}\sqrt{h_k}(\hat{\tau}_{Z_k,l}(h_k) - \tau_{Z_k})}{\hat{V}_{Z_k,l}(h_k)}.$$

Hence, we have

$$P(\hat{\psi}_{1,l,p}(h) \leq z_{\alpha/2}) \leq P \left(\frac{\sqrt{n}\sqrt{h_k}(\hat{\tau}_{Z_k,l}(h_k) - \tau_{Z_k})}{\hat{V}_{Z_k,l}(h_k)} \leq z_{\alpha/2} \right) \rightarrow \frac{\alpha}{2},$$

The same result holds for the case of $\max\{\tau_f, \tau_{Z_1}, \dots, \tau_{Z_d}\} = \tau_f$.

Next, suppose that $\min\{\tau_f, \tau_{Z_1}, \dots, \tau_{Z_d}\} \leq -\varepsilon$. Then, for the case of

$\min\{\tau_f, \tau_{Z_1}, \dots, \tau_{Z_d}\} = \tau_{Z_k}$, observe that

$$\hat{\psi}_{2,l,p}(h) \leq \frac{\sqrt{n}\sqrt{h_k}(\hat{\tau}_{Z_k,l}(h_k) + \varepsilon)}{\hat{V}_{Z_k,l}(h_k)} \leq \frac{\sqrt{n}\sqrt{h_k}(\hat{\tau}_{Z_k,l}(h_k) - \tau_{Z_k})}{\hat{V}_{Z_k,l}(h_k)}.$$

Hence, we have

$$P(\hat{\psi}_{2,l,p}(h) \geq z_{1-\alpha/2}) \leq P\left(\frac{\sqrt{n}\sqrt{h_k}(\hat{\tau}_{Z_k,l}(h_k) - \tau_{Z_k})}{\hat{V}_{Z_k,l}(h_k)} \geq z_{1-\alpha/2}\right) \rightarrow \frac{\alpha}{2},$$

The same result holds for the case of $\min\{\tau_f, \tau_{Z_1}, \dots, \tau_{Z_d}\} = \tau_f$.

Therefore, under H_0 , we have

$$\limsup_{n \rightarrow \infty} P\left(\hat{\psi}_{1,l,p}(h) \leq z_{\alpha/2} \text{ or } \hat{\psi}_{2,l,p}(h) \geq z_{1-\alpha/2}\right) \leq \alpha.$$

We next prove the statement under H_1 . Observe that

$$\begin{aligned} & P\left(\frac{\sqrt{n}\sqrt{h_k}(\hat{\tau}_{Z_k,l}(h_k) - \varepsilon)}{\hat{V}_{Z_k,l}(h_k)} \geq z_{\alpha/2}\right) \\ &= P\left(\frac{\sqrt{n}\sqrt{h_k}(\hat{\tau}_{Z_k,l}(h_k) - \tau_{Z_k})}{\hat{V}_{Z_k,l}(h_k)} - z_{\alpha/2} \geq \frac{\sqrt{n}\sqrt{h_k}(\varepsilon - \tau_{Z_k})}{\hat{V}_{Z_k,l}(h_k)}\right). \end{aligned}$$

Because we have

$$\begin{aligned} \frac{\sqrt{n}\sqrt{h_k}(\hat{\tau}_{Z_k,l}(h_k) - \tau_{Z_k})}{\hat{V}_{Z_k,l}(h_k)} - z_{\alpha/2} &\xrightarrow{d} N(0, 1) - z_{\alpha/2}, \\ \frac{\varepsilon - \tau_{Z_k}}{\hat{V}_{Z_k,l}(h_k)} &\xrightarrow{P} \frac{\varepsilon - \tau_{Z_k}}{V_{Z_k,l}}, \end{aligned}$$

and $nh_k \rightarrow \infty$, we obtain

$$\lim_{n \rightarrow \infty} P\left(\frac{\sqrt{n}\sqrt{h_k}(\hat{\tau}_{Z_k,l}(h_k) - \varepsilon)}{\hat{V}_{Z_k,l}(h_k)} \geq z_{\alpha/2}\right) = 0.$$

Similar result holds for $\hat{\tau}_{f,p+1}(h_f)$. Therefore, we obtain

$$\begin{aligned} & P(\hat{\psi}_{1,l,p}(h) \geq z_{\alpha/2}) \\ & \leq \sum_{k=1}^d P\left(\frac{\sqrt{n}\sqrt{h_k}(\hat{\tau}_{Z_k,l}(h_k) - \varepsilon)}{\hat{V}_{Z_k,l}(h_k)} \geq z_{\alpha/2}\right) + P\left(\frac{\sqrt{n}\sqrt{h_f}(\hat{\tau}_{f,p}(h_f) - \varepsilon)}{\hat{V}_{f,p}(h_f)} \geq z_{\alpha/2}\right) \\ & \rightarrow 0, \end{aligned}$$

which implies

$$\lim_{n \rightarrow \infty} P \left(\hat{\psi}_{1,l,p}(h) \geq z_{\alpha/2} \text{ and } \hat{\psi}_{2,l,p}(h) \leq z_{1-\alpha/2} \right) = 0.$$

□

Proof of Theorem A.1. Under the same assumption as in Theorem A.1, the asymptotic distribution for the local polynomial estimators, where the order is increased instead of eliminating the bias term, is as follows.

$$\begin{aligned} [\Delta \hat{\mu}_{Z_{1+,l+1}}(h_1), \dots, \Delta \hat{\mu}_{Z_{d+,l+1}}(h_d), \Delta \hat{f}_{+,p+1}(h_f)]' &\xrightarrow{d} N_{d+1}(0, V_{+,l+1,p+1}), \\ [\Delta \hat{\mu}_{Z_{1-,l+1}}(h_1), \dots, \Delta \hat{\mu}_{Z_{d-,l+1}}(h_d), \Delta \hat{f}_{-,p+1}(h_f)]' &\xrightarrow{d} N_{d+1}(0, V_{-,l+1,p+1}). \end{aligned}$$

This result and the stated result follow from a similar argument given in the proof of Lemma A.3 using the analogs of Lemmas A.1 and A.2. □

A.6 Auxiliary Lemma

The following lemma establishes convergence in the probability of the sample matrix $\Psi_{Z_j Z_{k+,p,q}}(h_j, h_k)$ to its population counterpart and characterizes this limit.

Lemma A.4. *Suppose that Assumptions 1-2 hold. If $h_{jk} \rightarrow 0$ and $nh_{jk} \rightarrow \infty$, then*

$$h_{jk} \Psi_{Z_j Z_{k+,p,q}}(h_j, h_k) = \tilde{\Psi}_{Z_j Z_{k+,p,q}}(h_j, h_k) + o_p(1), \quad (\text{A.25})$$

$$h_{jk} \Psi_{Z_j Z_{k-,p,q}}(h_j, h_k) = H_p(-1) \tilde{\Psi}_{Z_j Z_{k-,p,q}}(h_j, h_k) H_q(-1) + o_p(1), \quad (\text{A.26})$$

and

$$\tilde{\Psi}_{Z_j Z_{k+,p,q}}(h_j, h_k) = \sigma_{Z_j Z_{k+}}^2 f_+ \Psi_{jk,p,q} + o(1), \quad (\text{A.27})$$

$$\tilde{\Psi}_{Z_j Z_{k-,p,q}}(h_j, h_k) = \sigma_{Z_j Z_{k-}}^2 f_- \Psi_{jk,p,q} + o(1). \quad (\text{A.28})$$

Remark 9. In the proof of Lemma A.4, we use the compactness of the support of $K(\cdot)$ in the derivation of (A.27). We obtain (A.27) without assuming compactness in support of $K(\cdot)$. If $\rho_{jk} \rightarrow c_{jk} \in (0, \infty)$, (A.27) follows: continuity of $K(u)$, $r_p(u)$,

$\sigma_{Z_j Z_k}^4(u)$, and $f(u)$. For the other cases, we observe the following.

$$\begin{aligned}
& \tilde{\Psi}_{Z_j Z_{k+p,q}}(h_j, h_k) \\
&= \frac{1}{h_{jk}} \int_0^\infty K\left(\frac{x}{h_j}\right) K\left(\frac{x}{h_k}\right) r_p\left(\frac{x}{h_j}\right) r_q\left(\frac{x}{h_k}\right)' \sigma_{Z_j Z_k}^2(x) f(x) dx \\
&= \frac{m_{jk}}{h_{jk}} \int_0^\infty K\left(\frac{m_{jk}u}{h_j}\right) K\left(\frac{m_{jk}u}{h_k}\right) r_p\left(\frac{m_{jk}u}{h_j}\right) r_q\left(\frac{m_{jk}u}{h_k}\right)' \sigma_{Z_j Z_k}^2(um_{jk}) f(um_{jk}) du.
\end{aligned} \tag{A.29}$$

Suppose that $\rho_{jk,n} \rightarrow 0$. Subsequently, $h_{k,n} < h_{j,n}$; thus, $m_{jk,n}/h_{jk,n} = \rho_{jk,n}^{1/2}$ holds for a sufficiently large n . Hence, $m_{jk,n}/h_{jk,n} \rightarrow 0$, and (A.27) follows from (A.29). The case of $\rho_{jk,n}^{-1} \rightarrow 0$ follows from an analogous argument.

Proof of Lemma A.4. First, for $\Psi_{Z_j Z_{k+p,q}}(h_j, h_k)$, a change in the variables yields

$$\begin{aligned}
& E[h_{jk} \Psi_{Z_j Z_{k+p,q}}(h_j, h_k)] \\
&= E \left[\frac{1}{nh_{jk}} \sum_{i=1}^n 1(X_i \geq 0) K\left(\frac{X_i}{h_j}\right) K\left(\frac{X_i}{h_k}\right) r_p\left(\frac{X_i}{h_j}\right) r_q\left(\frac{X_i}{h_k}\right)' \sigma_{Z_j Z_k}^2(X_i) \right] \\
&= \frac{1}{h_{jk}} \int_0^\infty K\left(\frac{x}{h_j}\right) K\left(\frac{x}{h_k}\right) r_p\left(\frac{x}{h_j}\right) r_q\left(\frac{x}{h_k}\right)' \sigma_{Z_j Z_k}^2(x) f(x) dx \\
&= \int_0^\infty K\left(\frac{h_{jk}u}{h_j}\right) K\left(\frac{h_{jk}u}{h_k}\right) r_p\left(\frac{h_{jk}u}{h_j}\right) r_q\left(\frac{h_{jk}u}{h_k}\right)' \sigma_{Z_j Z_k}^2(uh_{jk}) f(uh_{jk}) du \\
&= \tilde{\Psi}_{Z_j Z_{k+p,q}}(h_j, h_k).
\end{aligned} \tag{A.30}$$

Let

$$\psi_{j,k,i} = 1(X_i \geq 0) K\left(\frac{X_i}{h_j}\right) K\left(\frac{X_i}{h_k}\right) r_p\left(\frac{X_i}{h_j}\right) r_q\left(\frac{X_i}{h_k}\right)' \sigma_{Z_j Z_k}^2(X_i), \tag{A.31}$$

where $\psi_{j,k,i} = \{\psi_{j,k,l,m,i}\}_{l=1,\dots,(p+1)}^{m=1,\dots,(q+1)}$ is a $(p+1) \times (q+1)$ -matrix. Additionally, let

$\psi_{j,k,l,m} = \sum_{i=1}^n \psi_{j,k,l,m,i}$ and $\psi_{j,k} = \sum_{i=1}^n \psi_{j,k,i}$. Observe that

$$\begin{aligned}
& h_{jk}^2 E[|\Psi_{Z_j Z_k+p,q}(h_j, h_k) - E[\Psi_{Z_j Z_k+p,q}(h_j, h_k)]|^2] \\
&= \frac{1}{n^2 h_{jk}^2} E[|\psi_{j,k} - E[\psi_{j,k}]|^2] = \frac{1}{n^2 h_{jk}^2} \sum_{l=1}^{p+1} \sum_{m=1}^{q+1} \text{Var}(\psi_{j,k,l,m}) \\
&= \frac{1}{n^2 h_{jk}^2} \sum_{l=1}^{p+1} \sum_{m=1}^{q+1} \sum_{i=1}^n \text{Var}(\psi_{j,k,l,m,i}) \\
&\leq \frac{1}{n^2 h_{jk}^2} \sum_{l=1}^{p+1} \sum_{m=1}^{q+1} \sum_{i=1}^n E[\psi_{j,k,l,m,i}^2] = \frac{1}{n^2 h_{jk}^2} \sum_{i=1}^n E[|\psi_{j,k,i}|^2]
\end{aligned} \tag{A.32}$$

and

$$\begin{aligned}
& \frac{1}{n^2 h_{jk}^2} \sum_{i=1}^n E[|\psi_{j,k,i}|^2] \\
&= \frac{1}{n h_{jk}^2} \int_0^\infty K\left(\frac{x}{h_j}\right)^2 K\left(\frac{x}{h_k}\right)^2 \left| r_p\left(\frac{x}{h_j}\right) \right|^2 \left| r_q\left(\frac{x}{h_k}\right) \right|^2 \sigma_{Z_j Z_k}^4(x) f(x) dx \\
&\leq \frac{1}{n m_{jk}^2} \int_0^\infty K\left(\frac{x}{h_j}\right)^2 K\left(\frac{x}{h_k}\right)^2 \left| r_p\left(\frac{x}{h_j}\right) \right|^2 \left| r_q\left(\frac{x}{h_k}\right) \right|^2 \sigma_{Z_j Z_k}^4(x) f(x) dx \\
&= \frac{1}{n m_{jk}} \int_0^\infty K\left(\frac{m_{jk}u}{h_j}\right)^2 K\left(\frac{m_{jk}u}{h_k}\right)^2 \\
&\quad \left| r_p\left(\frac{m_{jk}u}{h_j}\right) \right|^2 \left| r_q\left(\frac{m_{jk}u}{h_k}\right) \right|^2 \sigma_{Z_j Z_k}^4(um_{jk}) f(um_{jk}) du \\
&= O\left(\frac{1}{n m_{jk}}\right) = o(1).
\end{aligned} \tag{A.33}$$

Thus, (A.25) follows the Markov inequality. Second, (A.27) follows by continuity of $K(u)$, $r_p(u)$, $\sigma_{Z_j Z_k}^4(u)$, and $f(u)$, and the compactness of the support of $K(\cdot)$. \square

B Details on the search criterion

For the meta-analysis, we analyzed RD studies using diagnostic tests. There are two widely cited methodological papers, (McCrary, 2008 and Lee, 2008), and two widely cited survey papers, (Imbens and Lemieux, 2008 and Lee and Lemieux, 2010). We collected the citations of 2,697 unique papers on November 5, 2021, from the Web of

Science.²² Among 2,697 papers, we limited our focus to publications from the top five journals in economics (*American Economic Review*, *Econometrica*, *Journal of Political Economy*, *Quarterly Journal of Economics*, *Review of Economic Studies* in alphabetical order.). Among 98 in the top five publications, 60 papers reported at least one diagnostic test to validate their empirical analyses of RD designs. Furthermore, we removed one paper which meant to report the implausibility of an existing design by demonstrating the rejected diagnostic tests. We excluded surveys, theoretical contributions, and other uses of similar tests in manipulation detection or kink designs. Furthermore, we limited our focus to the density and balance or placebo tests in their *standard* procedures, excluding placebo or balance tests for predicted variables from covariates. We identified five studies that incorporated a joint test for multiple testing problems. However, we did not include these joint tests because all but one study did not incorporate the nonparametric nature of the RD estimates. The only considered study (Fort et al., 2020) used Canay and Kamat (2018).

From these 59 papers, we collected the balance, placebo, or density test results that appeared to be their *main* specifications. In practice, many researchers have run multiple versions of these tests using different bandwidths, kernels, and specifications. We collected the total number of tests separately, but our numerical analysis was limited to the main specifications. We computed p-values from the reported statistics when only the test statistics were reported.

C Details on the simulation data generating process

We conducted 3,000 replications to generate a random sample.

$$\{(X_i^+, X_i^-, \tilde{Z}_{1,i}, \dots, \tilde{Z}_{d,i}, U_i)' : i = 1, \dots, n\}$$

with size $n = 500, 1000$, $X_i^+ \sim tN(0, 0.12^2; [0, 1])$ with $tN(\mu, \sigma^2; [0, 1])$ denotes a truncated normal distribution with mean μ and variance σ^2 , lying within the interval $[0, 1]$, $X_i^- \stackrel{d}{=} -X_i^+$. $U_i \sim Unif[0, 1]$ with $Unif[0, 1]$ denoting a uniform distribution on the interval $[0, 1]$, $(\tilde{Z}_{1,i}, \dots, \tilde{Z}_{d,i})' \sim N_d(0, \tilde{\Sigma})$ with $\tilde{\Sigma}$ denoting a correlation matrix where each (j, k) entry is $1 > \rho \geq 0$ for $j \neq k$, and (X_i^+, X_i^-) , $(\tilde{Z}_{1,i}, \dots, \tilde{Z}_{d,i})$, and U_i

²²We used the Web of Science to limit our focus on published papers.

are mutually independent. The running variable X_i is generated as follows.

$$X_i = (1 - M_i)X_i^- + M_iX_i^+,$$

where $M_i = 1\{U_i \leq \bar{p}\}$ with $\bar{p} \geq 0.5$. For pre-treatment covariates $Z_i = (Z_{1,i}, \dots, Z_{d,i})'$, we consider two specifications: first, one of the d covariates sees a jump, and second, all the d covariates see a jump, but each jump size is divided by d . For the first specification, each $Z_{k,i}, k = 1, \dots, d$ is generated as follows.

$$Z_{k,i} = \begin{cases} \lambda(X_i) + \tilde{Z}_{k,i} & \text{for } k = 1, \dots, d-1 \\ \lambda(X_i) + aM_i + \tilde{Z}_{k,i} & \text{for } k = d \text{ with } a \geq 0, \end{cases}$$

where the functional form of $\lambda(x)$ is defined as

$$\lambda(x) = 0.48 + \begin{cases} 0.84x - 3.00x^2 + 7.99x^3 - 9.01x^4 + 3.56x^5, & \text{if } x \geq 0 \\ 1.27x + 7.18x^2 + 20.21x^3 + 21.54x^4 + 7.33x^5, & \text{otherwise.} \end{cases}$$

For the second specification, each $Z_{k,i}, k = 1, \dots, d$ is generated as follows.

$$Z_{k,i} = \lambda(X_i) + a/dM_i + \tilde{Z}_{k,i}.$$

Let $f^*(x)$ be the density of X_i^+ ,

$$f^*(x) = \frac{\phi(x/0.12)}{0.12(\Phi(1/0.12) - \Phi(0))},$$

where $\phi(x)$ and $\Phi(x)$ are the density and cumulative distribution functions, respectively, of the standard normal random variable. Using $f^*(x)$, the density of X_i can be expressed as

$$f(x) = \begin{cases} f^*(x)(1 - \bar{p}) & \text{if } x < 0 \\ f^*(x)\bar{p} & \text{if } x > 0, \end{cases}$$

and the discontinuity level of $f(x)$ at $x = 0$ is $\tau_f = f^*(0)(2\bar{p} - 1)$. Hence, we have $\tau_f = 0$ if and only if $\bar{p} = 0.5$, and $\tau_f > 0$ when $\bar{p} > 0.5$.

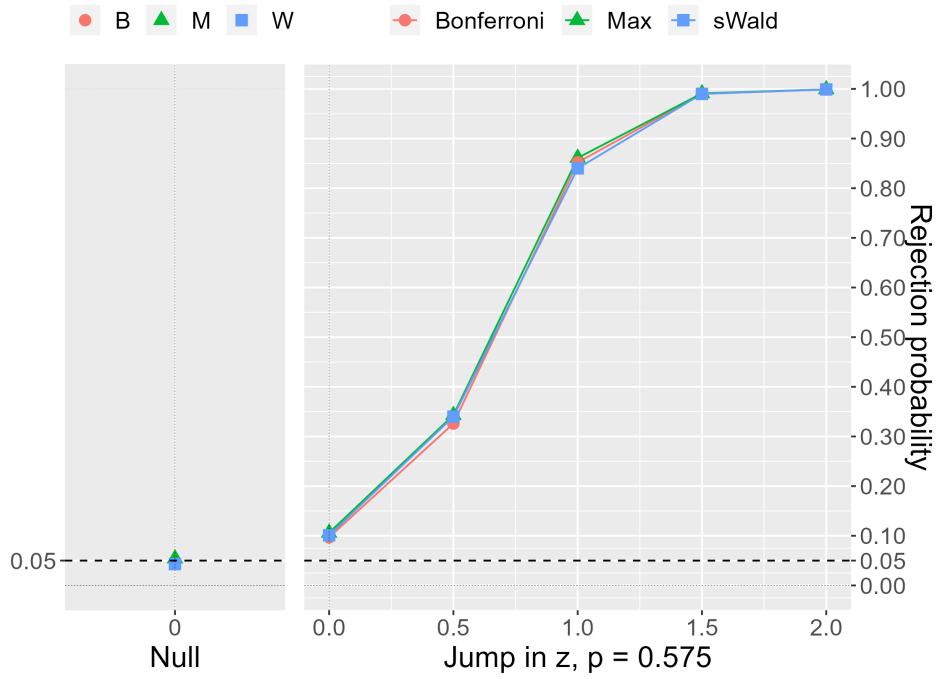
D Additional figures

D.1 Additional power plots

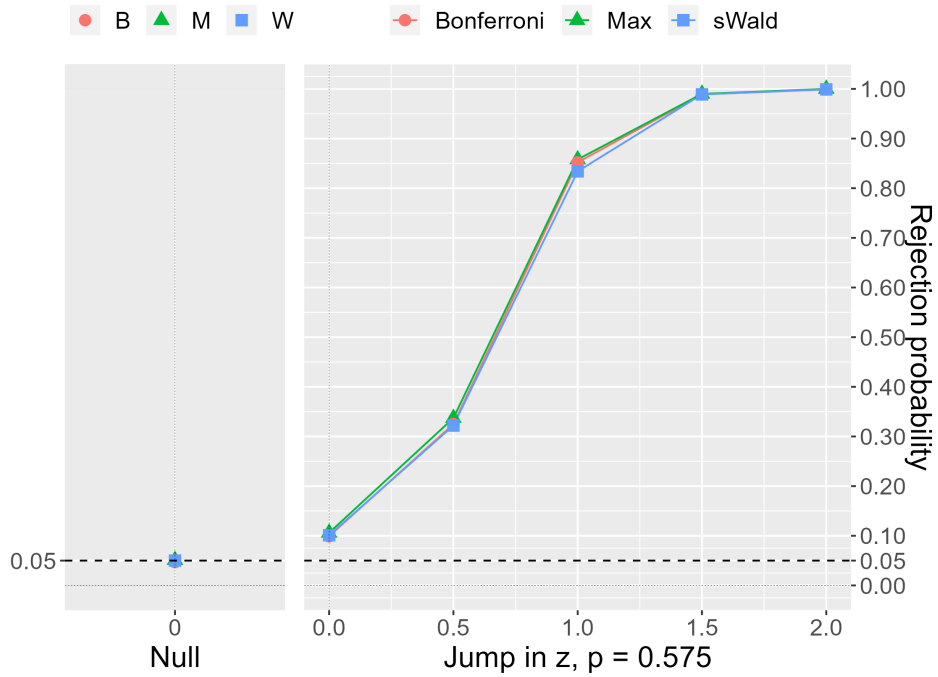
Appendix Figures 1-6 present the empirical power of the (ii) Bonferroni correction, (iv) Max test, and (v) sWald test under $p = 0.575$ and $\tau_{Z_d}(= a) = 0, 0.5, 1, 1.5, 2$ for different dimensions, and $d = 3, 5$ for the Monte Carlo experiment in Section 4. In Appendix Figures 1–4, each figure presents the results for different correlations, $\rho = 0, 0.3$, which are weaker than those in Figures 5-8 from the main text.

Appendix Figures 1 and 2 present the results when one of the d covariates jumps, and Appendix Figures 3 and 4 present the results when all d covariates jump. However, each jump size is divided by d for $d = 3, 5$. Although the difference between the Max test and Bonferroni correction is smaller, the simulation results show that the proposed joint testing methods exhibit power improvements similar to those shown in Section 4. Moreover, the power improvements in the sWald test are more significant when the correlation is weaker.

Appendix Figures 5 and 6 compare the results for positive and negative correlations when $d = 3$ and $|\rho| = 0.9$. In Appendix Figures 5 (b), and 6 (b), two of the three covariates have the same pairwise correlation coefficient of 0.9, and the remaining one has the pairwise correlation coefficient of -0.9 . Appendix Figure 5 presents the results when one of the three covariates jumps, and Appendix Figure 6 presents the results when all three covariates jump. Nevertheless, each jump size is divided by three. Although the sWald test is conservative when the correlation is strong, the Max test had more power than the Bonferroni correction in both cases. This suggests that the power improvements in the Max test are robust against negative correlations.

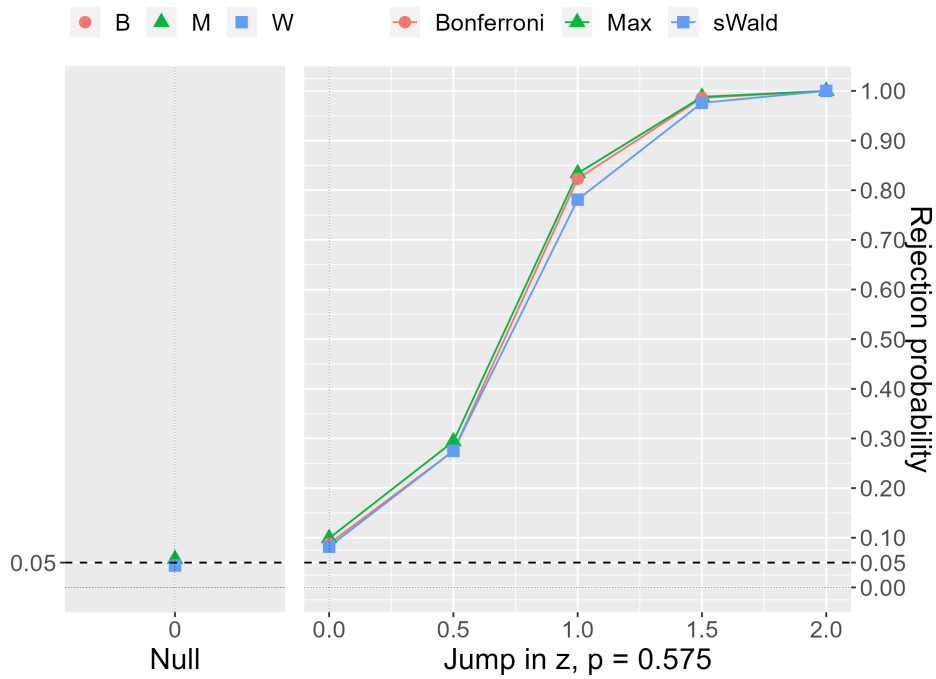


(a) Covariates have the same pairwise correlation coefficient of 0

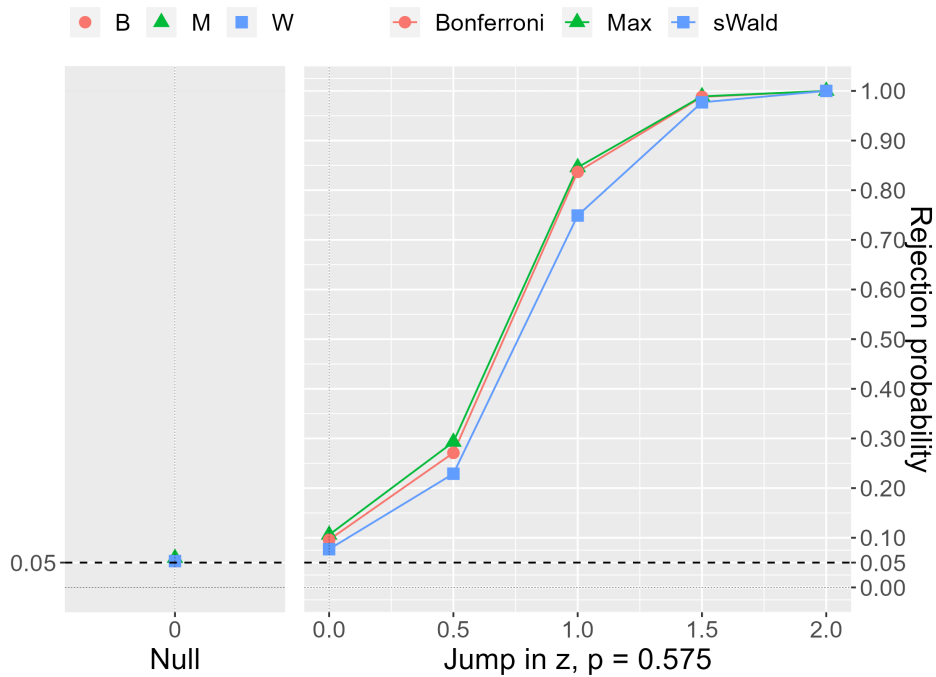


(b) Covariates have the same pairwise correlation coefficient of 0.3

Appendix Figure 1: A jump in the three covariates with a density, $n = 1000$

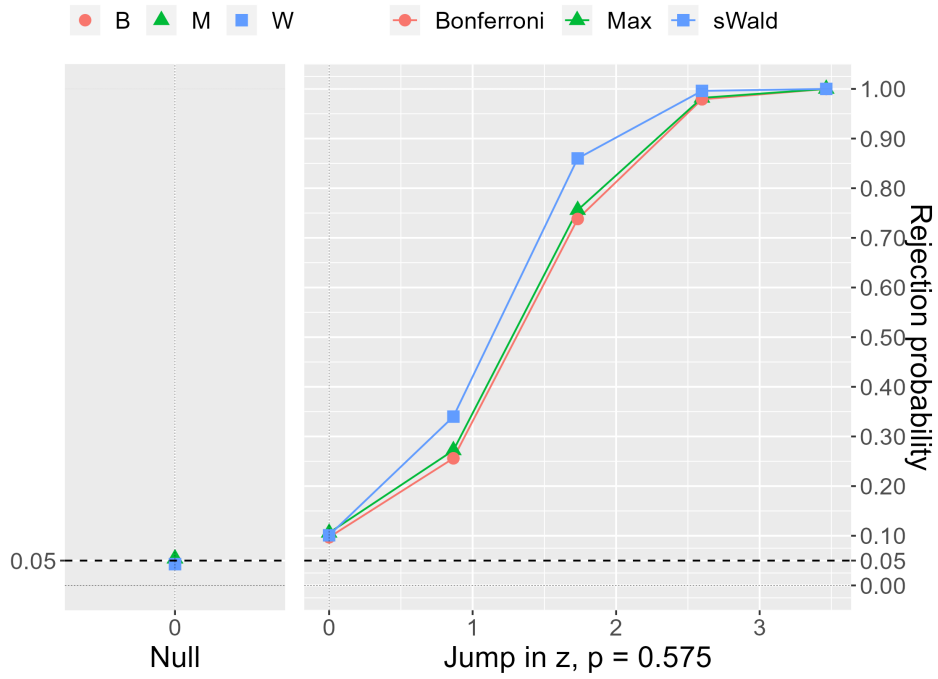


(a) Covariates have the same pairwise correlation coefficient of 0

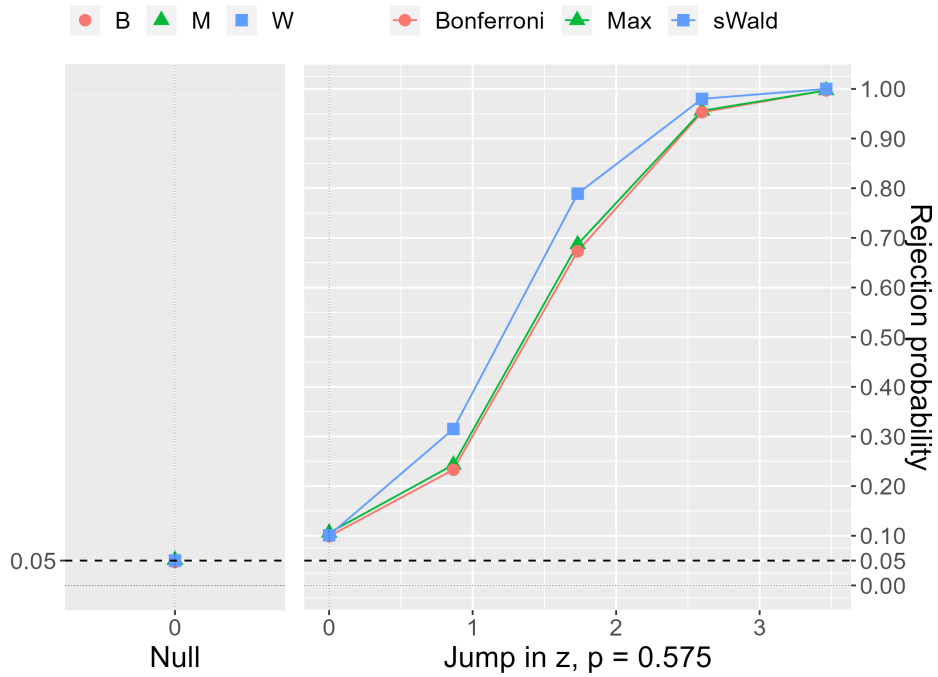


(b) Covariates have the same pairwise correlation coefficient of 0.3

Appendix Figure 2: A jump in the five covariates with a density, $n = 1000$

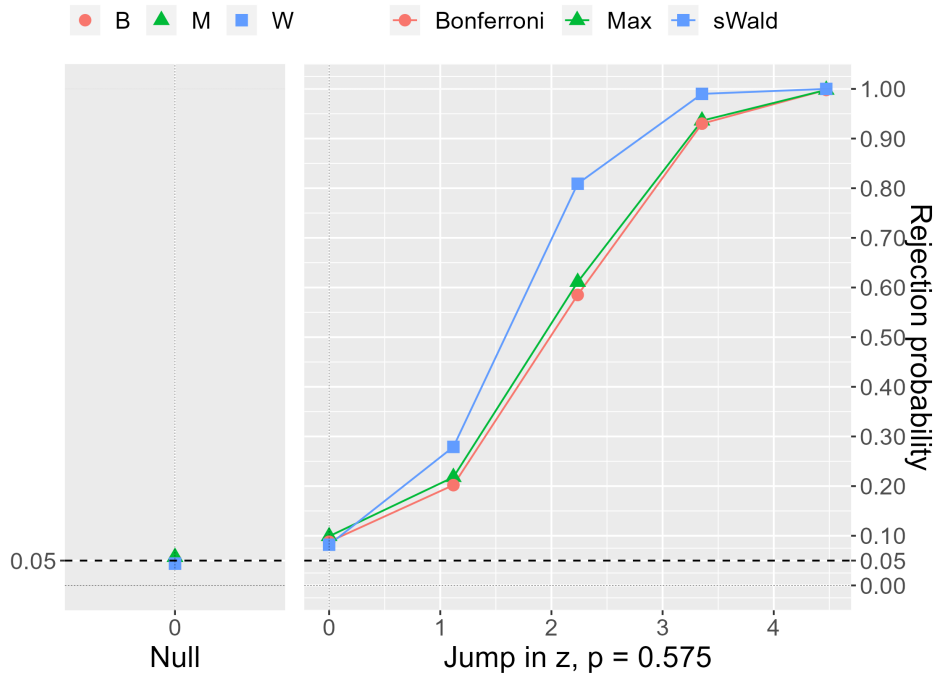


(a) Covariates have the same pairwise correlation coefficient of 0

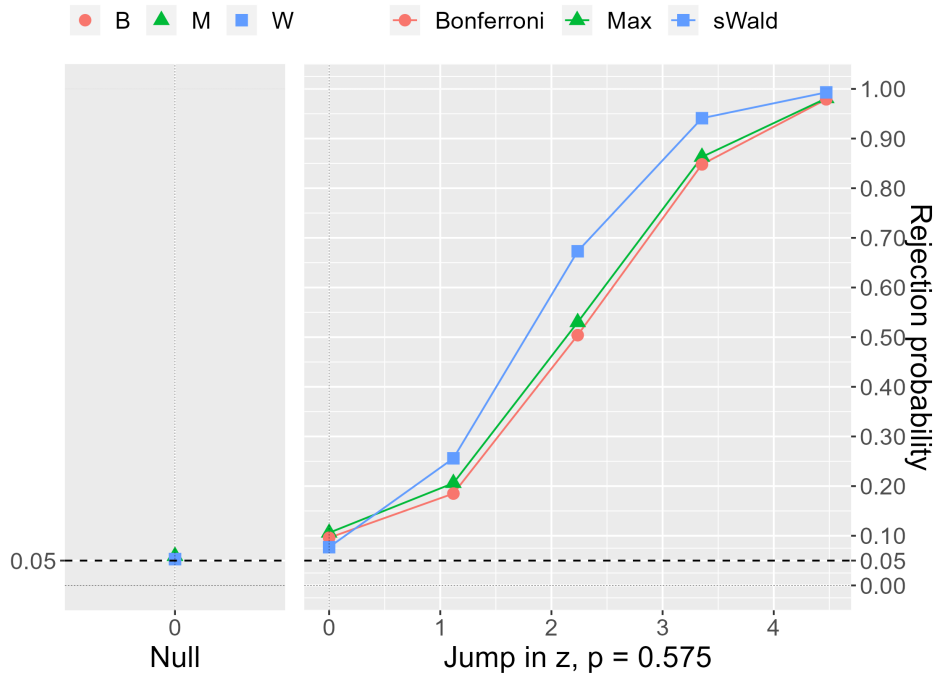


(b) Covariates have the same pairwise correlation coefficient of 0.3

Appendix Figure 3: 1/3 of jumps in all the three covariates with a density, $n = 1000$.

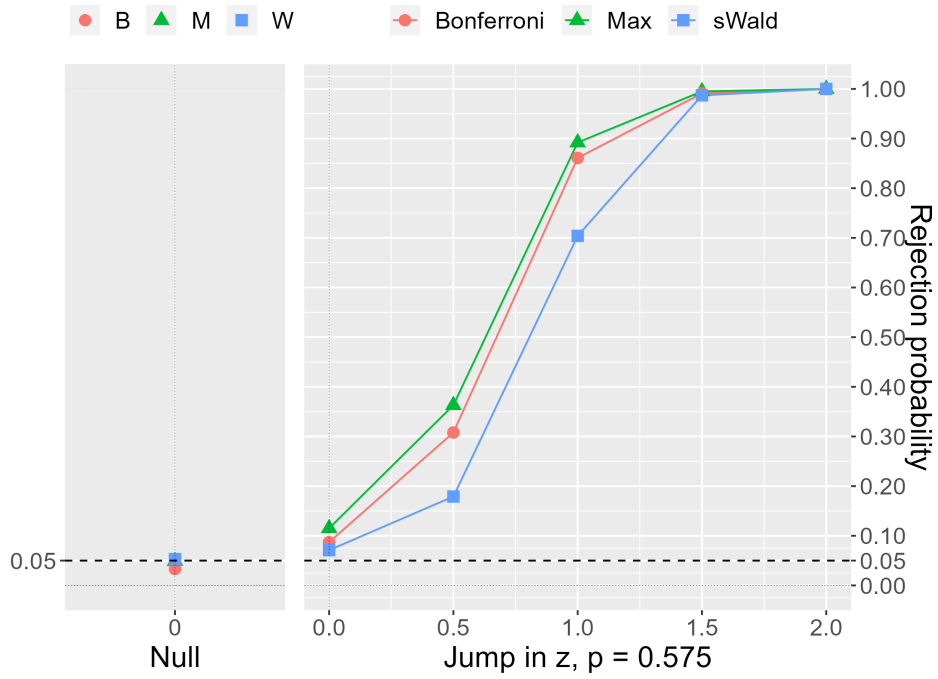


(a) Covariates have the same pairwise correlation coefficient of 0

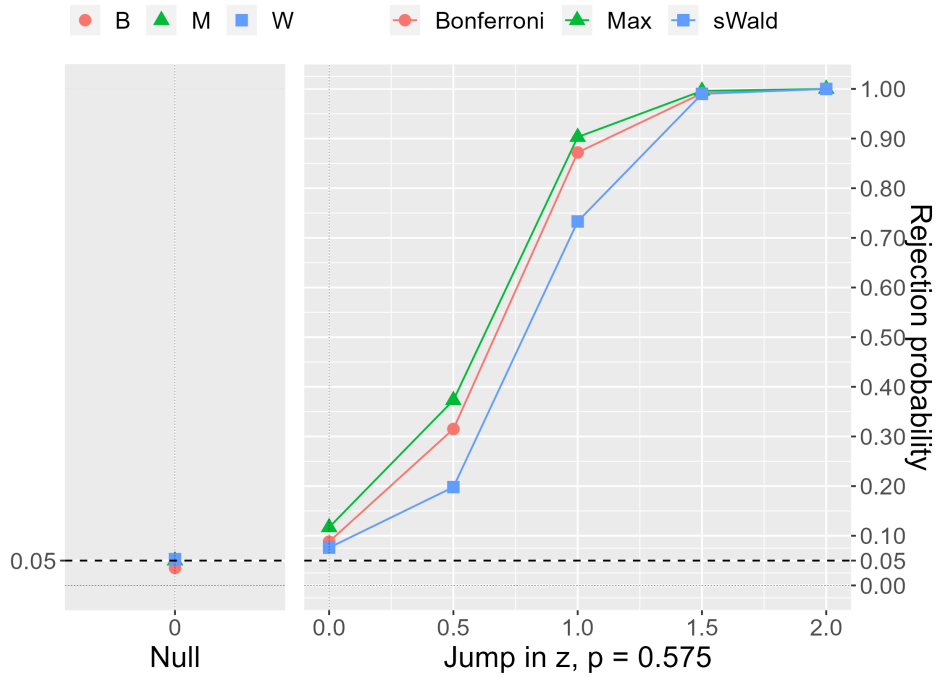


(b) Covariates have the same pairwise correlation coefficient of 0.3

Appendix Figure 4: 1/5 of jumps in all the five covariates with a density, $n = 1000$.

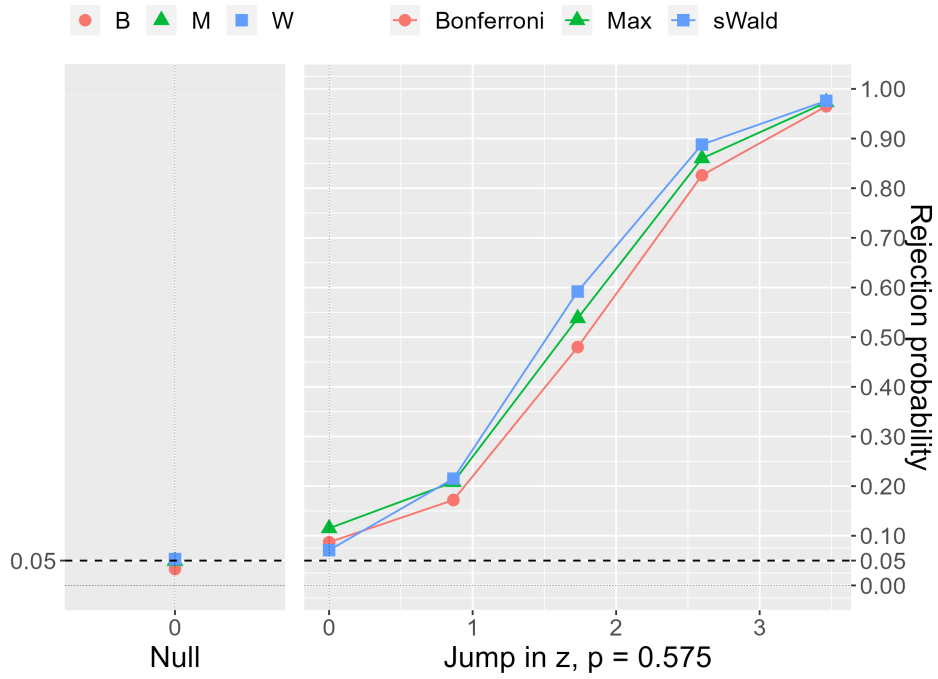


(a) The remaining one has the same pairwise correlation coefficient of 0.9.

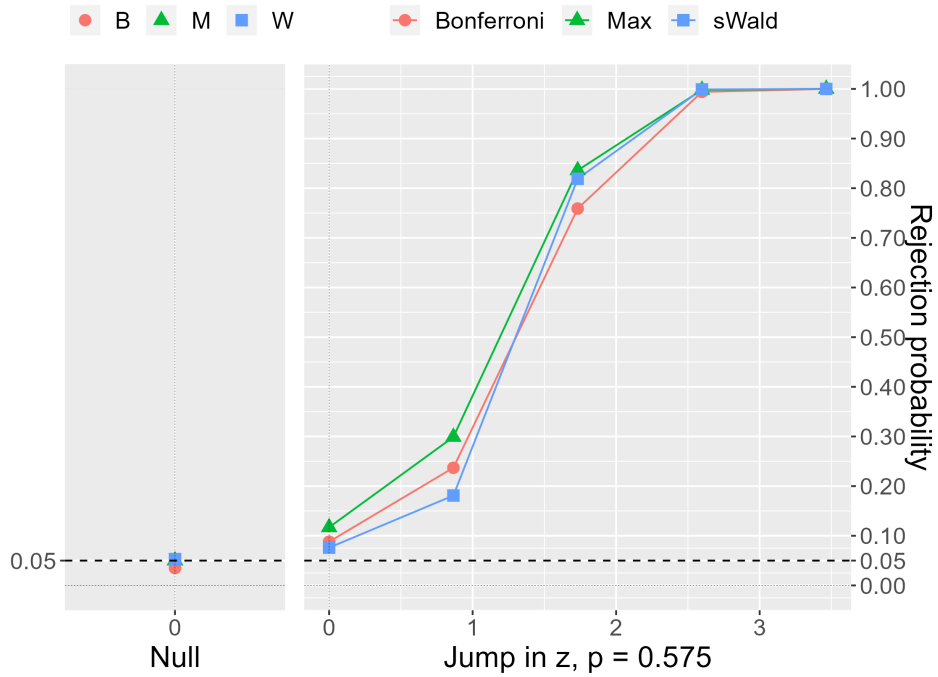


(b) The remaining one has the pairwise correlation coefficient of -0.9 .

Appendix Figure 5: A jump in the three covariates with a density, $n = 1000$. Two out of three covariates have the same pairwise correlation coefficient of 0.9



(a) The remaining one has the same pairwise correlation coefficient of 0.9.

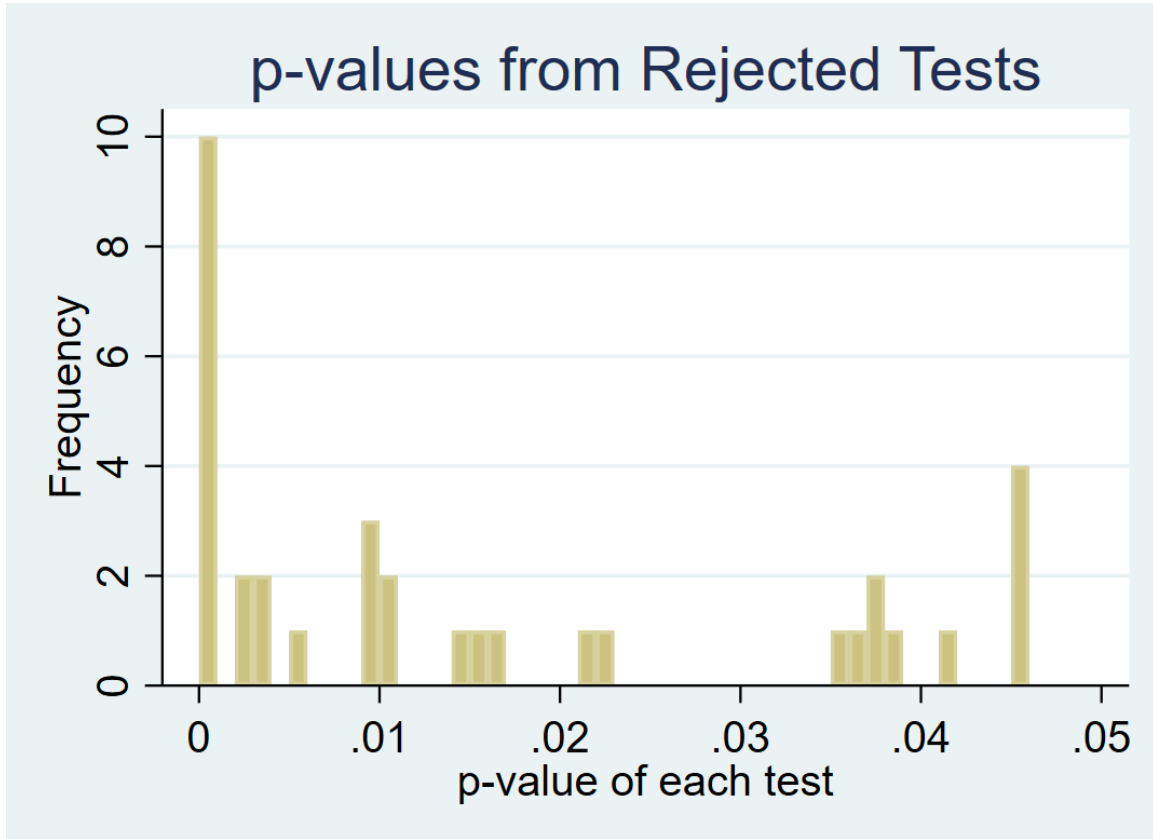


(b) The remaining one has the pairwise correlation coefficient of -0.9 .

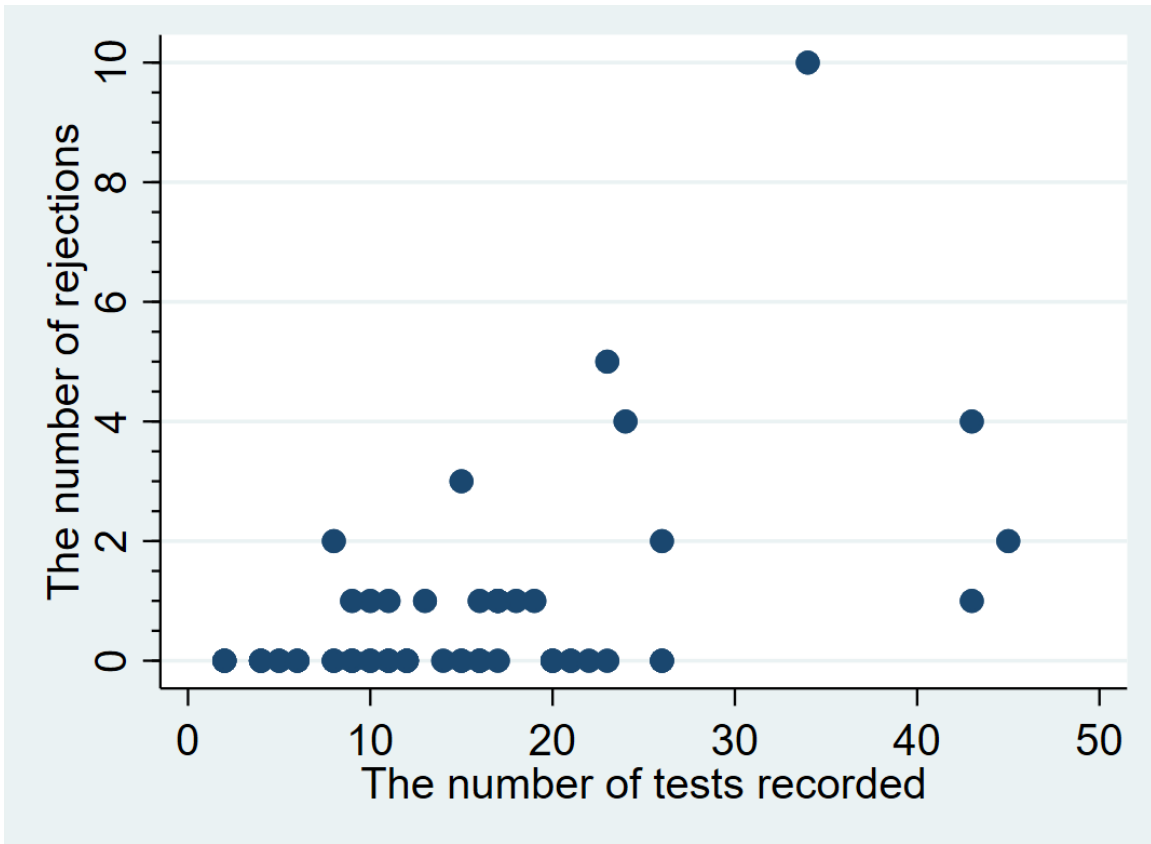
Appendix Figure 6: 1/3 of jumps in all the three covariates with a density, $n = 1000$. Two out of three covariates have the same pairwise correlation coefficient of 0.9

D.2 Additional meta-analysis plots

Appendix Figure 7: Histogram of p-values from rejected tests.

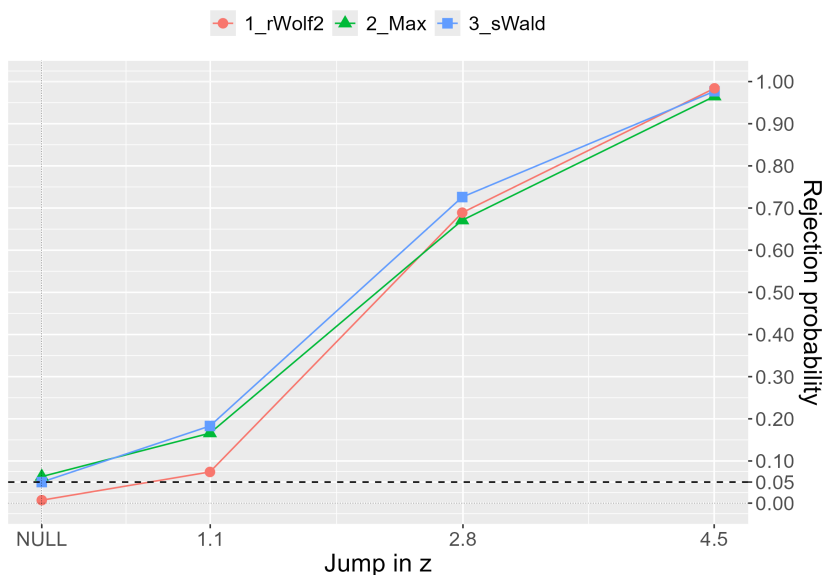


Notes: The distribution of the 34 tests are fairly uniform over 0 to 0.05. In the histogram of Appendix Figure 7, there are two masses due to rounding: the mass at 0 is rounding to 0 in the original reported p-value in the papers; the mass near 0.05 is at 0.0455 which is the p-value corresponding the computed t-statistics of 2 by dividing rounded numbers such as 0.02 over 0.01.

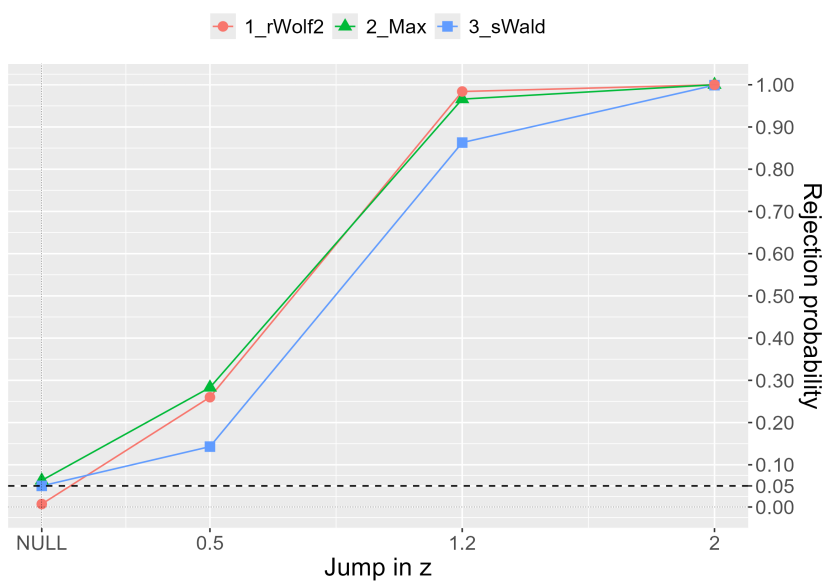


Appendix Figure 8: Scatter plot of the number of tests and the number of rejected tests.

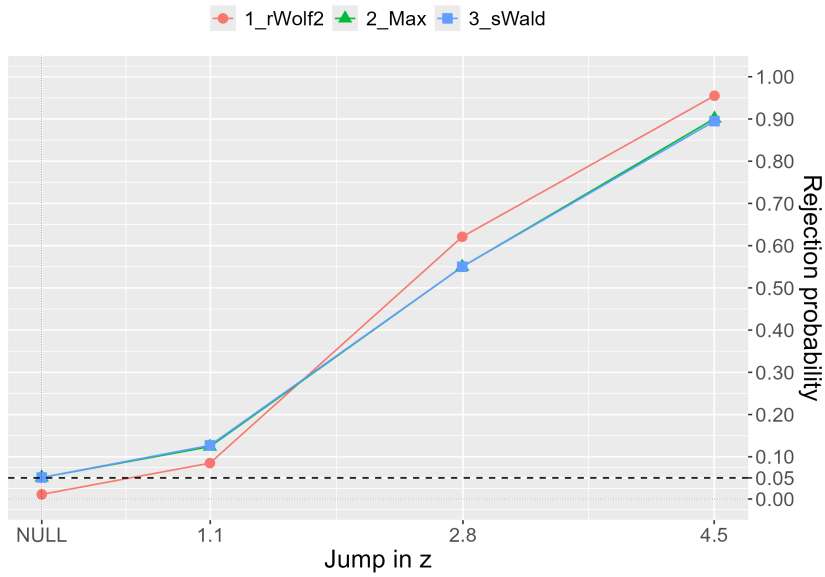
D.3 Additional power plots to compare with rwolf2 for balance tests only



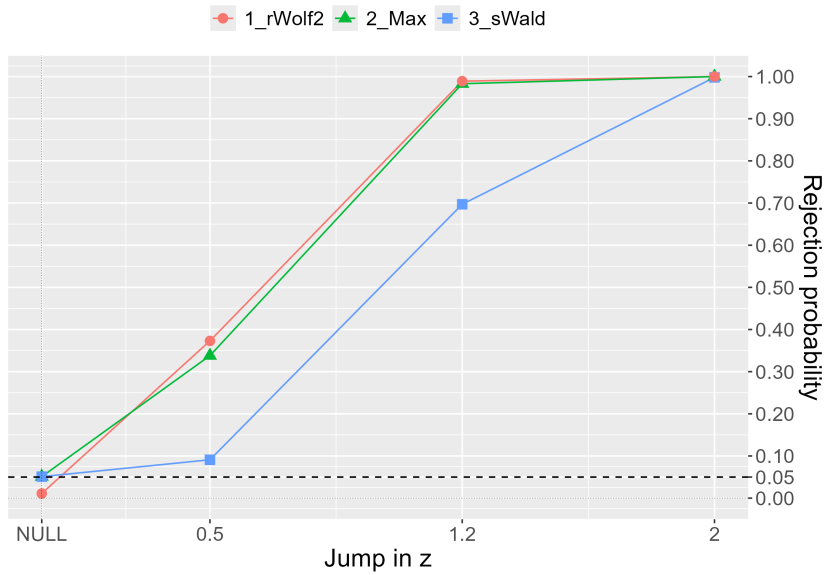
Appendix Figure 9: The unified balance test results compared with rwolf2. 1/5 of jumps in all the five covariates. Five covariates have the pairwise correlation coefficient of 0.5



Appendix Figure 10: The unified balance test results compared with rwolf2. One of five covariates have the jump. Five covariates have the pairwise correlation coefficient of 0.5



Appendix Figure 11: The unified balance test results compared with rwolf2. 1/5 of jumps in all the five covariates. Five covariates have the pairwise correlation coefficient of 0.9



Appendix Figure 12: The unified balance test results compared with rwolf2. One of five covariates have the jump. Five covariates have the pairwise correlation coefficient of 0.9

E Further discussions for the pretest analysis

Given the general case of the pretest analysis, we ran a few numerical analysis based on a simulated toy dataset and calibrated datasets from two empirical studies.

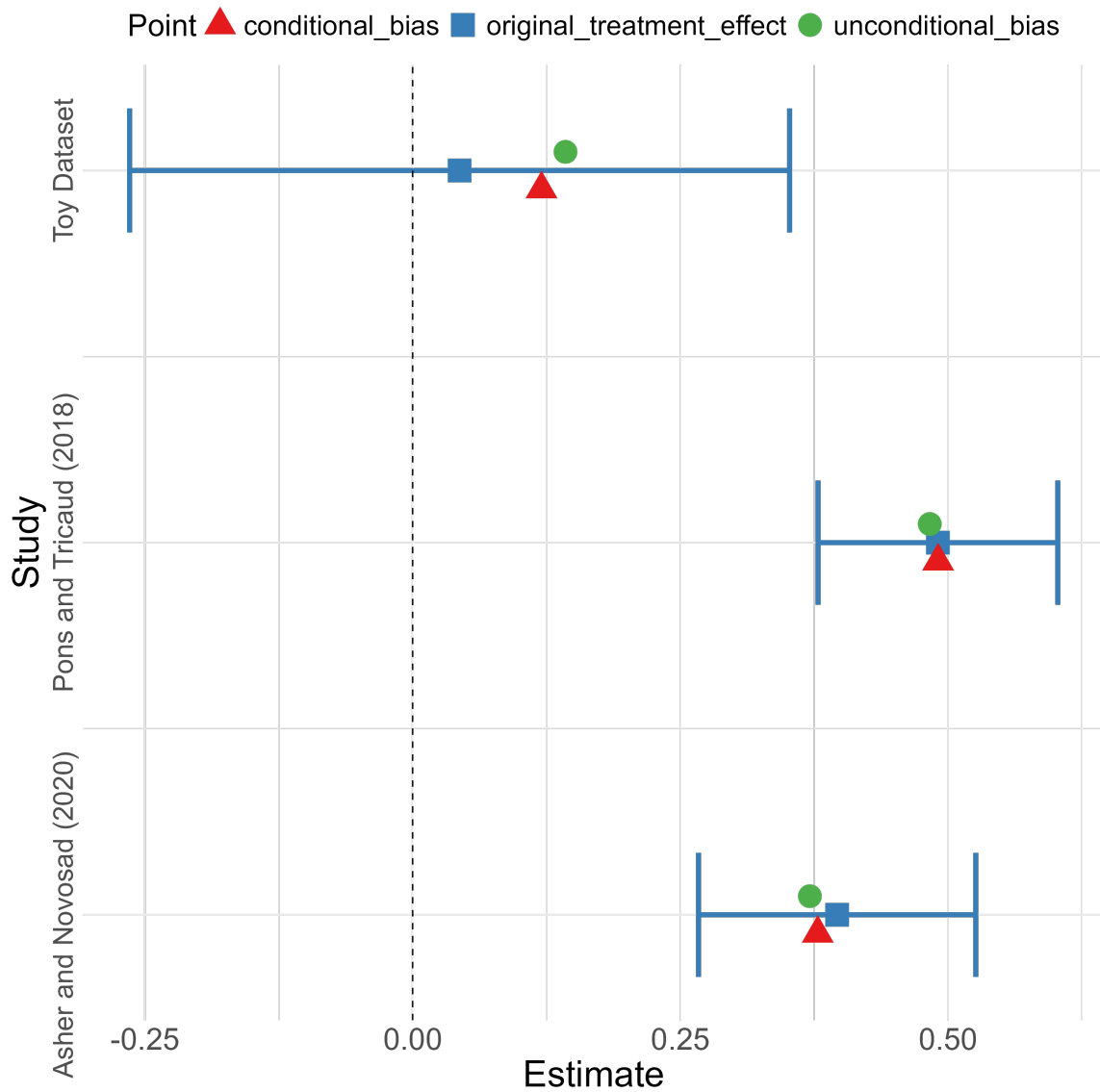
First, we consider a null RD design with a sample size of 3000 and four covariates. In the toy dataset, we generate the outcome using the following model

$$Y_i = \epsilon_i + Z_i' \beta$$

where $\epsilon_i \sim N(0, 1)$, $Z_i \sim N(0, I_4)$ and $\beta = [-0.05, 0.1, 0.2, -0.1]'$. Second, we use the dataset from two empirical studies, Pons and Tricaud (2018) and Asher and Novosad (2020). For Pons and Tricaud (2018), we use the five covariates for the balance test in the original study to evaluate the impact on the first stage binary treatment status. For Asher and Novosad (2020), we use the six covariates for the balance test in the original study to evaluate the impact on the first stage binary treatment status.

For three datasets, we conduct the following analysis as in Roth (2022). First, we set δ_Z so that the max test has 80% power. Second, run *rdrobust* with covariates option and obtain the treatment effect estimate $\hat{\tau}$ and the weights on the covariates $\hat{\beta}$. Finally, compute the mean δ_Y according to the linear model with $\hat{\beta}$ as the unconditional bias, and the conditional bias which is the mean δ_Y among simulated samples which accepts the null for the data generating process of δ_Z for the 80% power.

Appendix Figure 13 summarizes the results. In all three results, the unconditional bias is reduced towards the original estimate by conditioning on the draws which pass the max test. Hence, pretesting is bias-reducing at least for these cases.



Appendix Figure 13: Pretest numerical results

Notes: The figure compares the original estimates and confidence intervals with two points of the unconditional bias and (pretest) conditional bias plus the point estimates from a toy dataset and two empirical applications. The square points denote the original (bias corrected) point estimate, the range denote the confidence interval, the circle points denote the unconditional bias, the triangular points denote the conditional bias. In all three cases, conditioning reduces the bias towards the original point estimates.

References

- ABDULKADIROĞLU, A., J. ANGRIST, AND P. PATHAK (2014): “The Elite Illusion: Achievement Effects at Boston and New York Exam Schools,” *Econometrica*, 82, 137–196.
- ASHER, S. AND P. NOVOSAD (2020): “Rural Roads and Local Economic Development,” *American Economic Review*, 110, 797–823.
- BERTANHA, M. AND G. W. IMBENS (2020): “External Validity in Fuzzy Regression Discontinuity Designs,” *Journal of Business & Economic Statistics*, 38, 593–612.
- BUGNI, F. A. AND I. A. CANAY (2021): “Testing Continuity of a Density via g-order Statistics in the Regression Discontinuity Design,” *Journal of Econometrics*, 221, 138–159.
- CALONICO, S., M. D. CATTANEO, AND M. H. FARRELL (2020): “Optimal bandwidth choice for robust bias-corrected inference in regression discontinuity designs,” *The Econometrics Journal*, 23, 192–210.
- (2022): “Coverage Error Optimal Confidence Intervals for Local Polynomial Regression,” *Bernoulli*, 28, 2998–3022.
- CALONICO, S., M. D. CATTANEO, M. H. FARRELL, AND R. TITIUNIK (2017): “Rdrobust: Software for Regression-discontinuity Designs,” *The Stata Journal*, 17, 372–404.
- CALONICO, S., M. D. CATTANEO, AND R. TITIUNIK (2014): “Robust Nonparametric Confidence Intervals for Regression-Discontinuity Designs,” *Econometrica*, 82, 2295–2326.
- (2015): “Optimal data-driven regression discontinuity plots,” *Journal of the American Statistical Association*, 110, 1753–1769.
- CANAY, I. A. AND V. KAMAT (2018): “Approximate Permutation Tests and Induced Order Statistics in the Regression Discontinuity Design,” *The Review of Economic Studies*, 85, 1577–1608.

- CATTANEO, M. D., B. R. FRANDBEN, AND R. TITIUNIK (2015): “Randomization Inference in the Regression Discontinuity Design: An Application to Party Advantages in the U.S. Senate,” *Journal of Causal Inference*, 3, 1–24.
- CATTANEO, M. D., N. IDROBO, AND R. TITIUNIK (2019): *A Practical Introduction to Regression Discontinuity Designs: Foundations*, Cambridge University Press.
- (2024): *A Practical Introduction to Regression Discontinuity Designs: Extensions*, Cambridge University Press.
- CATTANEO, M. D., M. JANSSON, AND X. MA (2018): “Manipulation testing based on density discontinuity,” *The Stata Journal*, 18, 234–261.
- (2020): “Simple local polynomial density estimators,” *Journal of the American Statistical Association*, 115, 1449–1455.
- CATTANEO, M. D. AND R. TITIUNIK (2022): “Regression Discontinuity Designs,” *Annual Review of Economics*, 14, 821–851.
- CATTANEO, M. D., R. TITIUNIK, AND G. VAZQUEZ-BARE (2016): “Inference in Regression Discontinuity Designs under Local Randomization,” *The Stata Journal*, 16, 331–367.
- CATTANEO, M. D., R. TITIUNIK, AND G. VAZQUEZ-BARE (2017): “Comparing Inference Approaches for RD Designs: A Reexamination of the Effect of Head Start on Child Mortality,” *Journal of Policy Analysis and Management*, 36, 643–681.
- CLARKE, D. (2021): “Rwolf2 Implementation and Flexible Syntax,” *mimeo*.
- DURRETT, R. (2019): *Probability: theory and examples*, vol. 49, Cambridge university press.
- FAN, J. AND I. GIJBELS (1996): *Local polynomial modelling and its applications: monographs on statistics and applied probability 66*, vol. 66, CRC Press.
- FORT, M., A. ICHINO, AND G. ZANELLA (2020): “Cognitive and Noncognitive Costs of Day Care at Age 0–2 for Children in Advantaged Families,” *Journal of Political Economy*, 128, 158–205.

- HAHN, J., P. TODD, AND W. V. DER KLAUW (2001): “Identification and Estimation of Treatment Effects with a Regression-Discontinuity Design,” *Econometrica*, 69, 201–209.
- HARTMAN, E. (2021): “Equivalence testing for regression discontinuity designs,” *Political Analysis*, 29, 505–521.
- HARTMAN, E. AND F. D. HIDALGO (2018): “An equivalence approach to balance and placebo tests,” *American Journal of Political Science*, 62, 1000–1013.
- HSU, Y.-C. AND S. SHEN (2019): “Testing Treatment Effect Heterogeneity in Regression Discontinuity Designs,” *Journal of Econometrics*, 208, 468–486.
- (2021): “Testing Monotonicity of Conditional Treatment Effects under Regression Discontinuity Designs,” *Journal of Applied Econometrics*, 36, 346–366.
- HYTTINEN, A., J. MERILÄINEN, T. SAARIMAA, O. TOIVANEN, AND J. TUKIAINEN (2018): “When Does Regression Discontinuity Design Work? Evidence from Random Election Outcomes,” *Quantitative Economics*, 9, 1019–1051.
- IMBENS, G. W. AND T. LEMIEUX (2008): “Regression discontinuity designs: A guide to practice,” *Journal of Econometrics*, 142, 615–635.
- ISHIHARA, T. AND M. SAWADA (2023): “Manipulation-Robust Regression Discontinuity Designs,” *arXiv:2009.07551 [econ, stat]*.
- JÄGER, S., B. SCHOEFER, AND J. HEINING (2021): “Labor in the Boardroom*,” *The Quarterly Journal of Economics*, 136, 669–725.
- JOHNSON, M. S. (2020): “Regulation by Shaming: Deterrence Effects of Publicizing Violations of Workplace Safety and Health Laws,” *American Economic Review*, 110, 1866–1904.
- KORTING, C., C. LIEBERMAN, J. MATSUDAIRA, Z. PEI, AND Y. SHEN (2023): “Visual Inference and Graphical Representation in Regression Discontinuity Designs,” *The Quarterly Journal of Economics*, qjad011.
- LEE, D. S. (2008): “Randomized Experiments from Non-Random Selection in U.S. House Elections,” *Journal of Econometrics*, 142, 675–697.

- LEE, D. S. AND T. LEMIEUX (2010): “Regression Discontinuity Designs in Economics,” *Journal of Economic Literature*, 48, 281–355.
- MCCRARY, J. (2008): “Manipulation of the Running Variable in the Regression Discontinuity Design: A Density Test,” *Journal of Econometrics*, 142, 698–714.
- MEYERSSON, E. (2014): “Islamic Rule and the Empowerment of the Poor and Pious,” *Econometrica*, 82, 229–269.
- MONTIEL OLEA, J. L. AND M. PLAGBORG-MØLLER (2019): “Simultaneous Confidence Bands: Theory, Implementation, and an Application to SVARs,” *Journal of Applied Econometrics*, 34, 1–17.
- OTSU, T., K.-L. XU, AND Y. MATSUSHITA (2013): “Estimation and Inference of Discontinuity in Density,” *Journal of Business & Economic Statistics*, 31, 507–524.
- PONS, V. AND C. TRICAUD (2018): “Expressive Voting and Its Cost: Evidence From Runoffs With Two or Three Candidates,” *Econometrica*, 86, 1621–1649.
- ROMANO, J. P. AND M. WOLF (2005): “Exact and Approximate Stepdown Methods for Multiple Hypothesis Testing,” *Journal of the American Statistical Association*, 100, 94–108.
- (2016): “Efficient Computation of Adjusted p -Values for Resampling-Based Stepdown Multiple Testing,” *Statistics & Probability Letters*, 113, 38–40.
- ROTH, J. (2022): “Pretest with caution: Event-study estimates after testing for parallel trends,” *American Economic Review: Insights*, 4, 305–322.
- SERFLING, R. J. (1980): *Approximation theorems of mathematical statistics*, John Wiley & Sons.
- TYREFORS HINNERICH, B. AND P. PETTERSSON-LIDBOM (2014): “Democracy, Redistribution, and Political Participation: Evidence From Sweden 1919–1938,” *Econometrica*, 82, 961–993.
- VAN DER VAART, A. W. AND J. A. WELLNER (1996): *Weak convergence and empirical processes*, Springer New York, NY.
- WELLEK, S. (2010): *Testing Statistical Hypotheses of Equivalence and Noninferiority (2nd ed.)*, Chapman and Hall/CRC.